



NTNU – Trondheim
Norwegian University of
Science and Technology

The Håkåneset rockslide, Tinnsjø

Stability analysis of a potentially rock slope
instability.

Inger Lise Sollie

Geotechnology

Submission date: June 2014

Supervisor: Bjørn Nilsen, IGB

Norwegian University of Science and Technology
Department of Geology and Mineral Resources Engineering



MASTEROPPGAVEN

Kandidatens navn: Inger Lise Sollie

Oppgavens tittel: Håkåneset, Tinnsjø – Stability analysis of potential rock slope instability.

English title:

Utfyllende tekst:
1.

This master thesis is a follow-up of project work conducted by the candidate during the autumn semester 2013. Mapping of geomorphology, structural geology and geotechnical parameters, structural and kinematic analysis and discussion of a preliminary, simple stability model were performed during this project work. The aim of the master thesis is to perform more comprehensive stability analysis of the Håkåneset rock slide, with particular focus on:

- Reducing uncertainty of the structural model by supplementary structural analysis of LiDAR-data (ALS) in Coltop.
- Defining structural profiles in selected areas of the slope that will help to reduce the uncertainties of the kinematic model presented during the project work and will be used for:
 - Calculation of stress distribution and Factor of Safety in various parts of the rock slope by limit equilibrium analysis and numerical modeling techniques in for example Phase2 (Rocscience).
 - Including the effect of the water within the lower part of the slope in the stability analysis of the slope.
 - Measuring deformation of the rock slope by the use of land based TLS in Polyworks.
 - Combining structural profiles of the rock slope and deformation measurements for volume estimations.

The master thesis is organized in co-operation with NGU, with Reginald Hermanns as contact person and external co-supervisor.

Studieretning: Ingeniør- og miljøgeologi

Hovedprofil: Ingeniørgeologi og bergmekanikk

Tidsrom: 14.01.-10.06.2014

Bjørn Nilsen, Professor/hovedveileder

SKJEMAET TAS INN SOM SIDE 1 I MASTEROPPGAVEN
NTNU, 15 januar 2014

ABSTRACT

The Håkåneset rockslide is located on the west shore of Lake Tinnsjø (191 m.a.s.l), a fjordlake stretching 32 km with a SSE-NNW orientation in Telemark, southern Norway. The instability extends from 550 m.a.s.l. and down to approximately 300 m depth in the lake, making up a surface area of 0.54 km² under water and 0.50 km² on land. The rockslide comprises an anisotropic metavolcanic rock that is strongly fractured. Five discontinuity sets are identified with systematic field mapping supported by structural analysis of terrestrial laser scan (TLS) data. These are interpreted as gravitationally reactivated inherited tectonic structures. At the northern end the instability is limited by a steep south-east dipping joint (JF3 (~133/77)) that is one direction of a conjugate strike slip fault set (JF3, JF2 (~358/65)). Towards the south the limit to the stable bedrock is transitional. A back scarp is defined by a north-east dipping J1 (~074/59) surface that is mapped out at 550 m.a.s.l.

Kinematic analysis indicates that planar sliding, wedge sliding and toppling are feasible. However, because the joint sets are steeply dipping these failure mechanisms can only occur for small rock volumes and are limited to steep slope sections only. Large scale rock slope deformation can only be justified by assuming deformation along a combination of several anisotropies. This assumption is based on the presence of the ~50-65 degrees NE dipping J1 and the up to 19 degrees NNE dipping foliation, making bi-planar sliding a feasible mechanism in case of a massive failure of the entire slope instability. Numerical modelling using Phase² support assumption of bi-planar failure and indicate that significant rock damage by retrogressive failure mechanism is most likely for a stepped development of a basal sliding surface. The modeling results indicate that this sliding surface may daylight at a depth of ~100 m in the lake. By sensitivity tests for groundwater and different joint- and rock mass properties it is assumed that the instability is, besides the main structures, controlled principally by topography and rock strength conditions.

SAMMENDRAG

Det ustabile fjellpartiet ved Håkåneset er lokalisert på vestsiden av Tinnsjø (191 moh.) i Telemark i Sør-Norge. Innsjøen strekker seg 32 km i SSØ-NNV retning. Ustabiliteten starter på 550 moh. og går ned til omtrent 300m dybde i Tinnsjø, og tilsvarer 0,54 km² under vann og 0,50 km² på land. Bergmassen i området består av en anisotropisk metavulkansk bergart som er sterkt oppsprukket. Fem sprekkeseett er identifisert ved systematisk feltkartlegging, og har blitt bekreftet med strukturell analyse av "terrestrial laser scan" (TLS). Disse er tolket som gravitativt reaktiverte tektoniske strukturer. Den nordlige avgrensingen av ustabiliteten er definert av et bratt sør-øst fallende sprekkeseett (JF3 (~133/77)) som er tolket som en retning av et konjugert "strike-slip" forkastningssystem (JF3, JF2(~358/65)). Mot sør er det anslått å være en gradvis overgang til stabilt fjell. I bakkant er ustabiliteten avgrenset av en bakvegg med samme orientering som sprekkeseettet J1 (~074/59), og reiser seg fra ca. 550 m.o.h..

Kinematisk analyse av diskontinuitetene antyder at planær utgliding, kileformet utgliding og blokktoppling er mulig. På grunn av at det bratte fallet på samtlige sprekkeseett er disse bruddmekanismene mulig kun for små volum og kan kun forekomme i de bratteste delene av skråningen. For å forklare en massive utglidning av hele fjellpartiet må det antas at deformasjonen skjer langs en kombinasjon av flere anisotropier. I dette tilfellet er J1 som faller ~50-65 grader i NØ retning og det opp til 19 grader bratte NNØ fallende foliasjonen to sprekkeseett som gjør bi-planar utgliding av et stort volum av fjell til en mulig bruddmekanisme. Numerisk modeliering i Phase² støtter antakelsen om bi-planar utglidning og indikerer at utviklingen av et nedre bruddplan vil involvere betydelig ødeleggelser av intakt berg ved en retrogressiv bruddmekanisme. Resultatet fra modeleringen antyder at en sannsynlig lokalisering av et bruddplanet vil være på et nivå på ca. 100 m dybde i Tinnsjø. Sensitivitetstest av grunnvann og ulike sprekkeseett og bergmassestyrkeegenskaper antyder at stabiliteten av fjellsiden er kontrollert av diskontinuitetene, topografien og bergmassestyrkeparametre.

PREFACE AND ACKNOWLEDGEMENT

This thesis is the final work of my master degree at the Department of Geology and Mineral Resource Engineering at the Norwegian University of Science and Technology (NTNU), Trondheim. The master thesis is written in collaboration with the Norwegian Geological Survey (NGU). Reginald Hermanns (head of the landslide department at NGU) and Bjørn Nilsen (professor at the Department of Geology and Mineral Resource Engineering, NTNU) have been my supervisors.

I would like to thank Bjørn Nilsen and Reginald Hermanns for guiding me through the work with this master thesis. Thank you for always being so friendly set time for a meeting, to answer my questions and for all interesting discussions about geology - I have really learned a lot!

I am also very grateful for the help I have got from Gro Sandøy and Thierry Oppikofer at NGU and Nghia Quoc Trinh at SINTEF when applying the different software techniques.

Finally, I would like to speak to my classmates at NTNU. Thank you for early mornings and late night at "Lesesalen", ice cream in the sun, dancing in T-Town, good memories from field excursions and the years we have had together in Trondheim. You rock!

Trondheim, 10.06.2014

Inger Lise Sollie

TABLE OF CONTENTS

<i>Abstract</i>	<i>III</i>
<i>Sammendrag</i>	<i>V</i>
<i>Preface and acknowledgement</i>	<i>VII</i>
<i>Table of Contents</i>	<i>IX</i>
1 Introduction	1
1.1 Systematic mapping approach of large unstable rock slopes in Norway	1
1.2 Background	3
1.3 Aim and restrictions of the study	3
1.4 Available data and site specific literature	6
1.5 Previous work	7
1.5.1 Gvålviknatten rock fall monitoring project, Norwegian Public Roads Administration (Statens Vegvesen).....	7
1.5.2 Periodic monitoring with terrestrial laser scan (TLS), NGU.....	7
1.5.3 dGNSS displacement measurements (NGU, UiO).....	8
1.5.4 Student project assignment: Geological investigation of Håkåneset.....	8
2 Site information: Regional and geological settings	9
2.1 Location and topography	9
2.2 Climate and hydrogeological conditions	11
2.3 Geology	14
2.4 Historical events	15
3 General background about large natural rock slope instabilities	17
3.1 Development and definition of rockslide	17
3.2 Causes and controlling factors of rock slope instability	19
3.3 A case study of a subaerial-subaquatic rockslide: The Hochmais–Atemkopf rockslide system, Austria	19
4 Methods used of stability assessment of the Håkåneset rockslide	21
4.1 Digital elevation model (DEM) analysis	21

4.2	Terrestrial Laser scan (TLS) analyses	21
4.2.1	Structural analysis in Coltop-3D	22
4.2.2	Displacement analysis in Polyworks	24
4.3	Stability analysis.....	25
4.3.1	Numerical modeling with Finite Element Method (FEM) of the Håkåneset rock slide	27
5	<i>Results and findings from geological investigation of the Håkåneset rockslide</i> <i>(Includes results obtained in the project assignment).....</i>	31
5.1	Rock mass characterization	31
5.1.1	Field observations	31
5.1.2	Thin section analysis	32
5.2	Rock mass and discontinuity parameters	38
5.2.1	Justification of assumed homogeneous material type	38
5.2.2	Rock mass properties	38
5.2.3	Joint sets and structural domains	41
5.2.4	Discontinuity strength parameters	44
5.3	Major geomorphological features.....	48
5.4	Preliminary findings	50
5.4.1	Lateral limits of the rockslide.....	50
5.4.2	Results of kinematic feasibility test.....	50
6	<i>The FEM model used for the the Håkåneset rockslide</i>	53
6.1	Model geometry set up.....	53
6.2	Analysis set up	59
6.3	Input parameters for the Håkåneset rock mass	61
6.3.1	Material model and strength criterion of jointed rock mass	62
6.3.2	Material parameters.....	65
6.3.3	Discontinuity parameters.....	70
6.3.4	Stresses.....	79
6.3.5	Hydraulic material properties	81
6.4	Parameter study	82
6.4.1	Model and analyses overview	82
7	<i>Results.....</i>	84
7.1	Results from structural analysis of TLS-data in Coltop.....	84
7.1.1	Results from discontinuity mapping in COLTOP	84

7.1.2	Comparing the results from structural analysis of LiDAR-data with the structural analysis results based on field measurements	88
7.1.3	Conclusion	90
7.2	Results from deformation analysis of TLS-data in Polyworks	92
7.3	Results of stability analysis with numerical modeling in Phase2.....	95
7.3.1	Groundwater seepage analysis	95
7.3.2	Effect of submerged-subaquatic instability	99
7.3.3	Shear strength reduction (SSR) analysis	100
8	<i>Discussion</i>.....	118
8.1	Geological investigation of the Håkåneset rockslide.....	118
8.1.1	Structural analysis of field and TLS-data	118
8.1.1	Recorded slope deformation activity.....	120
8.1.2	Findings from SSR-analysis.....	121
8.2	Influence of Lake Tinnsjø on the stability of the Håkåneset rockslide	127
8.3	Volume estimation of the deforming mass in the Håkåneset rockslide.....	129
8.4	Uncertainties in the slope stability assessment of Håkåneset rockslide	132
8.5	Recommendations for further investigations	135
9	<i>Conclusion of the study</i>.....	137
10	<i>References</i>.....	139
	<i>Appendix</i>	A
	A1: Map: Structural orientations, lateral limits, locations (Project assignment)	A
	A2: dGNSS measurements (2012,2013), NGU, UiO.....	B
	A3: GSI estimate of the Håkåneset rock mass.....	C
	A4: Stereographic pole plots for structural domains.....	D
	A5: Normal stress calculation to potential failure surface	E
	A6: Rock mass strength conversion in RocLab.....	F
	A7: Calculation of joint stiffness.....	G
	A8: Phase2 contour plots.....	C
	A9: Geometry for volume calculations.....	F

1 INTRODUCTION

1.1 Systematic mapping approach of large unstable rock slopes in Norway

The Geological Survey of Norway (NGU) carries out the systematic geologic mapping of potentially unstable rock slopes in the Norway, while the Norwegian Water Resources and Energy Directorate (Norges vassdrags- og energidirektorat, NVE) is the finically responsible for this work (Hermanns et al., 2014). The systematic mapping has been carried out since 2005, were three of the 17 counties of Norway have been prioritized. By now, more than 300 unstable or possible unstable slopes have been found in Troms, Møre og Romsdal and Sogn og Fjordane (Hermanns et al., 2013). Due to this high number of instabilities, a hazard and risk classification system has been considered necessary. The established classification system gives guidelines for a systematic mapping that focuses on the geological data that is considered as relevant in order to effectively assess qualitatively the likelihood of failure of unstable rock slopes. Consequently, a hazard and risk classification system is fundamental in order to establish a database that allow to compare hazard and risk of unstable rock slopes from all over the country (Bunkholt et al., 2013). Such a database is required in order to prioritize time and resources for further investigation and follow-up activities on the most critical unstable slopes.

The Håkåneset rockslide is the first rockslide in Norway where detailed mapping show that the instability has a combination of a subaerial and a subaqueous component. It is one of 56 sites where periodical displacement measurements are carried out every year or in fixed yearly intervals by NGU. The interest for periodically measure displacement on this specific slope is based on the observations of geological features that indicate significant post-glacial deformation in the rock slope. Due to signs of deformation the Håkåneset rock slope is considered as a site which might have the potential to fail catastrophically in the future. By definition a catastrophic failure refers to a fast event with substantial fragmentation of the involved rock mass during the run and that impacts an area larger than that of the depositional angle of rock falls (Hermanns and Longva, 2012). Consequently, a catastrophic rock slope failure has the potential to cause severe material damage and loss of lives.

The hazard analysis provided by NGU (Hermanns et al., 2013) is based on two main steps: First a structural site investigation is undertaken in order to map out morphological expressions of deformation such as development of a back-scarp, lateral boundaries and basal sliding surface, and collect a statistically significant data set of orientation measurements of discontinuities in the assumed unstable rock mass. Further, a kinematic analysis of the structural data is performed, in order to investigate the feasibility for sliding and toppling failure based on slope orientation, persistence of main structures and morphologic expressions of the sliding surface. The geological investigation of the Håkåneset rockslide was undertaken by the candidate in a project assignment in the autumn semester 2013. The results from that work indicate that several failure mechanisms are kinematically feasible.

The second step in the hazard analysis involves analysis of slope activity primarily based on slide velocity, change of deformation rates, observation of rockfall activity, and historic or prehistoric events. These are factors that will be investigated in this master thesis by analysis of data obtained by terrestrial laser scanning (TLS) from the Håkåneset rock slope. In addition, the master thesis includes a structural analysis of TLS data where the aim is to confirm the structural model obtained by field measurements.

In order to improve the kinematic model of the Håkåneset rockslide a stability analysis by numerical modeling of the instability has been performed. With numerical modeling important factors such as persistence of main discontinuities, geotechnical properties of the rock mass, persistent morphological features and the effect of a submerged toe have been included in the analysis. All results from the undertaken work serve as a basis for the discussion of a stability model of the subaerial-subaqueous Håkåneset rockslide.

Chapter 2 presents regional and geological settings for the study area. In Chapter 3 some general aspects about large rock slope instability are defined. Next, Chapter 4 gives background information about the methods used in this study. Chapter 5 is important as it presents the most important results and interpretations from the geological investigation that are essential for the further stability analysis undertaken in this master thesis. A numerical modeling with the finite element method (FEM) is a major part of this thesis. Justification of the applied FEM model and the obtained results are presented in Chapter 6 and Chapter 7, respectively. Chapter 7 also includes result from structural analysis and deformation measurements undertaken with TLS data of the study area. Interpretations and discussion of all results obtained with the applied stability assessment techniques can be read in Chapter 8.

Experiences from the geological investigation are discussed to justify interesting results. A brief volume estimate for the deforming rock mass is calculated and suggestions for further work are given. Chapter 10 summarizes in short what is considered as the most important experiences from the undertaken study of the Håkåneset rockslide.

1.2 Background

Mapping large unstable rock slopes is an important work for the society as it helps to detect rock slopes that might fail catastrophically in future. Catastrophic rock slope failures have been experienced several times in the steep topography and high relief landscape in Norway, causing loss of lives and property (Blikra et al., 2006; Hermanns et al., 2012a). Such events will also occur in the future. It is important to remember that in most cases the rock slope failures are not the direct causes for the loss. Often the negative consequences to society are due to resulting displacement waves which run up along the shoreline, after being generated by the impact of the rockslide body into either a fjord or lake (Harbitz et al., 1993). Therefore, unstable rock slopes in Norway present a higher threat than in other mountain environments in the world because settlement and communities in Norway are concentrated along the coast line of the fjords and mountain lakes (Hermanns et al., 2012a).

The Håkåneset rockslide is located directly along the shore of the lake Tinnsjø in Telemark in southern Norway, and the instability has both a subaerial and subaqueous component. Thus, a rapid failure of this rock slope has the potential to cause a displacement wave. A potential displacement wave in Tinnsjø can reach the settlements in the multiple communities located around the lake and cause loss of life and property there. Therefore a hazard and risk classification of the Håkåneset rockslide site is considered as necessary.

1.3 Aim and restrictions of the study

The aim of this master thesis is to perform a stability assessment including numerical modeling of the unstable rock slope at Håkåneset, in order to provide information that will be used to discuss different failure scenarios of this unstable slope. The results from this master thesis provide information that will be used by the Norwegian Geological Survey (NGU) to

improve the monitoring network and to contribute to the hazard and risk classification of the Håkåneset rockslide. The exact classification will not be carried out in this master thesis.

A kinematic model and a simple preliminary stability model of the Håkåneset rockslide exists as an introductory project assignment conducted by the candidate in the autumn semester 2013. However, a more comprehensive stability analysis, taking into account important effects like scaling due to non-persistent discontinuities, rock mass strength in relation to failure of rock bridges and shearing of joint irregularities and the effect of a submerged toe, is required before the instability of the Håkåneset rockslide can be assessed satisfactorily.

This master thesis particularly focuses on:

1. Reducing the uncertainty of the existing preliminary structural model of the Håkåneset rockslide by supplementary structural analysis of LiDAR (Light Detection And Ranging) -data (aerial laser scans (ALS) and terrestrial laser scans (TLS)) in COLTOP 3D.
2. Reduce the uncertainties of the kinematic model discussed in the project assignment and discuss a stability model of the Håkåneset rockslide, by including joint surface conditions and rock mass properties in the analysis. This is obtained by defining a structural profile along the slope selected that area interpreted to be most critical regarding the stability of the slope, which are used for:
 - Calculation of stress distribution and Factor of Safety in various parts of the rock slope by numerical modelling techniques in Phase2 (Rocscience), in order to detect the most likely failure surfaces.
 - Including the effect of the water within the lower part of the slope in the stability analysis.
 - Measuring deformation of the rock slope by the use of land based TLS in PolyWorks.
 - Combining the structural profile of the rock slope and deformation measurements for volume estimations.

Adjustment of the thesis description

Some adjustments are made on the original thesis description in consultation with the main supervisor Bjørn Nilsen. The adjustments are:

1. Only one topographic profile is used for the numerical model. This was decided because it was evaluated to be important to focus the analyses to what is considered as the most critical area.
2. Limit equilibrium modelling has not been used in this study. A numerical model with FEM was suggested by the main supervisor as the best approach of this study due to the pre-known information about the study area.
3. The undertaken deformation measurement did not give sufficient information for carry out a volume calculation. However, volume estimation is performed based on the numerical modeling results and interpretation of a digital elevation model (DEM) of the study area.

1.4 Available data and site specific literature

An overview of data from the Håkåneset rockslide site available for the master thesis is listed in Table 1 below.

Table 1: Available site specific data from the Håkåneset rockslide used in this master thesis.

Available data from the Håkåneset site:	Source
<ul style="list-style-type: none"> Gvålviknatten rock fall monitoring reports from 2002/2003 and 2006. 	(Frisvold, 2006, 2007)
<ul style="list-style-type: none"> 1x1m resolution elevation model from Airborn Laser Scanning LiDAR data 	Statens Kartverk
<ul style="list-style-type: none"> Bathymetric data 	NGU, Eilertsen (2013)
<ul style="list-style-type: none"> High resolution TLS data from 2011, 2012 and 2013 	NGU
<ul style="list-style-type: none"> Air photos of the Håkåneset site 	Statens Vegvesen
<ul style="list-style-type: none"> Deformation measurements obtained by Global Navigation Satellite System (GNSS) from 2012 to 2013 	(Eiken, 2013)
<ul style="list-style-type: none"> Project assignment: <i>Håkåneset, Tinnsjø - Geological investigation of potentially rockslide.</i> (summarized in Chapter 5) 	(Sollie, 2013)

1.5 Previous work

1.5.1 GVÅLVIKNATTEN ROCK FALL MONITORING PROJECT, NORWEGIAN PUBLIC ROADS ADMINISTRATION (STATENS VEGVESEN)

Highway 37, Tinnsjøvegen, cuts through the unstable rock slope at Håkåneset, and is a road that regularly experiences rockfall activity. The "Gvålviknatten rockfall monitoring project" was started by the Norwegian Public Roads Administration (Statens Vegvesen, SVV) in 2001, with the aim to establish systematic displacement monitoring of bedrock, blocks and soil by the application of air photos of areas with frequent rock fall activity along the road (Frisvold, 2006, 2007). In addition, GPS control points were installed on selected outcrops for regular displacement measurements. In particular an exposed outcrop of dissected rock, 200 m above the highway, named Gvålviknatten (see Appendix 1), was in focus of the project. Gvålviknatten is located in the central part of the defined limits of the study area. Two GPS points that were installed on the block area of Gvålviknatten indicate displacement of 3.1 ± 0.8 cm horizontally and 0.6 ± 0.2 cm vertically from 2003 to 2006. This correspond to a yearly rate of 10 mm horizontally and 2 mm vertically, which will be within the accuracy interval of GPS measurements (1-2 cm horizontally and 2-3 cm vertically). The project did not detect any critical areas that require continuous monitoring. The Gvålviknatten monitoring project is not in any progress by SVV itself at present time (Langelid, 2013).

1.5.2 PERIODIC MONITORING WITH TERRESTRIAL LASER SCAN (TLS), NGU

During the elaboration of the national hazard mapping plan for Norway, the county geologist of Telemark, Sven Dahlgren, suggested the unstable area in Håkåneset along Tinnsjø as a potential high risk site. The national systematic mapping project by NGU initially focused on the three counties Troms, Møre og Romsdal and Sogn og Fjordane, and therefore the Håkåneset site was included in a "rest Norway"-project. During the first recognition to the Håkåneset site it was decided as necessary to define the lateral limits of the instability with further investigations. TLS has been carried out in 2011, 2012 and 2013. The first year the survey was obtained from the road with a scanner that has an operative range of approximately 600 m. However, since 2012 the scanning has been set up at two different localities in a distance of approximately 2.5 km from the opposite side of Lake Tinnsjø.

1.5.3 DGNSS DISPLACEMENT MEASUREMENTS (NGU, UIO)

Displacement measurements of the Håkåneset rockslide have been undertaken by the Norwegian Geological Survey (NGU) on a yearly basis since 2012 (June 2012 and June 2013). The work is performed in cooperation with the Department of Geoscience at the University of Oslo (UiO). Measurements are obtained with a Topcon two-frequent GNSS (Global Navigation Satellite System) by registration of the displacement vectors between two rover points within the instability and two fixed points (TIN-1 and TIN-2) along the highway (see Appendix 1). The rover points were installed on what is described as "relative big blocks" (Eiken, 2013). The study area at Håkåneset is heavily vegetated, which make it challenging to obtain measurements of satisfactory quality.

The results from the first year of monitoring are given in Appendix 2. Rover point TIN-1 is located at Gvålviknatten, while rover point TIN-2 is located in the most upslope exposed block area within the study area (see Appendix 1).

By experience, significant values for rockslide displacement monitoring are 1-3 mm for horizontal displacement and 2-6 mm for vertical displacement (Eiken, 2013). Significant displacement is only measured at TIN-2 (Appendix 2), where a horizontal displacement of 9 mm is registered. The direction of this significant displacement is in WSW-direction, i.e. directed into the slope.

1.5.4 STUDENT PROJECT ASSIGNMENT: GEOLOGICAL INVESTIGATION OF HÅKÅNESET

A detailed study of the Håkåneset rockslide was performed as a project assignment conducted by the candidate of this master thesis in the autumn semester 2013. The work included mapping of geomorphology, structural geology and geotechnical parameters, laboratory work for estimation of rock mass strength parameter, kinematic feasibility test and discussion of a simple preliminary stability model of the Håkåneset rockslide. Important observations and results obtained during the project assignment are presented in Chapter 5, and serve as a basis for the further stability analysis performed in this master thesis.

2 SITE INFORMATION: REGIONAL AND GEOLOGICAL SETTINGS

2.1 Location and topography

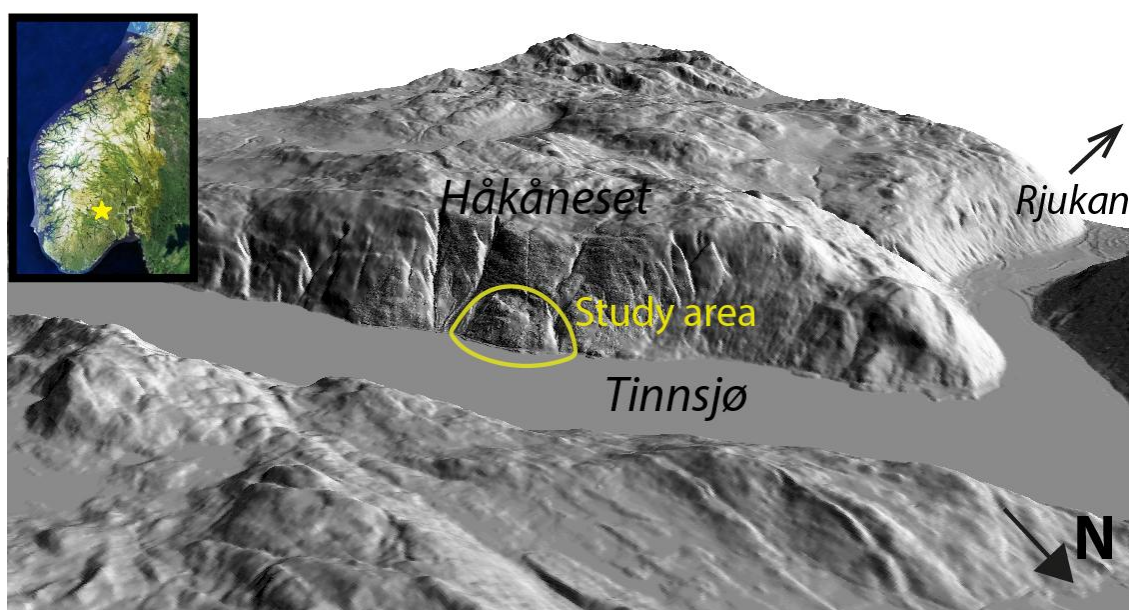


Figure 1: The unstable rock slope in this study is located at the foot of the Håkåneset Mountain, on a ENE facing slope along the shore of the lake Tinnsjø. This shaded relief model is derived from a 10x10 m resolutions DEM model.

The Håkåneset rockslide is located at the north-west shore of Lake Tinnsjø in the county Telemark in southern Norway. Tinnsjø stretches 32 km with a SSE-NNW orientation, 191 meter a.s.l (Dons and Jorde, 1978). The unstable rockslope is a combined subaerial and submerged slope in the foot of the mountain Håkåneset. The mountain goes up to 1249 m.a.s.l. In the project assignment the instability was identified to extend from approximately 300 meters depth in Tinnsjø and up to 550 m.a.s.l on the subaerial mountain slope.

The topography in Telemark is characterized by deeply eroded U-shaped glacial valleys, with an increasing relief from east to west. The main valleys in Telemark were formed in the Quaternary by erosion that cut down into the old paleic surface (Jansen, 1986), which is the pene plane of the original Mesoproterozoic Sveconorwegian orogen of the Fennoscandian Shield (Viola et al., 2009). Glacial processes followed these primary erosional features and

formed deep U-shaped valleys. The deglaciation of the Scandinavian Ice Sheet started in the Old Dryas, about 18,000 years ago. Tinnsjø was at the ice margin approximately 10 600 years ago (Figure 2, Ramberg (2008)).

The orientation of Tinnsjø is parallel to the main glacial movement direction during the last glacial maximum in the area, Figure 3. In glacially eroded mountain setting valley profiles have extra deep submersions downstream meeting points of two or more valleys. In such areas the merging of several valley glaciers increases the erosion effect, causing deep thresholds (Jansen, 1986). Today these thresholds are filled with water and forming lakes such as Lake Tinnsjø, which is located south of five merging valleys. Tinnsjø is measured to be up to 460 m deep (<http://www.nve.no/>).



Figure 2: Map showing the stages of the retreat of the Scandinavian Ice Sheet. Ages for the various position of the ice margin are shown in thousands of calendar years. Tinnsjø (yellow star) was at the ice margin approximately 10 600 years ago (outlined with yellow line). The line marked "12.5-11.6" (blue) denotes the outer limit during the Younger Dryas stadial. (ed. after J. Kleman and A. Strømberg published by Ramberg (2008)).



Figure 3: Extracted section of glacial map of Norway showing the main glacial movement (black arrows) in the area of the study area. The Håkåneset rockslide is located at the west shore of Tinnsjø, outlined in red. (Holtedahl and Andersen, 1960)

2.2 Climate and hydrogeological conditions

There are no detailed sources or maps of the local hydrogeological conditions of the study area. In order to get an impression of the regional climate and hydrogeological conditions in Telemark, regional maps published at seNorge.no have been studied. seNorge.no is an open portal on the Internet that shows daily updated maps of snow, weather and water conditions and climate in Norway.

Ground water

Norway's national catchment database is called REGINE, established and maintained by Norwegian Water Resources and Energy Directorate (NVE). REGINE divides Norway into major and subordinate reference units along the coastline, rivers and catchments, where the subdivision defines the structure in the hydrological system. Maps and information are provided at (atlas.nve.no).



Figure 4: Extraction of hydrogeological map of the study area (atlas.nve.no). No particular conditions are reported within the limits of the study area.

To get an impression of the local hydrogeological conditions of the study area, the hydrogeological map of the Tinn sjø REGINE unit (no. 016.G42) was studied, see Figure 4. The Tinn sjø unit is a part of catchment of Skien ("Skienvassdraget"), and covers an surface area of 23.15 km². On average the seepage is 13.27 mill m³/yr based on measurements in the

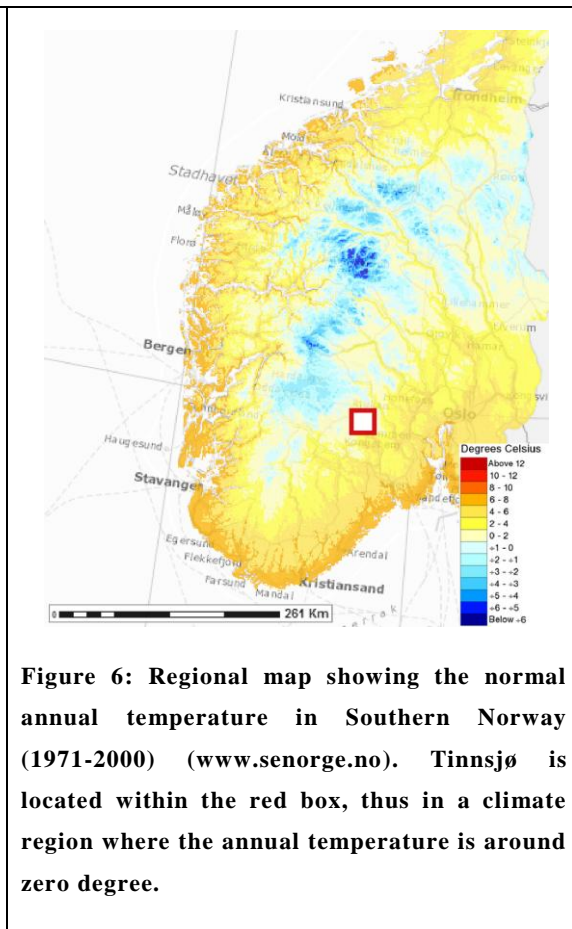
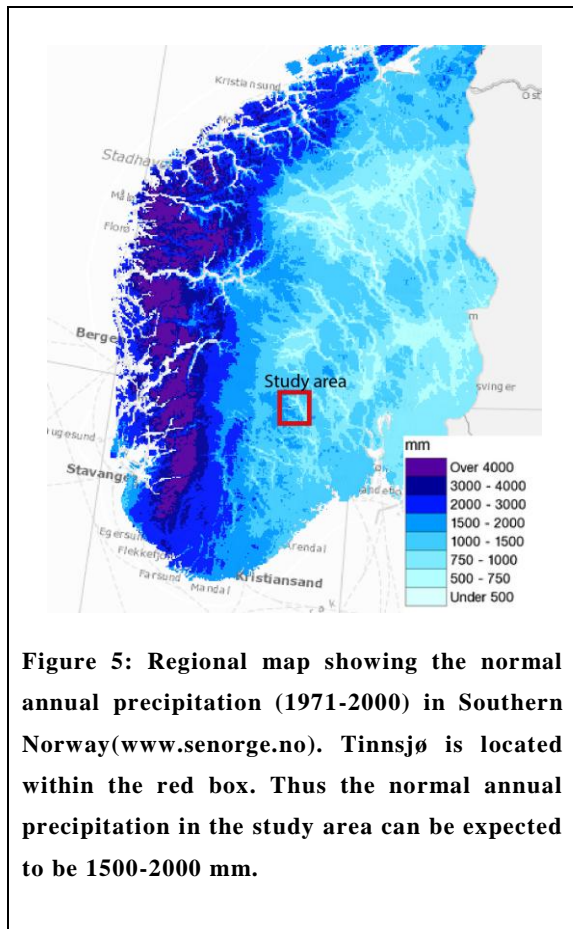
period 1961-1990 (atlas.nve.no). North of the instability of the Håkåneset rockslide is Bjørnebekken, which is the drainage channel of several mountain lakes at the Håkåneset mountain plateau that is located directly above the instability. Also, in the south of the study area there are two topographical depressions that are possible drainage channels.

Precipitation

The normal annual precipitation in the region of the study area is 1500-2000 mm, based on climate registrations in the period 1971-2000, see Figure 5 (www.senorge.no).

Temperature and permafrost

Permafrost thaw is thought to be an important mechanism through which climate controls slope stability (Gruber and Haeberli, 2007). Figure 6 is a regional map showing the normal annual temperature in Southern Norway (1971-2000) extracted from the national climate database at (www.senorge.no). Tinnsjø is located within the red box, thus in a climate region where the annual mean air temperature is around zero degree. Consequently, conditions related to permafrost and slope stability is not important for the study of the Håkåneset rockslide.



Water level in Tinnsjø

The Håkåneset rockslide is directly in contact with Lake Tinnsjø, which implies that the groundwater table in the slope will be sensitive to fluctuations in the lake surface level. Due to the last statutory regulation of the Tinnsjø lake dated to 17.11.2006, maximum fluctuations of $\pm 4\text{m}$ is allowed (Østhus, 2012).

2.3 Geology

The so called "Telemarksuiten" is dominated by rock of Precambrian age (Jansen, 1986). These are metasediments and metavolcanic rocks. The Håkåneset rockslide is located within the lowest geological unit "Rjukangruppen", which is characterized by metarhyolite and metamorphosed tuff, some quartzite and conglomerates/agglomerates (Dons and Jorde, 1978). Figure 7 gives the location of the study area (red box) on a lithological map (geo.ngu.no). The Precambrian bedrock in Telemark is in general dissected by several faults and joint sets that are the result of different deformation phases in the geological history, where characteristic main sets have a SW-NE and NW-SE orientation (Jansen, 1986).

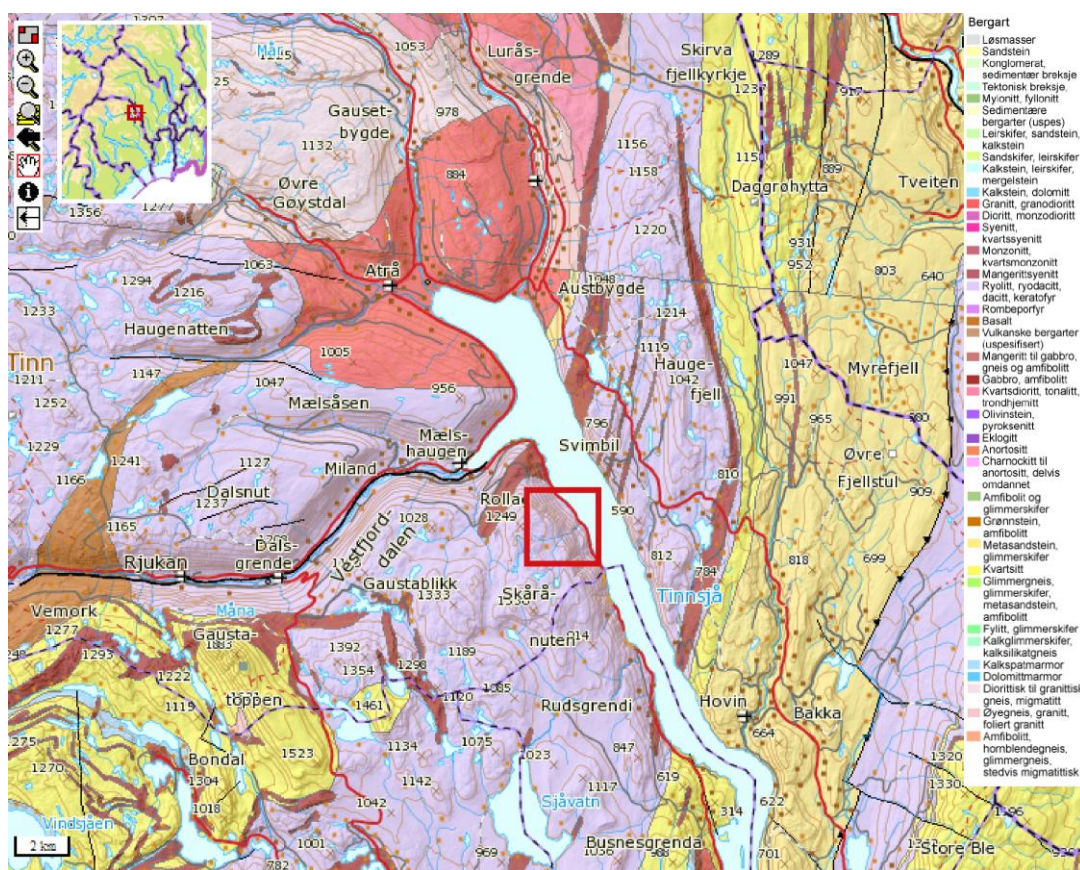


Figure 7: N250 map showing the regional main bedrock types around Tinnssjø. The study area (outlined with red the box) is located within a metarhyolitic/metamorphic tuff unit (geo.ngu.no).

In Figure 7 it is seen that directly on the opposite side of the lake (at the north-east shore) to the study area several bands of amphibolites, metagabbro and amphibolgneiss are mapped (geo.ngu.no). These bands are trending south-west, i.e. in the direction of the study area, and

therefore bedrock of the latter mentioned types can also be expected to be found within the study area of the Håkåneset rockslide even though they are not mapped out.

The bedrock in the study was further identified during the geological investigation undertaken by the candidate. Important observations are presented in Chapter 5.

2.4 Historical events

Historical data about the spatial distribution of gravitational slope processes in Norwegian mountain slopes are vital information when assessing the likelihood of new rock slope failures in an area. Statistically, areas where a large activity is recorded in historical times have a higher likelihood to experience new events in the future (Blikra et al., 2006). The Norwegian Water Resources and Energy Directorate (NVE) provide a historical geohazard database (Skredhendelsesdatabasen), with information about all historically recorded geohazards in Norway. By definition, a geohazard event in this database is an event that has caused damage of life and property (www.nve.no).

A high number of gravitational slope processes events are recorded along the shore of Tinnsjø (Figure 8). The highest concentration of events is along the west shore of the lake, where also the study area is located. 220 events are recorded here (www.nve.no). These are mainly rock fall events. The high frequency of recorded events at the west shore compared to the east shore of the lake can be explained with a combination of two effects related to construction of Tinnsjøvegen: 1) a high number of events due to undercutting of the natural slope, and 2) frequently records of events by road authorities.

37 gravitational slope processes events are registered within the study area of the Håkåneset rockslide, where 35 are rock fall events, see Figure 9. The records within the study area are dated from 1993 - 2013.

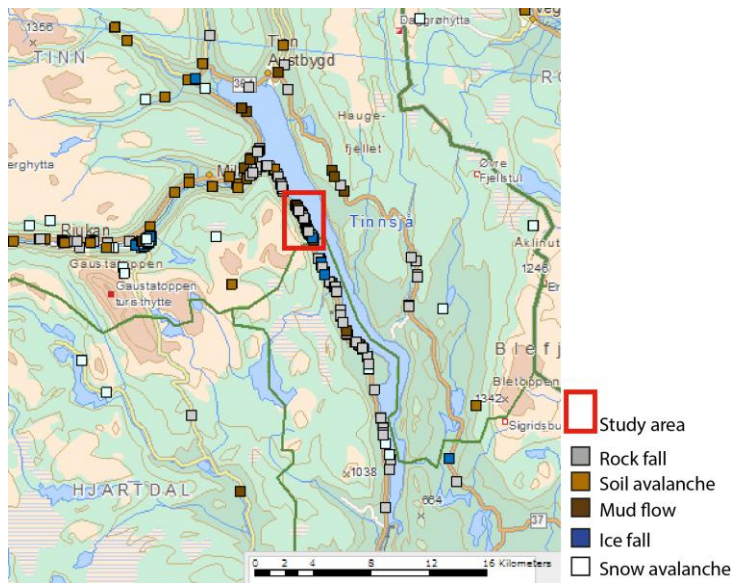


Figure 8: Recorded historical landslide and rock fall activity along Tinn sjø (www.nve.no)

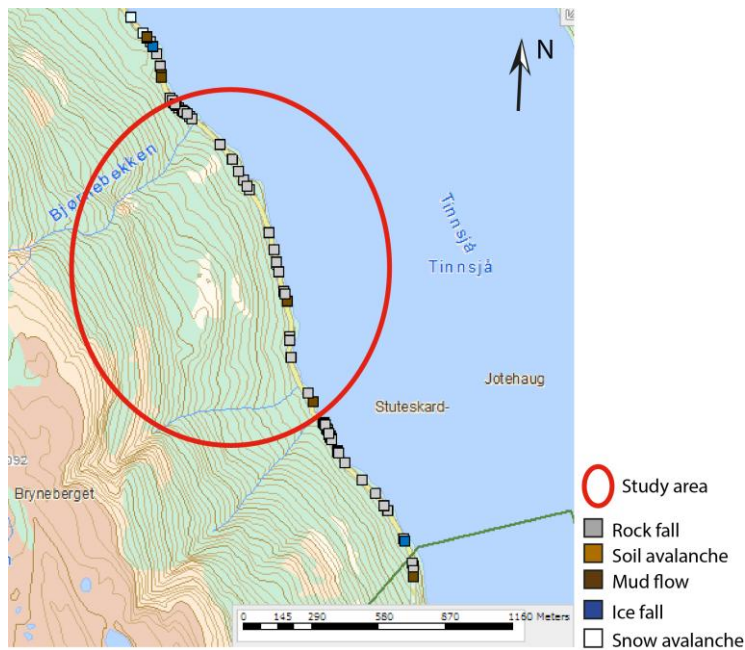


Figure 9: 35 historic rock fall events are recorded within the study area of the Håkåneset rockslide (www.nve.no).

3 GENERAL BACKGROUND ABOUT LARGE NATURAL ROCK SLOPE INSTABILITIES

3.1 Development and definition of rockslide

A rockslide is by definition a landslide that involves movement of rock material (e.g. Hungr et al. (2012)). According to Terzaghi (1950) and Leroueil et al. (1996) in Hungr et al. (2012) is a landslide a mechanical system that develops in time through several stages. These stages of mass movement may be divided in pre-failure deformations, the failure itself and post-failure displacements (Skempton and Hutchinson, 1969). Hungr et al. (2012) purposes the following definition of the term "failure":

"Failure is the single most significant movement episode in the known or anticipated history of a landslide, which usually involves the first formation of a fully-developed rupture surfaces as a displacement or strain discontinuity."

When assessing a possible landslide it is essential to evaluate what stages that dominates in the unstable slope, as it may help to predict future behaviour and explain kinematic trends. In addition, it may help to obtain more reliable estimates of material properties as the degree of strength loss during deformation and failure (e.g. peak, vs. residual strength) can be taken account of. The Håkåneset rockslide is anticipated to be in the pre-failure stage.

Table 2 Classification of slope instabilities involving movement of rock material based on the Varnes classification system of landslide (ed. Hungr et al. (2012))

Type of movement	Classification based on involved failure mechanisms
Fall	Rock fall
Topple	Rock block topple
	Rock flexural topple
Slide	Rock rotational slide
	Rock planar slide
	Rock wedge slide
	Rock compound slide
	Rock irregular slide
Spread	Rock slope spread
Flow	Rock avalanche
Slope deformation	Mountain slope deformation
	Rock slope deformation

A classification system for landslides in rock based on movement type is the modified Varnes classification system of landslides in Hungr et al. (2012). As seen in Table 2 can a rockslide be divided in five subgroups that describes the involved failure mechanisms in the deformation that brings the slope to a critical state of failure.

The description of the rockslide types defined in the Varnes classification system is presented in Table 3

Table 3: Varnes classification of rockslide types based on involved failure mechanisms and the character of the movement.

<p>Rock rotational slide (“rock slump”): Sliding of a mass of weak rock on a cylindrical or ellipsoidal rupture surface which is not structurally-controlled. Little internal deformation. A large main scarp and characteristic back-tilted bench at the head. Usually slow to moderately slow.</p>
<p>Rock planar slide (“block slide”): Sliding of a mass of rock on a planar rupture surface. The surface may be stepped forward. No internal deformation. The slide head may be separating from stable rock along a deep, vertical tension crack. Usually extremely rapid.</p>
<p>Rock wedge slide: Sliding of a mass of rock on a rupture surface formed of two planes with downslope-oriented intersection. No internal deformation. Usually extremely rapid.</p>
<p>Rock compound slide: Sliding of a mass of rock on a rupture surface consisting of several planes, or a surface of uneven curvature, so that motion is kinematically possible only if accompanied by significant internal distortion of the moving mass. Horst-and-graben features at the head and many secondary shear surfaces are typical. Parts of the rupture surface may develop by shearing through the rock structure. Slow or rapid.</p>
<p>Rock irregular slide (“rock collapse”): Sliding of a rock mass on an irregular rupture surface consisting of a number of randomly-oriented joints, separated by segments of intact rock (“rock bridges”). Occurs in strong rocks with non-systematic structure. Failure mechanism is very complex and often difficult to describe. May include elements of toppling. Often very sudden and extremely rapid</p>

3.2 Causes and controlling factors of rock slope instability

According to Stead and Eberhardt (2013) is a rock slope instability a result of high degree of rock damage that varies both spatially and temporally, where characteristic damage distribution is in particular associated with variation in:

- Slope topography
- Failure surface morphology
- Failure surface geometry
- Failure mechanism
- Lithology
- Geological structure

Certain areas of a slope may be predisposed to increased damage either in relation to 1) driving forces, 2) water pressure or 3) due to the existence of pre-existing tectonic damage (Stead and Eberhardt, 2013). Moreover, factors that govern an existing rock slope instability are in particular (Nilsen et al., 2000):

- Rock type boundaries and mechanical properties
- Faults and weakness zones
- Detailed jointing
- Groundwater and climate conditions
- Rock stresses

3.3 A case study of a subaerial-subaquatic rockslide: The Hochmais–Atemkopf rockslide system, Austria

The Hochmais–Atemkopf rockslide system is a mass movement in a more than 1000 m high E-facing slope above the Gepatsch dam reservoir in Northern Tyrol, Austria (Zangerl et al., 2010). The bedrock comprises a foliated, paragneissic rock unit (Schneider-Muntau and Zangerl, 2005). According to Schneider-Muntau and Zangerl (2005) can the deforming slope be divided in four individual sliding masses, Figure 10. Between sliding mass 3 and 4 in Figure 10 there are moraine deposits, resulting from the postglacial sliding of a fractured paragneiss slab. The instability is largely influenced by pre-existing mesoscale discontinuities (i.e. tensile joints and shear fractures) aligned subperpendicular to the foliation.

Displacements in the range of 3 to 4 cm per year is recorded in the lower part of the slope and are mainly directed parallel down slopes, which suggests a translational sliding mechanism.

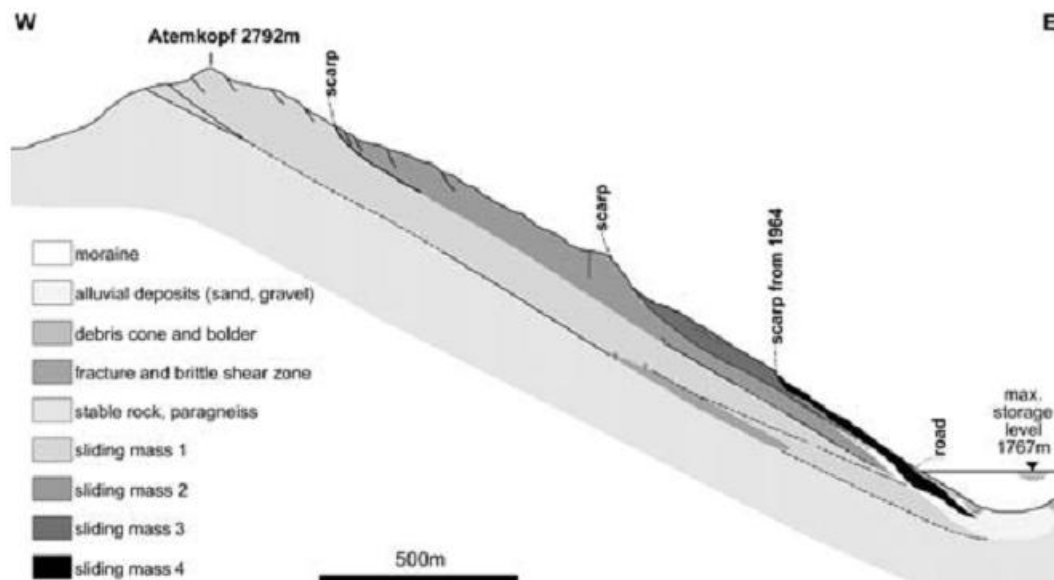


Figure 10: W-E geological cross section of the Hochmais–Atemkopf rockslide system (Schneider-Muntau and Zangerl, 2005).

The lowest sliding plane interacts directly with the water level in the reservoir. According to Zangerl et al. (2010) could recorded temporal slope accelerations not be explained by rainfall and snow melt periods. The annual fluctuations in the reservoir level on the other hand were justified as the main controlling factor on the slope movement. The importance of water level as a driving factor of the slope stability is also supported by a limit equilibrium (LE) analysis undertaken by Schneider-Muntau and Zangerl (2005). Two more observations regarding the effect of the reservoir water level was indicated in this LE study: 1) the destabilizing effect due to the buoyancy forces on the submerged rock mass is more significant than the destabilizing effect due to an increased groundwater table elevation, and 2) the hydrostatic pressure affect the rate of displacement.

4 METHODS USED OF STABILITY ASSESSMENT OF THE HÅKÅNESET ROCKSLIDE

4.1 Digital elevation model (DEM) analysis

Digital elevation model (DEM) is a high resolution three dimensional representation of the terrain and is an efficient tool in slope stability analysis for both visualization and interpretations (Bitelli et al., 2004). DEM are derived by a Light Detection And Ranging (LiDAR) technique that is a remote sensing technique widely used in studies on rock slope instabilities. The basic principle of the LiDAR technique is to providing high-resolution point clouds of the topography, generated by terrestrial laser scans (TLS) or airborne laser scans (ALS). DEM can be combined with high resolution bathymetric data if that is of interest. In particular, morphological structures related to rock slope instabilities (e.g. faults, open cracks forming a back scarp, bulges) can be investigated by DEM analysis.

A DEM model of the study area, processed from a 1 m resolution ALS, was combined with a bathymetric depth model and adapted in the geographical information software ArcMap10.1 (Esri, 2012) for further analyses. The DEM of the study area was used for:

- Interpretation of major geomorphology.
- Defining lateral limits of the instability.
- Extracting a scaled topographic profile of the instability.
- Estimation of surface area of the instability.

In addition was high-resolution DEM of TLS data of the study area used for structural and displacement measurements.

4.2 Terrestrial Laser scan (TLS) analyses

Terrestrial Laser Scanning (TLS) is widely used in slope stability assessment as an efficient tool for structural analysis and for displacement measurements using multi-temporal TLS data (Oppikofer et al., 2012). In this master thesis TLS data from the study area used for structural and displacement analyses. Figure 11 presents an overview of the steps involved in this approach. A brief description of each can be read in e.g. by Oppikofer et al. (2012).

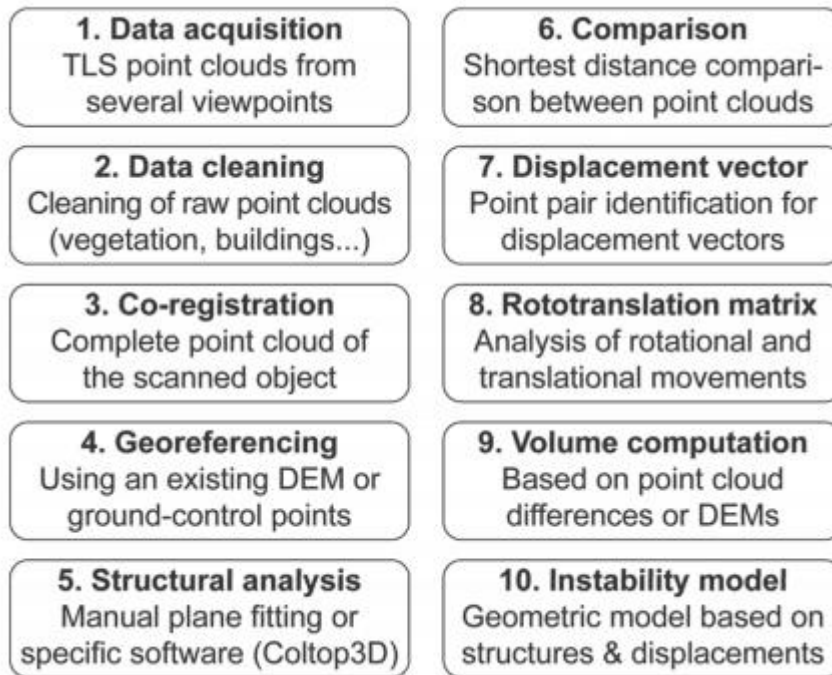


Figure 11: Flowchart for the acquisition, treatment and analysis of TLS data for structural analysis and deformation calculation. Step 1-5 applies for single acquisition and Step 6-10 require multi-temporal point cloud.

The structural analysis approach refers to step 5 in Figure 11. Next, the displacement measurement approach is undertaken in step 1-6.

4.2.1 STRUCTURAL ANALYSIS IN COLTOP-3D

First step in the TLS approach, seen in Figure 11, is pre-processing the files, where the software PifEdit from Terranum (2013) can be used. The pre-processing involves removal of vegetation and other scatter points. Secondly the point cloud is georeferenced by a fitting procedure with a DEM. After georeferencing a structural analysis can be undertaken in the software COLTOP-3D (InnovMetric, 2014). In short, the COLTOP-3D analysis is based on calculating the spatial orientation of each point in the georeferenced point cloud of the TLS data with respect to its neighborhood (Jaboyedoff et al., 2007). The obtained orientation is displayed by coloring the point with a orientation-specific color, illustrated in Figure 12. Consequently, adjacent points with the same color will be visible in the software as surfaces with homogeneous color which can be mapped out by creating polygons. Further, the orientation data collected with the polygons can be exported to the structural orientation software DiPS (Rocscience, 2013) and the mean orientation and variability of each

discontinuity set is determined. A basic assumption in COLTOP-3D is that topographic surfaces is considered to reflect the discontinuity sets that exist in the slope.

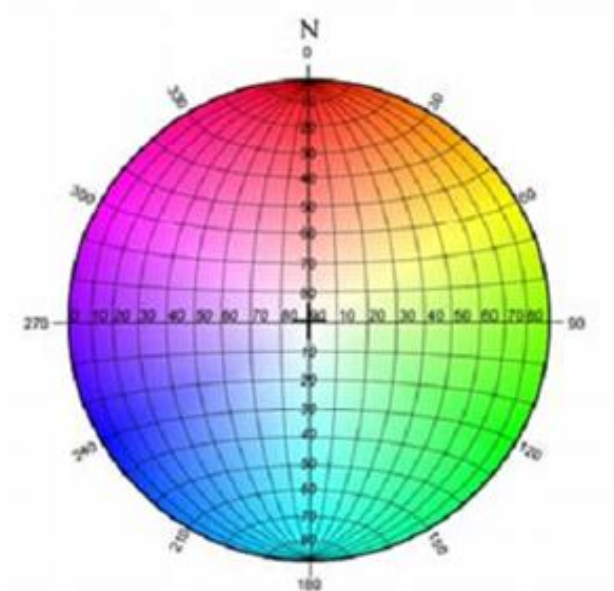


Figure 12: COLTOP-3D color scheme. The scheme is a colored stereonet that is used to represent the spatial orientation of a point in the DEM point cloud. The color represent the aspect and the intensity represents the dip angle (modified from (Hanssen (1998); Jaboyedoff et al. (2007))).

Due to the high accuracy of the technique, geometrical properties such as persistence and roughness can also be obtained from the structural analysis in COLTOP-3D. Hence, structural mapping by TLS data is favorable compared to traditional geological field mapping when the instability is located in areas that are not easy accessible. Because LiDAR scans cover a larger section of the slope it provides better mapping of major persistent structures that controls the large-scale stability of the slope and is an efficient tool for justifying that all major discontinuity sets have been mapped during the field investigation. Moreover, the information obtained from TLS-data are more statistically representative, thus it can be used to reduce the uncertainty of a structural model that are based on field measurements.

As for all analytical tools there are limitations and uncertainties also related to structural analysis with TLS data. Before applying the obtained results for further analyses it is necessary to evaluate the reliability. Therefore, results obtained by structural mapping in TLS

data should whenever possible be justified with results from other investigation techniques. For an overview of publications that deals with several aspects of the application of TLS to rock slope assessment, see Abellán et al. (2014)

4.2.2 DISPLACEMENT ANALYSIS IN POLYWORKS

The software Polyworks (Terranum, 2013) can be applied for a deformation analysis of a rockslide, see e.g. Abellán et al. (2014). The software detects volume changes in the slope by comparison of temporal TLS-data that are scanned with exactly the same orientation. First step in the displacement analysis is to combine temporal TLS point cloud models. In the undertaken study data from 2012 and 2013 were used. This was performed by applying tools in IMAlign in Polyworks. Further the combined model was imported to IMInspect (Polyworks), in which the analysis displacement was carried out. A comprehensive description of the displacement measuring approach can be read in Loftesnes (2010).

In particular, detection of areas with increased rock fall activity is important to detect in a large rock slope stability analysis, because rock fall areas might reflect zones of higher slope deformation activity.

4.3 Stability analysis

The factors that are considered when choosing an analysis method for a rock slope analysis are mainly 1) the complexity of the geological conditions 2) time and costs. Stead et al. (2006) gives recommendations of preferred analysis method based on the complexity of the geological conditions, which are illustrated and described in Figure 13 and briefly described in the further text:

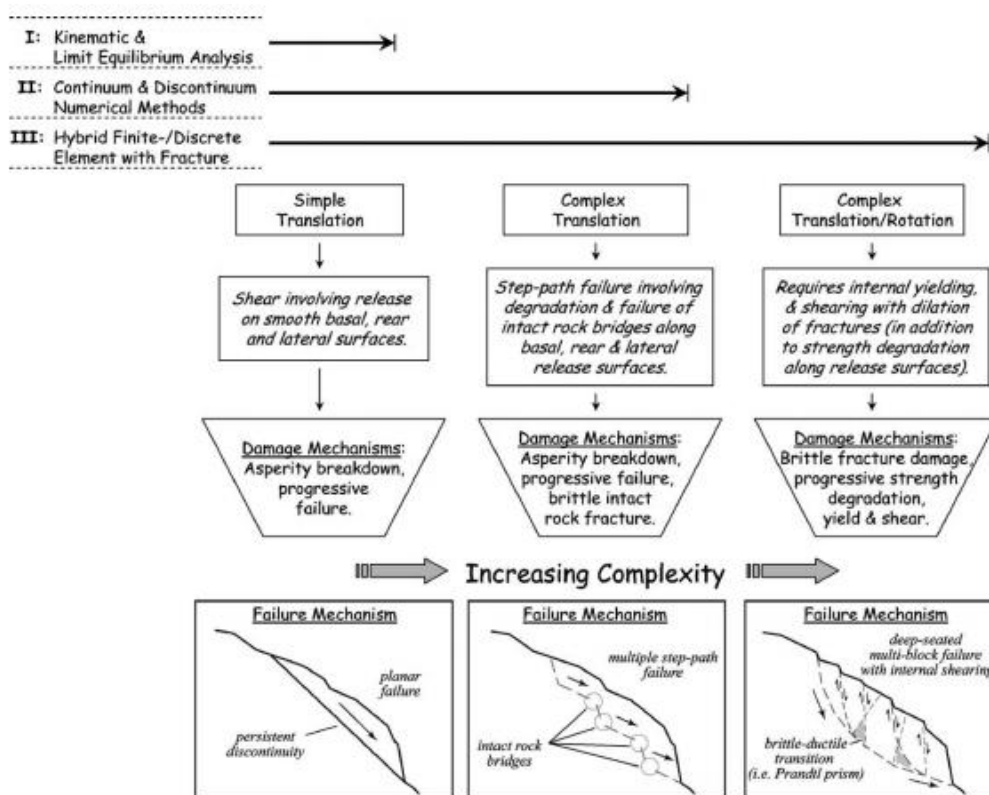


Figure 13: This figure gives recommendation for preferred slope stability analysis method based on the complexity of the assumed dominant failure mechanism forming a sliding surface (Stead et al., 2006)

I. Kinematic and Limit equilibrium analysis: Before applying numerical modeling a slope stability problem is usually identified by a kinematic feasibility test. Kinematic feasibility tests assess the possibilities for different failure mechanisms (planar sliding, wedge sliding and toppling failure) based on the discontinuity orientations with respect to the slope orientation. A kinematic feasibility test was undertaken for the Håkåneset rockslide in the project assignment, and is presented in Chapter 5.4.2.

When a failure mechanism is defined as kinematically feasible the stability can be evaluated with limit equilibrium (LE) analysis to determine a factor of safety (FS). LE is a mathematical method that is time and cost effective and has therefore been an efficient tool in slope stability analysis for years. However, in order to obtain a satisfactory result with LE calculations, the geology usually have to be oversimplified by assuming that the failure is translational and involves release on smooth basal, rear and lateral surfaces where the principle active damage mechanisms are progressive failure and/or asperity breakdown (Stead et al., 2006).

II. Numerical methods: Numerical modeling in slope stability analysis is use for stress and deformation calculations (Stead et al., 2006). The fast development of computers that can handle a large quantity of data has led to the development of numerical models that can perform calculations on complex models. In rock engineering this means that essential complexities like geometry, material anisotropy, non-linear behavior, in situ stresses, the presence of several coupled processes, e.g.: pore pressures and seismic loading, can be more reliable represented compared to when a limit equilibrium model is used for stability analysis. This means that the effect of step-path failure involving internal deformation and fracturing of intact rock can be taken account of if a numerical modeling is applied in a slope stability analysis. Consequently, one of the major advantages with numerical modeling contra limit equilibrium analysis is that the calculations can be performed without pre-defining failure planes. As a result, a more reliable estimate can be obtained, however this is fully dependent on the quality of the input parameters that are used. It is crucial to remember that numerical analysis basically is about investigating the *sensitivity* of the model due to changing input parameters, and should never be interpreted as exact calculations with definite answers (Nilsen et al., 2000). Numerical modeling is only a tool that can provide information that helps to understand the conditions in a unstable rock mass, and the results obtained with the modeling should always be verified with field observations.

Numerical methods are divided into continuous models and discontinuous models, where

1. **Continuous models** consider the material as continuous through the whole model. Consequently, rock mass behavior is essential in these models, and they

are best suited for the analysis of slopes that comprises massive, intact rock, weak rock and soil-like or heavily jointed rock masses.

2. ***Discontinuous models*** dissect the material into blocks that represents discontinuities. Thus, the representation of discontinuity orientation, location and behavior become of fundamental importance. Discontinuous models are favorable to apply in cases where the instability is controlled by discontinuity behavior.

III. Hybride methods involve analyses where continuum–discontinuum codes with fracture simulation capabilities are combined. These codes are expensive and slow, thus mostly used to complex translation/rotational instabilities where failure requires internal yielding, brittle fracturing and shearing (in addition to strength degradation along release surfaces).

4.3.1 NUMERICAL MODELING WITH FINITE ELEMENT METHOD (FEM) OF THE HÅKÅNESET ROCK SLIDE

For the stability assessment of the Håkåneset rockslide it was suggested by the main supervisor Nilsen (2014) to use the software Phase², which is a continuous numerical *Finite Element Method (FEM)* including the application of a *Shear Strength Reduction (SSR)* method. The main reasons for choosing this method are its applicability and easily available license at NTNU. This chapter justifies the application of a FEM as a suitable numerical model for investigating the aims of study of the Håkåneset rockslide.

Finite Element Method (FEM) in general

Finite Element Method (FEM) is a continuous numerical modelling technique that is widely applied to slope stability analysis. (Hammah et al., 2007). Hammah et al. (2007) lists the following as the primarily reasons for its popularity:

1. *Can handle multiple materials in a single model (material heterogeneity)*
2. *Readily accommodate non-linear material responses*
3. *Model complex boundary conditions, and*
4. *Easily available software*

Slope failure in FEM is assumed to occur "naturally" through the zones in which the shear strength of the material is insufficient to resist the shear stresses (Griffiths and Lane, 1999). This assumption is the basis for defining factor of safety (FS) as (Wyllie and Mah, 2004) :

$$FS = \frac{\textit{Shear strength of the material}}{\textit{Minimum shear strength required to prevent failure}} \quad (\text{Eq. 1})$$

By this definition FS can be used to reflect a calculated stability of a slope, where $FS < 1$ indicate unstable slope conditions.

Software: Phase² (Rocscience)

The two-dimensional software Phase² (Rocscience, 2014a) is used in this study. Phase² is an efficiently tool for model progressive failure, where the calculation basically involves determining relative displacements and stress conditions in a slope model. Several analysis techniques in Phase² can be applied to investigate these conditions. This study includes a *Groundwater Seepage analysis* and a *Shear Strength Reduction (SSR) analysis* that provides a FS for the slope model based on defined input parameter values. In addition, maximum shear strain and displacement contour plots are provided (among others) that can be used for visual analysis to get an impression of the stability conditions in the slope. Model set up, analysis settings and input parameters used for the FEM analysis in this study is discussed in Chapter 6.

Groundwater Seepage analysis

A groundwater seepage analysis in Phase² allow for modeling the pore pressure distribution and the location of a groundwater table (pore pressure = 0) in the slope model based on defined hydraulic material parameters (Rocscience, 2014b). The results from the groundwater analysis are automatically added to the stress analysis. In this way the modeling is performed with effective stress values. Since there is no information about the location of the groundwater table in the mountains slope at Håkåneset, this was analysis option was considered efficient to use.

Finite Element Shear Strength Reduction Analysis (FE-SSR)

By the definition of Hammah et al. (2004):

"The Shear Strength Reduction (SSR) technique of a finite element model is a simple slope stability analysis approach that involves a systematic search for a stress reduction factor (SRF) or factor of safety (SF) value that brings a slope to the very limits of failure."

As defined by Eq. 1, the factor of safety is defined as the ratio of the actual shear strength to the minimum shear strength required to prevent failure. Wyllie and Mah (2004) describe a SSR analysis as a process that basically involves a systematic reduction of the shear strength until collapse occurs in the model, and the *critical stress reduction factor* (CSR_F) is the ratio between the rock's actual strength to the reduced shear strength at failure. This systematic reduction of the shear strength is simulated by running series with an increasing *trial factor of safety*, f . If Mohr-Coulomb material is assumed, f determines the reduction of the actual shear strength properties, cohesion (c) and friction angle (φ) for each series (Wyllie and Mah, 2004). The trial factor of safety is increased gradually until the slope fails. At failure, the factor of safety equals the trial factor of safety. At this point the numerical solution does not converge because equilibrium cannot be established for the stress- and displacement distribution calculations when the particular simulated material strength are used as input for the calculations (Griffiths and Lane, 1999).

Parameter study

Due to high uncertainty related to input parameter values for the rock mass, a parameter study has been performed on assumed critical parameters. This involves a systematic change of the chosen input parameters to see how it affects the conditions of CSR_F, shear strain concentrations. An overview of all the analyses that has been performed in this study of the Håkåneset rockslide is presented in Chapter 6.4.

Justification of methods used for Håkåneset study

As defined in the project assignment, does the rock mass at Håkåneset comprise of brittle metavolcanic rock that is heavily dissected by 5 main discontinuity sets of non-persistent joints, see Chapter 5. As recommended by Stead et al. (2006), Figure 13, numerical methods should be applied to model scenarios where the development of a failure plane involves

complex translation, meaning that a high degree of asperity breakdown, progressive failure, fracturing of brittle intact rock are expected. The fact that no failure surface is identified for the Håkåneset rockslide and the non-persistence of the joints are the reason for interpreting the geology to be so complex that numerical modeling is chosen over LE for investigating the stability of this slope. According to Hammah et al. (2007) can the use of FE-SSR analysis on blocky rock mass failure mechanisms (planar, wedge, toppling) with absolutely no a priori assumptions on the modes, shapes or locations of these mechanisms be justified if the material is so evenly jointed that it can be assumed as a continuum. With this basic assumption, FE-SSR is considered as a suitable to used to predict the development of a failure plane in the heavily dissected rock masses in the rockslope at Håkåneset.

The Håkåneset rockslide slides into the Lake Tinnsjø, thus hydrogeological conditions are essential to include in the model in order to get the most realistic model. Simultaneously, adding the hydrogeological parameters also adds new uncertainties to the model. Because no groundwater measurement exists for the study area, the automatic groundwater seepage analysis in Phase² was chosen as a good approach for including pore pressure calculations in the slope model.

5 RESULTS AND FINDINGS FROM GEOLOGICAL INVESTIGATION OF THE HÅKÅNESET ROCKSLIDE

(INCLUDES RESULTS OBTAINED IN THE PROJECT ASSIGNMENT)

This chapter is a summary of the project assignment *Håkåneset, Tinnsjø - Geological investigation of potentially rockslide* performed by the candidate as an introductory study to this master thesis. In addition, results from a supplementary thin section analysis performed during the master thesis are also presented. This chapter gives information about: identified joint sets, important mapped and interpreted geological features, geotechnical parameters for the rock mass and the joint surfaces in the study area and the result of a kinematic feasibility test.

5.1 Rock mass characterization

5.1.1 FIELD OBSERVATIONS

During the field investigation two main rock type units was observed: 1) a dark rock with quartz, calcite and amphibolites crystallizations of various character, interpreted as a metarhyolitic rock, and 2) a light rock type with visible foliation planes, interpreted as a gneissic rock. The lithological boundary between these units could not be mapped out as a distinct boundary. Observations along the road cut gave the impression of dark metarhyolitic rock at the lowest elevations in the road cut and a transitional transformation to the lighter rock type further up. Mostly the assumed gneissic bedrock was observed at the locations up slopes of the road. The most distinct bedrock characteristics are shown in Figure 14.

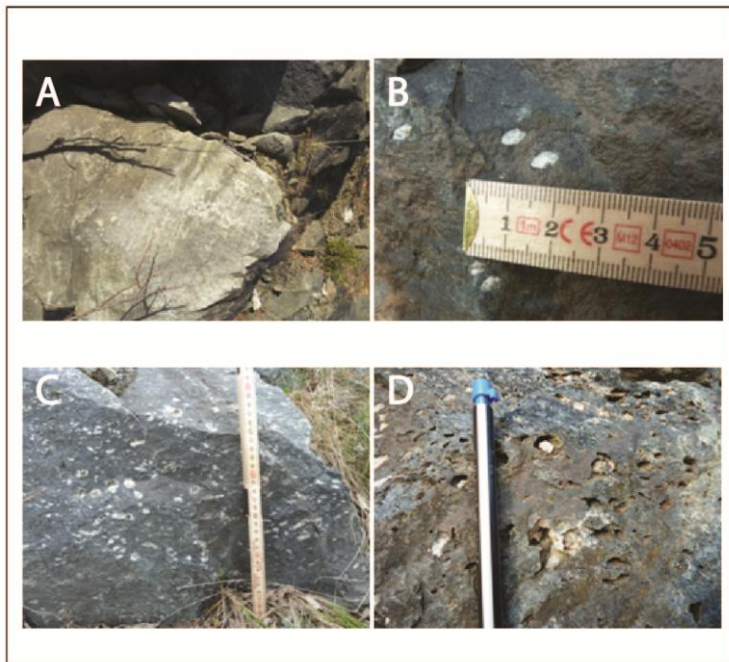


Figure 14: Some rock type characteristic observed in the area during field work. A) Gneissic rock with poorly developed schistose foliation. B) Metavolcanic ryholite with calcite (white) and brown FE-mineralized surface. C) Metarhyolite with quartz and calcite minerals. D) Porous ryholite with re-crystallized calcite and quartz in the pore holes.

5.1.2 THIN SECTION ANALYSIS

Four thin sections were prepared to analyze the texture and mineralogy of the in situ rock. The in situ rock samples were taken in the road cut close to Location 1 and 2 in Appendix 1. Thin section #1 is prepared from a rock sample of the light colored rock unit and thin section #2, #3 and #4 were prepared from the dark colored rock unit explained in Chapter 5.1.1. Thin section #1, #2 and #3 were prepared with orientations in order to investigate the presence and orientation of foliation and possible microfractures. Several photos of the analyzed thin sections prepared in the laboratory at NTNU can be seen in Figure 15, Figure 16 and Figure 17. All photos are taken with the same settings with plain light (ppl) polarisor crossed (xpl) and with fluorescence.

Mineralogy

All thin sections are dominated by a fine grained matrix of feldspar, quartz, mica and epidote. Muscovite is identified in thin section #1 (visible as "disco" colored grains in 1_xpl Figure 15b). In thin section #3 (Figure 16) and #4 (Figure 17) the fine grained matrix has high biotite content (brownish color in 3_ppl (Figure 16a) and 4_ppl (Figure 17a)), whereas in section 1_ppl (Figure 15a) the amount of biotite is significantly lower. Also, the fine grained matrix in all thin sections have mineral grains of oxides (black, non-transparent), calcite (cross-hatched cleavage pattern), feldspar and quartz that are of bigger size than the matrix itself. The major dark colored area in section 1_xpl (Figure 15b) is interpreted as a phenocrystal (Sørensen, 2014).

Texture: deformation and foliation

The texture of the grains is clearly deformed, which can be seen from the rounded shape of the feldspar grains and the asymmetric shape of the oxides in all thin sections. All thin sections also show a foliation due to a preferred orientation of deformed mineral grains, and mica sheets oriented parallel to the deformed grains, see e.g. Figure 16a/b. In #1 (Figure 15) the oriented mica sheets are mainly muscovite, while in #2, #3 (Figure 16) and #4 (Figure 17) there are mainly biotite defining the foliation. The foliation trends NE in #1 and N-S in #3.

Micro fractures

Microfractures are identified in thin section #3 (Figure 16c) and #4a-b (Figure 17 c and f) (yellow color), developed parallel to the foliation. The microfractures are filled with calcite. It can be seen that the presence of coarse grains in the fine grained matrix affect the fracture development by changing its orientation, as can be seen in thin section #4b Figure 17b. In #4a the interaction between the fracture development and the foliation is clear: the microfractures appear more scattered within the biotite layer which illustrates the weakening effect of foliations.

Interpretations

The following interpretations are made based on the thin section analysis of the rock at material from Håkåneset:

- The difference between the light colored and dark colored rock units observed in field is due to variable biotite content. However, since the texture is the same it is considered reasonable that for further stability analysis a homogeneous rock type can be assumed.
- The presence of phenocrystals confirms that the rock mass is of magmatic origin (Sørensen, 2014).
- The rounded and asymmetric shaped feldspar and oxide grains may in addition to the dominance of fine grained matrix be interpreted as an evidence that the rock mass has undergone significant deformation (Sørensen, 2014). This justifies that the rock has undergone shear deformation and metamorphism.
- The rock is clearly foliated due to deformed grains and mica sheets oriented parallel to the deformed grains. The foliation appears with N-NE trend. Hence, significant strength anisotropy in the rock is expected.
- Microfractures development is disturbed by the presence of coarser mineral in the fine grained matrix.
- The microfractures are developed approximately parallel to the foliation.

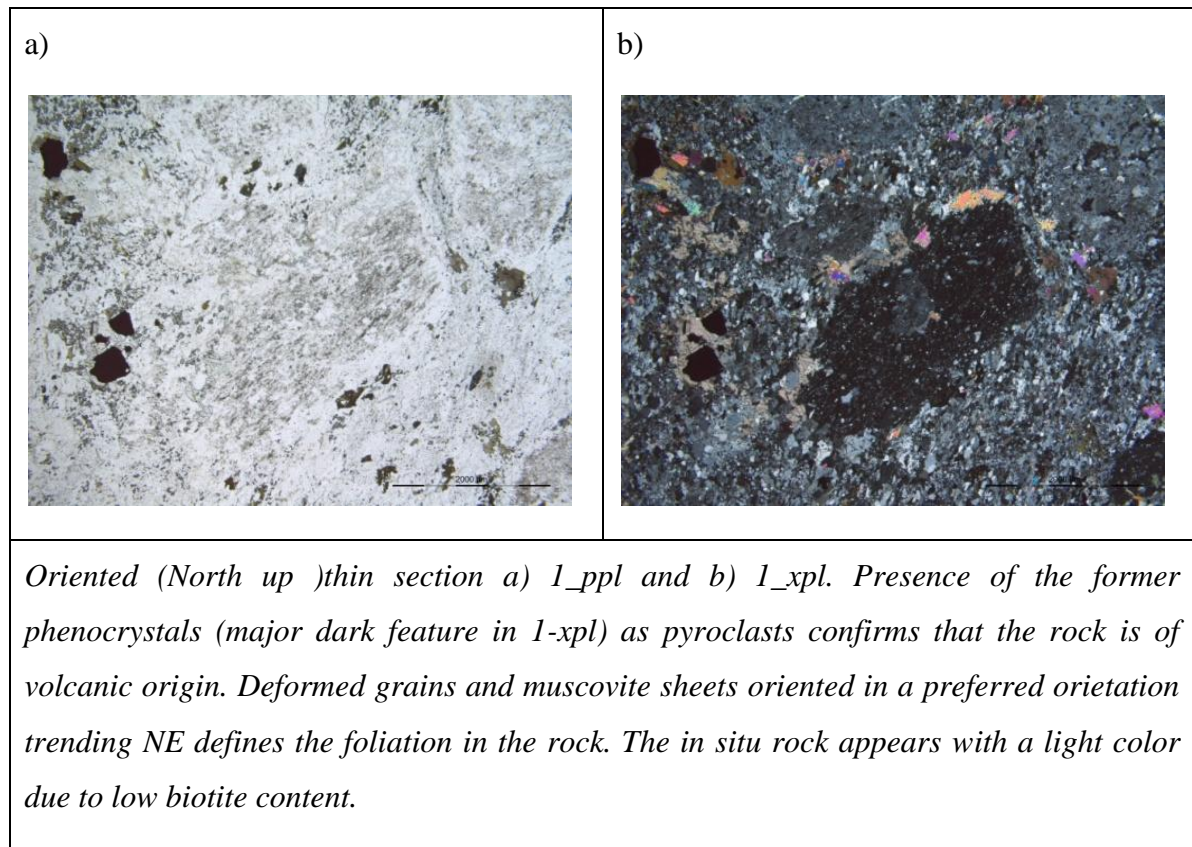


Figure 15: Oriented (North up) thin section #1 of the light colored in situ rock type within the Håkåneset instability.

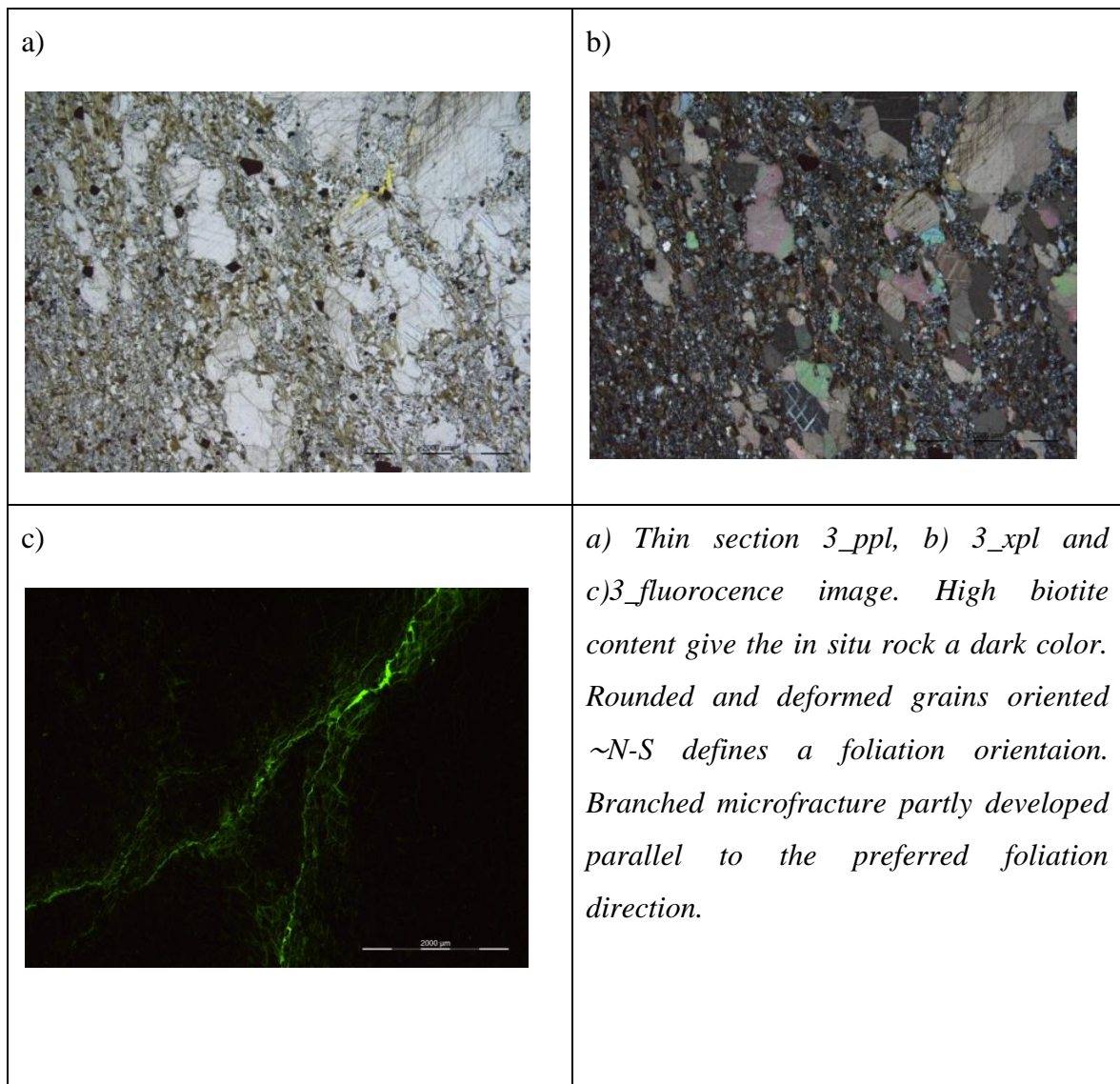


Figure 16: Oriented (North up) thin section #3 prepared from the dark colored situ rock within the Håkåneset instability.

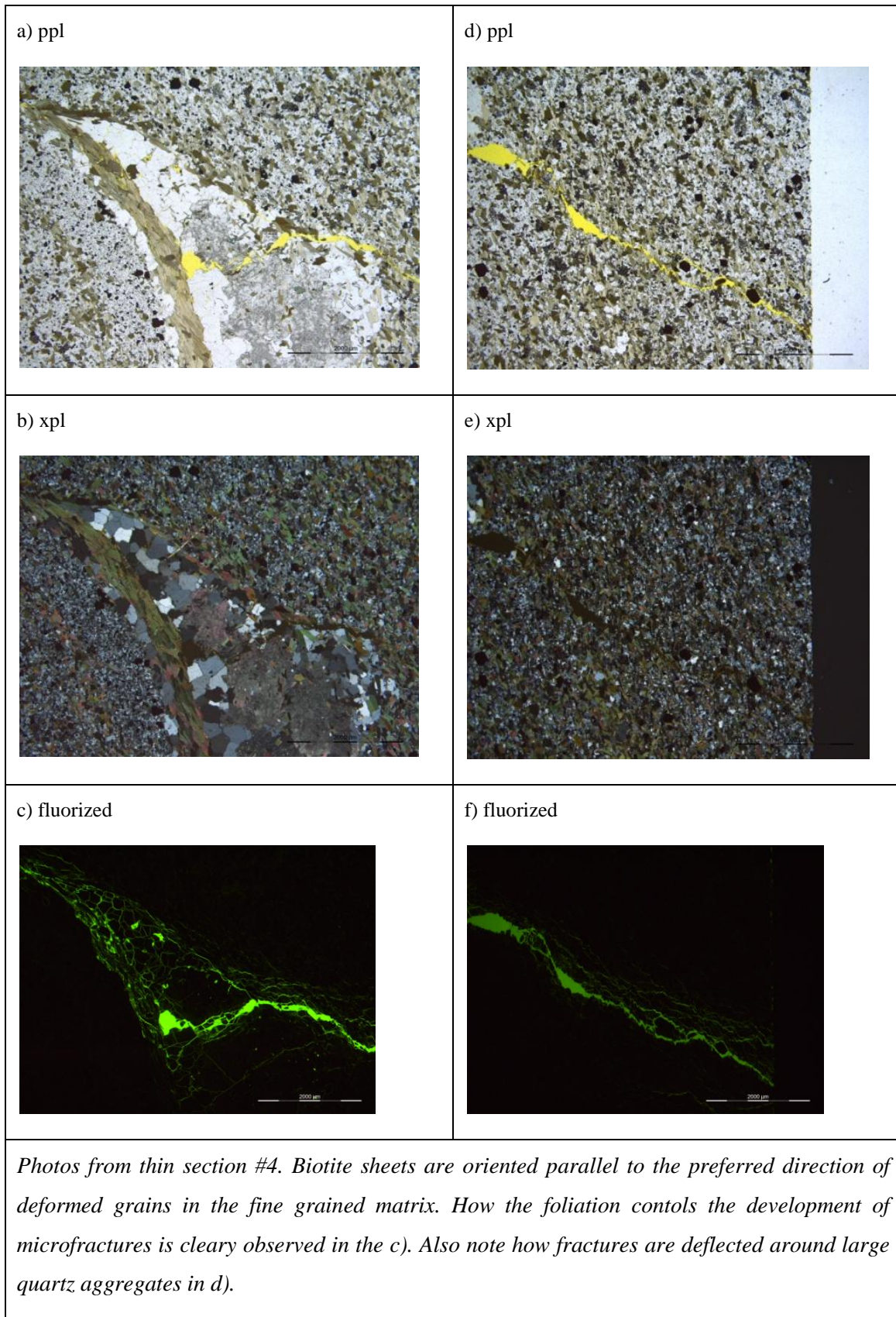


Figure 17: Thin section #4 (not oriented) of dark colored in situ rock sample within the Håkåneset instability.

5.2 Rock mass and discontinuity parameters

5.2.1 JUSTIFICATION OF ASSUMED HOMOGENEOUS MATERIAL TYPE

The rock mass in the unstable rock slope at Håkåneset comprises a metavolcanic rock that appears both as light and dark colored units. There are not observed any distinct lithological boundary between these units. Thin section analysis of in situ rock samples revealed that the rock mass of both units have the same texture. In general both units have high mica content; however in the light colored rock muscovite is dominant, while biotite dominates in the dark colored rock, thus being an explanation to the color difference. The mica sheets are oriented parallel to a preferred direction of deformed grains, giving the rock strong anisotropic character due to foliation. For anisotropic rock material will the strength estimates obtained by uniaxial compressive strength test be highly dependent on the load direction relative to the anisotropy. However, the anisotropy of the in situ rock material from Håkåneset was not taken into account in the laboratory work conducted in this study, and therefore it was evaluated that calculating the mean of all obtained test, independent on rock unit, would be the best approach to obtain a representative estimate for the rock strength. The lack of lithological boundary in field, same texture in all thin sections, and insufficient shear strength parameters to distinguish between the light and dark rock units are all factors that justifies that for a stability model the rock mass in the rock slope at Håkåneset can be considered as anisotropic homogeneous metavolcanic rock.

5.2.2 ROCK MASS PROPERTIES

Geotechnical properties

Deformability parameters (E , ν), unconfined compressive strength (UCS) and basic friction angle (ϕ_b) are necessary input parameters in the numerical modelling approach (Wyllie and Mah, 2004). These parameters were determined by laboratory tests on cores of rock material collected from the Håkåneset site during the project assignment. All tests were performed at the Geological Engineering Laboratory of NTNU/SINTEF, Trondheim, Norway, following the standard of ISRM (2007) and Barton-Bandis standard procedures described in (Grøneng and Nilsen, 2009). The test results are given in Table 4.

Table 4: Geotechnical data (mean values and standard deviation) of rock material taken from the site of Håkåneset rock slide. Blue numbers represent the number of tested specimens.

Rock sample location	Rock type	E [GPa] (#)	ν (#)	γ [kN/m ³]	UCS [MPa] (#)	Failure angle* (#)	Tilt angle [φ _b] (#)
Weakness zone (J1-fault)	Meta-volcanic	45,6 ± 4,6 (6)	0,21 ± 0,013 (6)	30	81,3 ± 22,6 (3)	23 ± 6 (3)	27,7 ± 2,2 (2)
Possible rupture surface (J1 surface)	Meta-volcanic	33,1 ± 3,3 (3)	0,13 ± 0,006 (3)	30	59,5 ± 4,6 (3)	29 ± 1 (1)	27,3 ± 1,7 (1)
Road cut	Meta-volcanic	54,4 ± 4,3 (3)	0,18 ± 0,030 (3)	30	154,3 ± 29,4 (2)	18 ± 3 (2)	28,4 ± 1,2 (1)
Average mean		44,3	0,17	30	98,4	23	27,8

#: number of tested specimens

* Measured on the failed specimens from uniaxial compressive strength test

Reliability of the laboratory estimates

Estimation of rock mass parameter can be challenging and involves several uncertainties regarding both the representativeness of the tested material and the laboratory approach. For the values for the in situ rock from Håkåneset provided in Table 4, the following comments are considered as important:

- The rock samples used for the testing was partly detached and taken from the road cut, which imply that it can be strongly affected by the road construction.
- The rock material is strongly anisotropic due to foliation, thus the loading direction is essential in the compressive strength test. Because the foliation was difficult to recognize on the rock samples, the loading direction relative to the foliation is not

uniform for the tested samples. This will be a significant bias in the obtained strength estimates for the rock material.

- Even though the specimens seemed to have different character (described in the project assignment) the material is assumed homogenous.

Geological strength index (GSI)

The geotechnical rock properties presented in Table 4 are values measured for intact rock conditions. However, the actual rock mass in nature is highly disturbed and dissected by discontinuities, which implies a significant reduction in the strength of the geological unit. The Geological Strength Index (GSI) provides a number which, when combined with the intact rock properties, can be used for estimating the reduction in rock mass strength for different geological conditions (Hoek, 2007). The in situ rock mass at Håkåneset is blocky, where four joint sets are dominant. The joint surfaces conditions are: slightly weathered, Fe-mineralization, planar, undulating rough (see Table 6, Chapter 5.2.2), which is best classified as good "Good" surface conditions, as defined in Hoek (2007) and will indicate a GSI value of the range 60 to 80, see Appendix 3. At some localities the surface conditions were smoother and better described as "Fair", implying a GSI value of 40 to 60.

5.2.3 JOINT SETS AND STRUCTURAL DOMAINS

The rock mass at Håkåneset is heavily dissected by discontinuities, as can be seen on the air photo in Figure 18. These were all interpreted as inherited tectonic structures that are gravitationally reactivated. 1100 orientation measurements of distinct discontinuities and foliation in the study area were mapped during field work. The entire unstable slope was covered. The measurements were plotted in stereographic projection (*lower hemisphere, equal angle, Fisher distribution*), using the structural data analyzing program *DiPS 6.0 (Rocscience)*, and four joint sets were very clear. The orientations (dip direction/dip) of these

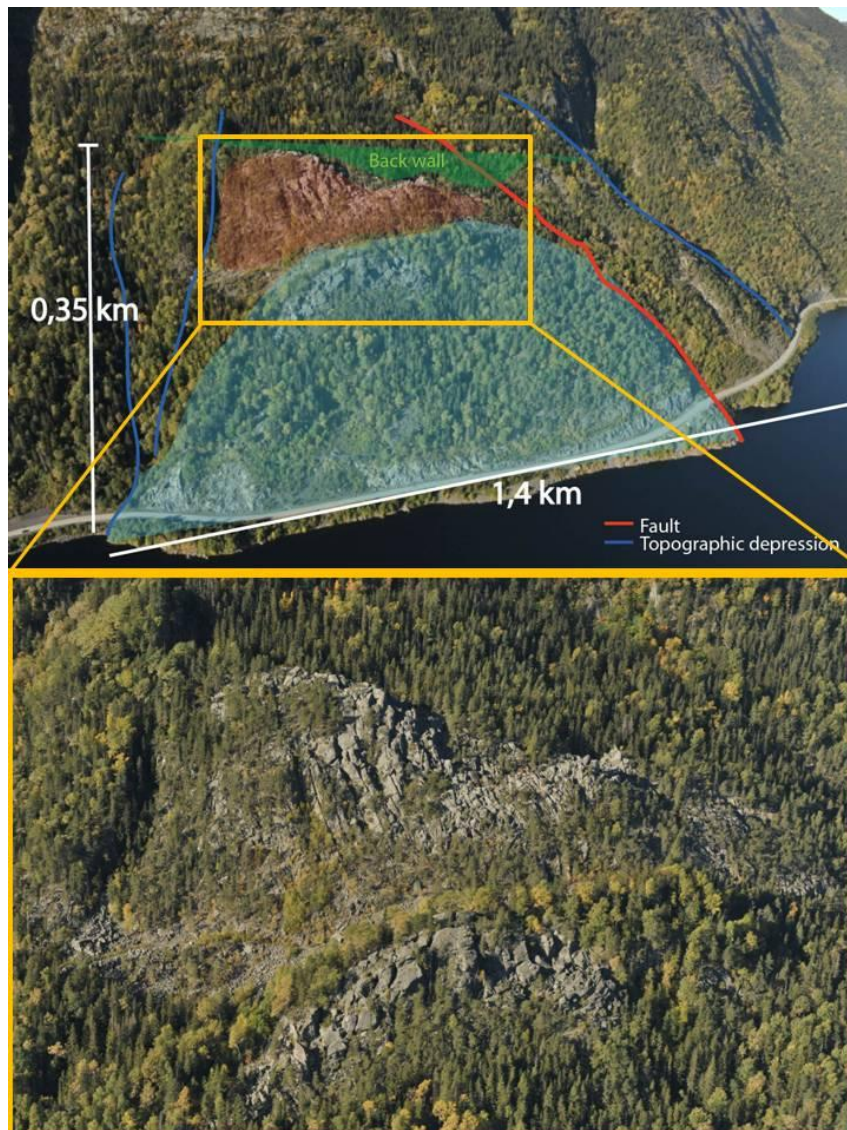


Figure 18: The rock mass at Håkåneset is heavily dissected by multiple joint sets that were mapped out during the project assignment. Structural domains (blue and red shaded area) and geological structures and geomorphology is described in Chapter 5.3. Photo: SVV, Audun Langelid

were determined by cluster analysis, which involve defining windows around the pole clusters. The contour range was set to 2-10 for this analysis. The joint sets are labeled as J1, JF2, JF3 and J4 (corresponding to J1, J2, J3 and J4 in the project assignment). Additionally, a less distinct and more variable oriented foliation and coincident foliation planes were recognized and referred to as schistose foliation, SF. Further, the measurements were organized and plotted as stereonet for 20 localities on a base map of the study area (Appendix 1). Even though the measurements are very consistent, a systematic change in the orientation of joint set J1 and J4 was identified. Together with mapped major tectonic features (described in Chapter 5.3), this systematic change was the basis for dividing the study site in three subaerial domains, see Figure 19. Dip and dip direction of the joint sets for each domain are given in Table 5, and visualized in Appendix 4. All joint sets are mapped in all domains. However, some joint sets were not statistically significant with the chosen criteria for the cluster analysis (contour range 2-10). In these cases the contour range was increased to 1-10, and the set window was drawn based on this for the particular joint set cluster. Joint set orientations that are determined with an increased contour range are written with grey color and italicized style in Table 5. The joint set characteristics based on the field observations are briefly summarized in Table 6.

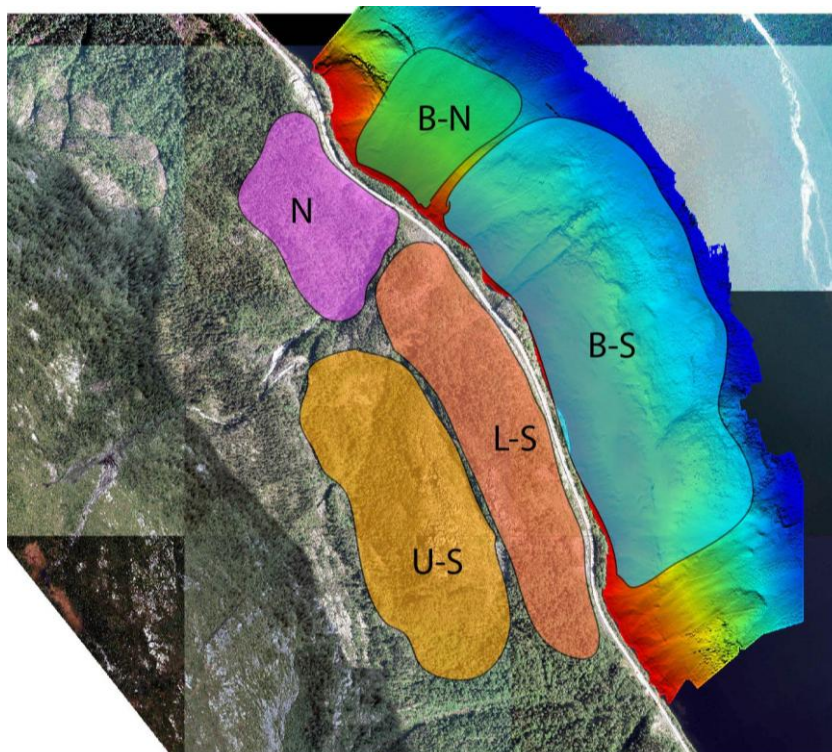


Figure 19: Defined structural domains for the study area: Subaerial domains are called North (N), Upper-South (U-S) and Lower-South (L-S), and are based on a systematic spatial variability in discontinuity orientations. Subaqueous domains are Bathymetric-North (B-N) and Bathymetric-South (B-S) and are divided based on geomorphological features that are visible on bathymetric images.

Table 5: Mean dip and dip direction (Fisher distribution) of identified joint sets given for the whole study area (ALL) and for each defined subdomain (North, Lower-South, Upper-South). Joint set orientations in black are determined with a contour range of 2-10 in DiPS (Rocscience). Grey colored and italicized style represent orientations where the contour range was increased to 1-10 in order make the joint set statistically significant.

Joint set	Discontinuity type	Average all domains (DipDir/Dip)	Domain North (DipDir/Dip)	Domain Lower-South (DipDir/Dip)	Domain Upper-South (DipDir/Dip)
J1	Exfoliation	074°/59° ± 20°	071°/62° ± 16°	076°/51° ± 19°	075°/63° ± 14°
JF2	Fault plane (conjugate)	358°/65° ± 18°	359°/69° ± 18°	355°/51° ± 14°	360°/67° ± 16°
JF3	Fault plane (conjugate)	133°/77° ± 20°	137°/72° ± 14°	138°/79° ± 14°	140°/78° ± 8°
J4	Joint	208°/76° ± 16°	237°/62° ± 13°	213°/76° ± 10°	<i>207°/71° ± 15°</i>
SF	Schistose foliation	237°/19° ± 21°	<i>284°/11° ± 16°</i>	031°/16° ± 14°	<i>277°/15° ± 18°</i>

Table 6: Field descriptions of the identified joint sets at Håkåneset.

Joint set	Discontinuity type	Dip direction	Consistency	Surface condition	Spacing	Persistence	Features
J1	Exfoliation	NE	Steeper in Upper-South domain than Lower-South domain	Slightly weathered, planar to undulated, stepped, rough. Brown weathering surface with thin spots of quartz/feldspar	0,1 - 2,6m	0,2 - 3,4 m ($\pm 0,2$), also 10s of meters	Slickensided lineations (trend/plunge: 044/42) Groove marks (trend/plunge: 081/47)
JF2	Tectonic (conjugate)	N	Consistent	Mostly planar and smooth. Brown Fe-mineralization	0,1-10m	1m to more than 10 m	Well developed mineral lineations formed at least partially by muscovite sheets. Subhorizontal (13/279 (trend/plunge)), thus indication strike slip movement.
JF3	Tectonic (conjugate)	SE	Consistent	Undulating to stepped. Mainly rough. Fe-mineralization. Quarts/feldspar mineralization	0,2-2m	0,2-10m	Fault: ~ 1 km
J4	Joint	SW	Dip direction more north in the North domain compared to the south domain	Smooth to rough, angular or planar. Brown Fe-mineralization	0,2-0,5m	0,1 m to more than 10 meter	
SF	Schistose foliation	variable	Difficult to map	-	-	-	-

5.2.4 DISCONTINUITY STRENGTH PARAMETERS

The shear strength of rock joints are most commonly estimated after Barton-Bandis empirical method. Barton-Bandis parameters are: joint roughness coefficient (JRC), joint compressive strength (JCS) and residual friction angle (φ_r). A standard NTNU methodology for obtaining these parameters are given by Grøneng and Nilsen (2009) and was followed in the work related to this study.

JRC

JRC is an empirical index used for surface roughness characterization, and was determined in field by directly measuring the surface roughness amplitude from a straight stick (1m). The scale effect is corrected for following the procedure presented in Grøneng and Nilsen (2009), and mean values and description for each joint set are given in Table 7.

JCS

JCS is an index that represents the strength of the rock at the discontinuity surface. JCS was estimated by applying Schmidt hammer test on three natural, weathered surfaces, following the procedure in Grøneng and Nilsen (2009). The Schmidt hammer values were converted to representative JCS values that are presented in Table 8 below. According to Grøneng and Nilsen (2009) can JCS be assumed equal to the unconfined compressive strength (UCS, σ_c) of the intact rock if the joints are completely unweathered. In reality natural joint surfaces will always be weathered to some extent, and JCS will be lower than UCS tested on specimens in laboratory. UCS estimate of the intact rock from Håkåneset determined in the laboratory was in the range 60-154MPa (Table 4), whereas mean JCS values ranges from 120-223MPa (Table 8). Due to the fact that JCS values obtained with Schmidt hammer is greater than the UCS values determined in the laboratory on intact rock, the Schmidt hammer results has been considered not reliable. The unrealistic correlation may also be explained with the fact that some specimens was loaded subperpendicular to the foliation, thus a low value is obtained.

It was decided to use the laboratory estimate as input value for further investigations, as this will give the most conservative result.. A widely accepted estimate for JCS on weathered joints based on laboratory rock strength estimates are $1/4 \sigma_c$, recommended by Barton and Choubey (1977). With a mean value for USC of 98MPa for the tested Håkåneset rock mass, 25MPa is assumed as an acceptable input JCS value for the natural joints in the study area.

Basic friction angle (φ_b) and residual friction angle (φ_r)

By the definition in Grøneng and Nilsen (2009) can the basic friction angle (φ_b) be considered as a material constant and refers to smooth, planar surfaces in fresh rock. The residual friction angle (φ_r) refers to the residual condition of natural joint surfaces after shear displacement. Empirical formulas have been developed for determining φ_r from φ_b . In this study φ_b was determined with tilt test in the laboratory, after the recommendations in Grøneng and Nilsen (2009). Four specimens were tested, and the tilt angle was assumed to be a representative value for φ_b , as justified in (Grøneng and Nilsen, 2009). The results of the tilt test are given in Table 4. According to Barton (1973) can φ_r for natural joints be assumed equal the φ_b for sawn surfaces (the tilt angle) of the same rock material, and is usually in the range between 25° and 35°. This assumption is used for the discontinuities in the Håkåneset rock mass, thus $\varphi_r = \varphi_b = 28^\circ$ is assumed as representative value.

Table 7: Estimated JRC for the defined joint sets. Estimated after a standard NTNU methodology presented by Grøneng and Nilsen (2009)

Joint set	JRC	Description	Source
J1	13,7 ± 4,7	planar to undulated, stepped, rough	Field estimate
JF2	4,7 ± 1,5	planar, smooth	Field estimate
JF3	> 20	rough, undulating	Field estimate
J4	9,5 ± 2,1	smooth to rough, angular or planar	Field estimate
SF	5 ± 1	smooth, stepped	Chart value

Table 8: Estimated JCS (USC) for natural discontinuity surfaces at the Håkåneset site obtained with Schmidt hammer as presented in Grøneng and Nilsen (2009). Suggested empirical estimate calculated from UCS obtained in the laboratory

Joint set	Assumed geological feature	Rock type	JCS (MPa)	Source
J1	Back scarp	Granitic	195 ± 60	Field work
J1	Sliding plane	Metarhyolitic	120 ± 32	Field work
JF3	Weakness zone	Metarhyolitic	223 ± 27	Field work
$1/4\sigma_c$	Laboratory specimens	Granitic/metarhyolitic	~25	Empirical formula by Barton and Choubey (1977)

Estimated discontinuity shear strength of J1

Determinations of the shear strength of discontinuities, that are assumed to be important sliding surfaces, are essential in a slope stability analysis (Grøneng and Nilsen, 2009). Grøneng and Nilsen (2009) assumes that the shear strength of a discontinuity is defined by four geological properties: 1) the surface roughness, 2) the strength of rock at the discontinuity surface, 3) the normal stress acting on the discontinuity and 4) the amount of shear displacement. These are represented by three index parameters; the joint roughness coefficient, JRC, the joint wall compressive strength, JCS, and the residual friction angle, ϕ_r , in addition to the normal stress, σ_n , action on the surface. Figure 20 gives the relationship between shear strength and normal stress on a representative J1 surface within the study area. This relationship is calculated after a modified Coulomb criteria after the procedure given by Grøneng and Nilsen (2009). The non-linear relationship between peak shear strength and normal stress for low stress levels is justified in for instance Nilsen et al. (2000). An average value of the estimated JCS given in Table 8 for J1 is used in the calculation.

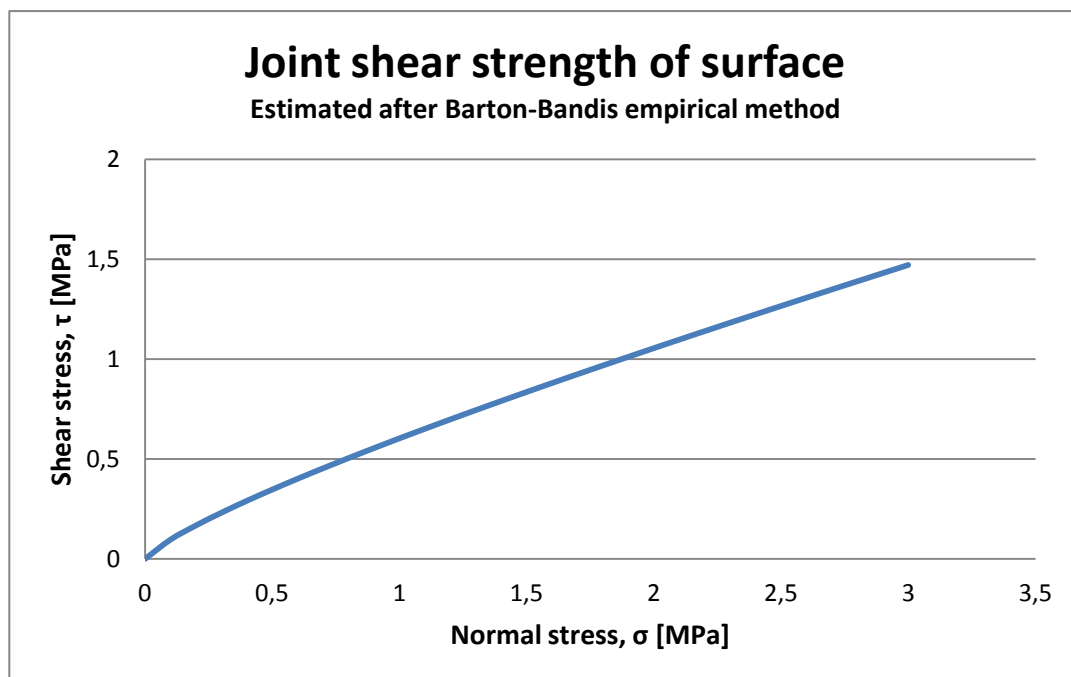


Figure 20: Estimated joint shear strength for the Håkåneset slope. The estimation is performed after the empirical method of Barton-Bandis, described in Grøneng and Nilsen (2009). Input values found in Table 4, Table 7 and Table 8

5.3 Major geomorphological features

Several geomorphological features could be mapped on both air photos and in the field, and these are assumed to affect and control the stability of the slope. These features are outlined in Figure 21. A brief description of these structures is given in the following text. A more detailed description can be read in the project assignment

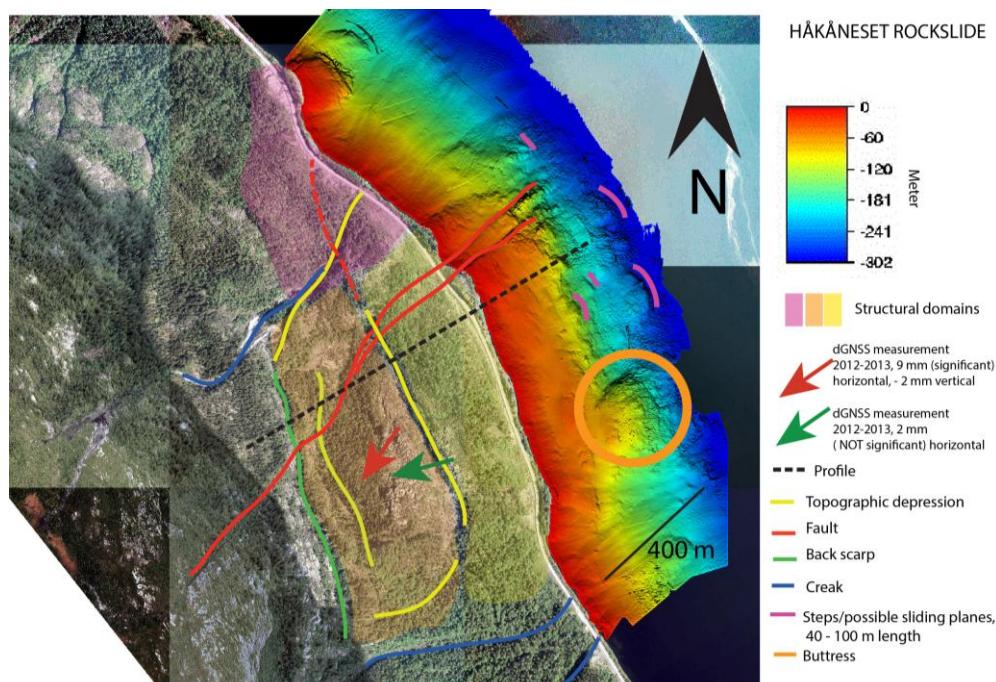


Figure 21: Important geomorphological features that are assumed to be affecting and controlling the stability of the slope. The three defined structural domains are highlighted and arrows show the direction of the measured movement in the slope by dGNSS (not in scale).

Subaerial features

J1-fault zone: A weakness zone (red dotted line) in Figure 21 is recorded to daylighting in the road cut in the north domain (Location 6 in Appendix 1). The width is estimated to be 8,0 m. The weakness zone material consists of highly fractured rock mass with lense structures and fine grained joint filling down to clay size (fault breccia) and high mica content. Estimated GSI value is 27-50. The material characteristic indicates that the damage is a result of tectonic activity. The tectonic activity interpretation is supported by observations of mineral lineations (13/279) on a JF2 (63/007) surface within the weakness zone material and slicken sides (42/044) at a J1 (53/077) surface below the weakness zone. The same J1 surface have groove

marks (47/081) (not statistically significant), that is interpreted as evidence of gravitationally reactivation of the fault. On air photos the weakness zone seems to continue as a NNW-SSE trending depression, defining the boundary between the U-S and L-S domains in Figure 19 (yellow line in Figure 21). i.e. congruent with the orientation of joint set J1.

Back scarp: The upper limit of the instability is defined by a back scarp at an elevation of approximately 550 m a.s.l. The orientation of this steeply dipping wall is 65/070 ($\pm 06/\pm 012$) (calculated from 18 measurements), thus it is parallel to J1 surfaces.

JF3-fault zone: A distinct SW-NW trending fault zone (red solid line) is interpreted as the northern limit of the instability. This linear feature is also clear on the bathymetric map (see Figure 21), and continues down to approximately 300 meters depth. Based on field measurements the orientation of the fault is 78/314, thus congruent with joint set JF3.

Subaquatic features

Spatially variable bedrock structures: The bathymetric map reveals that subaquatic a southern area with significantly bedrock structures can be seen relative to a northern area where the bedrock surfaces appear smoother, see Figure 21. This is the reason for dividing the submerged slope in a northern and a southern domain. The bedrock structures in the southern domain are prominent in the north and less distinct in the south.

Multiple sliding planes: Several linear SE-NW trending features of 40 - 100 m length can be seen in the prominent subaquatic bedrock structures at 200 - 300 meters depth (purple lines in Figure 21). In the far north of the southern domain two SW-NE trending steps are observed. These linear features and steps are interpreted as an indication that multiple sliding planes exists in the slowly deforming rock mass.

Buttress: South in the southern domain is a dome like feature. This feature stands out from a typical glacial eroded valley profile, and is therefore assumed to be a buttress of hard rock that was resistant to the glacial erosion in (see Figure 21).

5.4 Preliminary findings

5.4.1 LATERAL LIMITS OF THE ROCKSLIDE

The lateral limits of the instability have been determined by geomorphological mapping and interpretation of aerial photos and bathymetric images. The surface area has been calculated to be 0,50 km² subaerial and 0,54km² subaqueous by the 3D Analyst tool in ArcMap (ArcGIS, ESRI).

Two distinct faults striking SW-NE parallel to joint set J3 form the northern lateral release surface. Such a clear release surface does not occur in the south and the bathymetric data rather suggest that the limit of the unstable area in the south is transitional.

5.4.2 RESULTS OF KINEMATIC FEASIBILITY TEST

Based on the geological investigation of the Håkåneset the instability was concluded to be structurally controlled by the discontinuities. In the project assignment a kinematic feasibility test was performed for each of the subaerial domains, testing for the possibility of planar sliding, wedge failure and block toppling. The test was performed under the criteria in NGU's hazard analysis published by Hermanns et al. (2012b). Maximum slope inclination determined in ArcMap 10.1 (Esri, 2012) is assumed. The results are illustrated by Figure 22. For detailed description about how to interpret the plots, see Hermanns et al. (2012b).

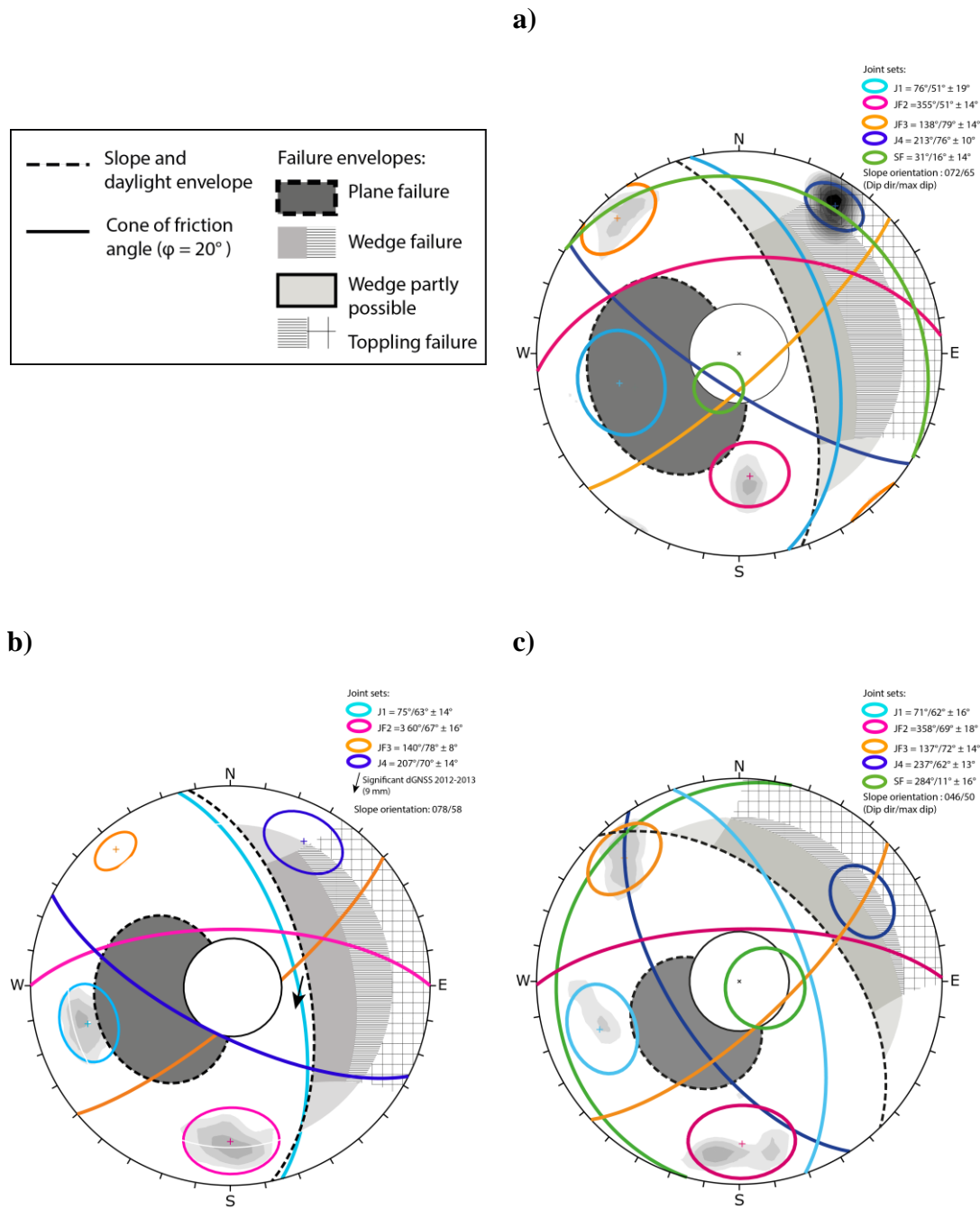


Figure 22: Kinematic feasibility test results for a) Lower-South (L-S) domain. b) Upper-South (U-S) domain. c) North (N) domain. The feasibility for planar, wedge and toppling failure are tested assuming maximum slope inclination. Guidelines given for the risk and hazard classification system provided by NGU (Hermanns et al., 2012b) are followed.

Based on the interpretation of the kinematic feasibility test in Figure 22 there are five important failure mechanisms that are considered as relevant for the further stability analysis of the Håkåneset rock slide:

1. Planar sliding is feasible in steep parts of the slope along planes of minimum dipping values of an exfoliation plane (J1) dipping 40-80 degree in NE direction towards Tinnsjø.
2. Either steeply dipping J1 surfaces like along the back scarp, or joint set (J4) dipping 40-90 degree into the slope, can form rear release surfaces.
3. Bi-planar sliding is feasible along a compound sliding surface defined by the exfoliation J1 and the variable schistose, SF.
4. Wedge sliding formed by the intersection of the conjugate joint sets J2 and J3 is feasible where the slope is steeper than 50-60 degrees.
5. Toppling of small rock volumes. (Not important for a massive failure of the slope.)

6 THE FEM MODEL USED FOR THE HÅKÅNESET ROCKSLIDE

This chapter presents all settings and input parameters which serves as a basis for the stability analysis of the Håkåneset rockslide undertaken in this study. It gives all the information that should be known before interpreting (Chapter 7).

The stability analysis performed in this study is undertaken by applying the numerical modeling software Phase² (Rocscience, 2014a). A description of this software and reason for choosing it for the slope stability of the Håkåneset rockslide is discussed in more detail in Chapter 4.5.1. This chapter first verifies the construction of a representative model for the studied slope, presented in Chapter 6.1. The chosen analysis settings are presented in Chapter 6.2. Chapter 6.3 presents the structure of the parameter study undertaken in the following analysis, and lists the different slope models that have been analyzed. The discussion for choosing input rock mass parameter values are summarized in Chapter 6.4.

6.1 Model geometry set up

The numerical modeling in this study is carried out on a 2-dimensional one stage model. The model is constructed based on a scaled cross section profile of the Håkåneset rock slope. The profile was extracted from a 1m resolution DEM in ArcMap 10.1 (Esri, 2012) using the 3D Analyst tool. The location of the profile is through the central part of the study area, illustrated in Figure 23 as a red line. This location is chosen to include the assumed most active part of the slope with respect to slope deformation. The assumption about increased activity in the north of the study area is based on an interpretation of bedrock structures on bathymetric images, where pronounced structures appear in the central part of the study area, as described in Chapter 3.2. The profile is oriented perpendicular to the valley slope and rises from the bottom of the lake at 300 meters depth in Lake Tinnsjø and up to the mountain plateau at 962 m.a.s.l. In addition, it has been essential to have a favorable orientation of the profile with respect to mapped structural and geomorphological features that are assumed as controlling factors for the slope stability. Thus, the profile intersects with the exfoliation joint set J1, the prominent SW-NE striking JF3-fault system and the NW-SE striking J1-fault cutting through the slope. The characterization of these geomorphological features can be read in Chapter 5.3.

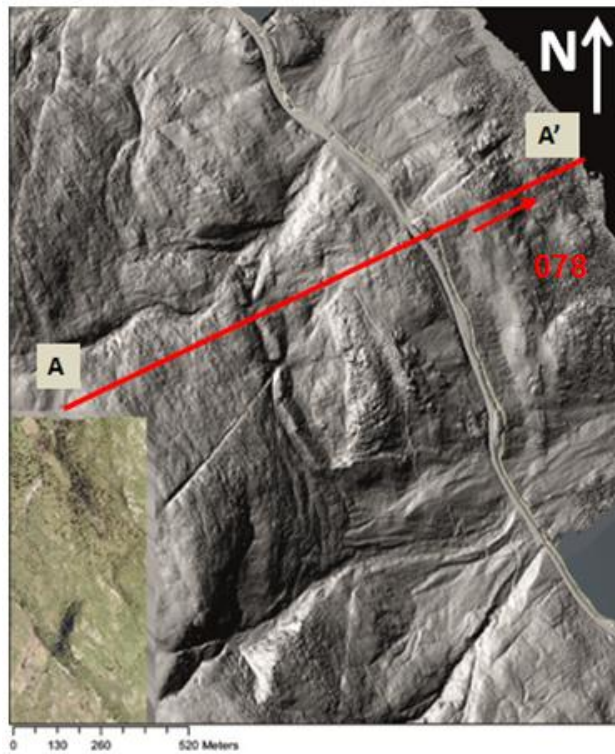


Figure 23: AA' is the trend of the cross section profile used to construct the Phase2 model. Profile constructed from 1m resolution DEM in Esri (2012)

Boundary conditions

The geometry of the model is constructed on the basis of recommendations given in Wyllie and Mah (2004), see Figure 24, in order to avoid boundary effects. Boundary effects in this matter are related to the artificial boundaries of the model, i.e. far-field boundaries that do not correspond to natural ground surface boundaries. In reality no artificial boundaries exist, thus they may influence the analysis results if they are located too close to the area representing the slope stability problem in the model. In any numerical model for slope stability analysis the condition of the artificial boundaries must be specified either as prescribed displacement or as prescribed stress. Prescribed displacement are most commonly used for slope stability problems (Wyllie and Mah, 2004), therefore also applied in this study. Table 9 gives an overview of the displacement boundary set up of Håkåneset rockslide model.

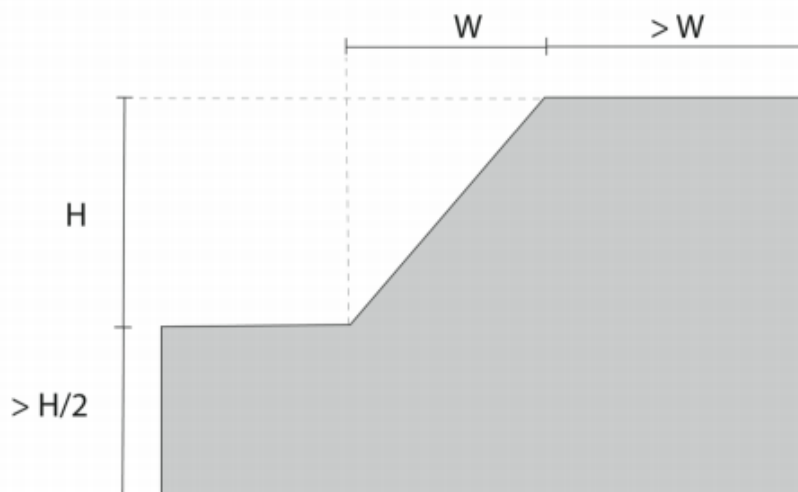


Figure 24: Recommended location of artificial far-field boundaries in a model for slope stability analysis given by (Wyllie and Mah, 2004)

Table 9: Displacement boundary set up of the Håkåneset rockslide model in this study.

Boundary	Condition	Recommendation
Ground surface	Free to move in all directions	(Rocscience, 2014b)
Left and right vertical boundaries	Allowed to move in vertical (y) direction, but not in horizontal (x) direction. This allows deformation and prevents stress concentration.	(Sandøy, 2012)
Horizontal base	Fixed in both vertical and horizontal directions in order to inhibit rotation of the model.	(Wyllie and Mah, 2004)

Figure 25 show the final model used for this study of the Håkåneset rockslide. The applied mesh and the added water representing Lake Tinnsjø, is commented in the following text.

Mesh setup

For the numerical modeling approach in *Phase 2* the rock mass is considered as a continuous material that is subdivided in triangular or quadrilateral elements by generating a finite element mesh (Rocscience, 2014b). The performed analysis in this study is based on a mesh

of 3-noded triangular elements, following recommendation given by Trinh (2014). This mesh set up gives a fast modeling but still with a satisfactorily quality of the computation. A "Graded" mesh is used, by recommendation given in Rocscience (2014b).

The size of the elements or the density of the mesh in the model is determined by applying the Advanced Mesh Region option under the Mesh Setup option in Phase². By defining a mesh region it is possible to construct a more time effective model where the mesh has a higher density in the interesting part of the model, i.e. around the unstable slope, and lower density mesh in the parts that are not close to the unstable slope region. The mesh region was assigned to the model of this study within the same area that is defined as a SSR Search Area (see Shear Strength Reduction analysis set up in Chapter 7. 2) in Figure 25. The density of the mesh is determined by defining an element length of 75 m, which means that the length between the elements at the model boundary within the region (corresponding to the slope face at this model) is 75 m. The mesh type within the region was chosen as Uniform, because this gives an uniformly meshed rock mass over the instability of the study and the quality of the calculations are equal for all depths in the slope model. This is considered to give the most representative analysis in the search for a feasible sliding plane.

Outside the defined mesh region, a graded mesh type was chosen. When using Advanced Mesh Region the *Default Number of Nodes on External* is not affecting the meshing of the model. However, the mesh is dependent on the *Gradiation factor* of the graded mesh outside the mesh region, as this factor determine the discretization of all boundaries outside the defined mesh region. A Gradiation factor of 0,1 (default) is used for this model. With this, the model has a generated mesh with 994 elements and 534 nodes, which is assumed to be a satisfactorily mesh quality for this study (confirmed by Trinh (2014)).

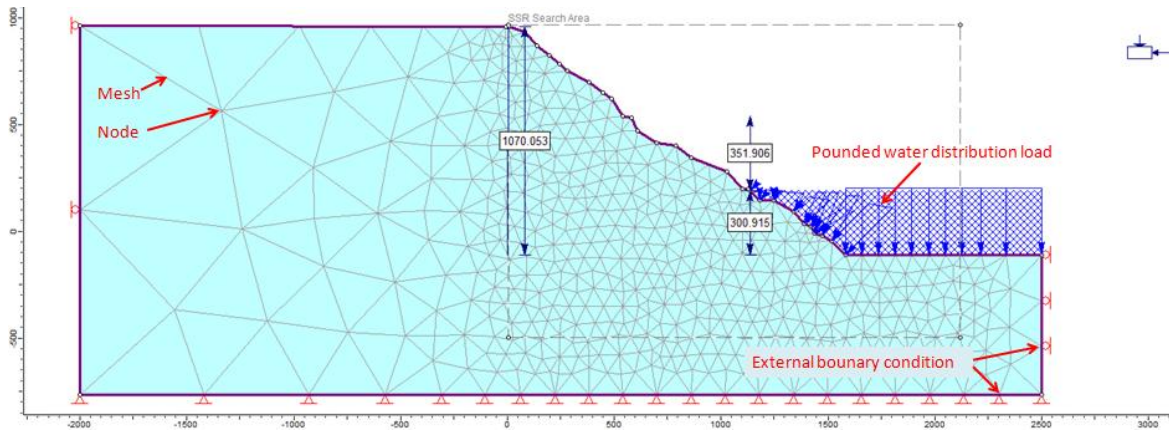
Pounded lake water

The unstable slope at Håkåneset has both a subaerial and a subaquatic component, thus the Lake Tinnsjø should be included in the model to make it as close to the reality as possible. In a Phase² model the effect of a lake can be investigated by constructing a "pounded water" in the model (Rocscience, 2014a). Rocscience (2014b) defines pounded water as water which is impounded against a dam or a slope, and is represented as a blue hatch pattern above the ground surface, as shown in Figure 25a,b). The pounded water conditions are assigned to the model by defining the *Set Boundary Conditions* under the *Groundwater* option, as described

in tutorials given by Rocscience (2014b). The boundary type *Total Head* are used, which require input on the elevation of the phreatic surface at the external boundaries. Since the surface elevation of the Lake Tinnsjø is 191 m.a.s.l., a Total Head Value of 191m was assigned to the right external boundary from the lower right corner and up to the level of 191 m in the model, thus representing the elevation of the assumed phreatic surface. Selection mode was defined as *Boundary Segments*.

Pounded water applies an additional stress to the slope due to the weight of the water (Rocscience, 2014b). However, the *Total Head Boundary Conditions* described above do not define the weight of the pounded water. Therefore, the weight of the pounded water must be defined by adding a *Pounded Water distributed load* to the model. The pounded water load is found under the *Loading* option in Phase². The water is modeled as an equivalent distributed load, and is represented as blue arrows in the model in Figure 25a). A pounded water load, also with a Total Head Value corresponding to the elevation of the lake surface at 191 m.a.s.l., was defined.

a)



b)

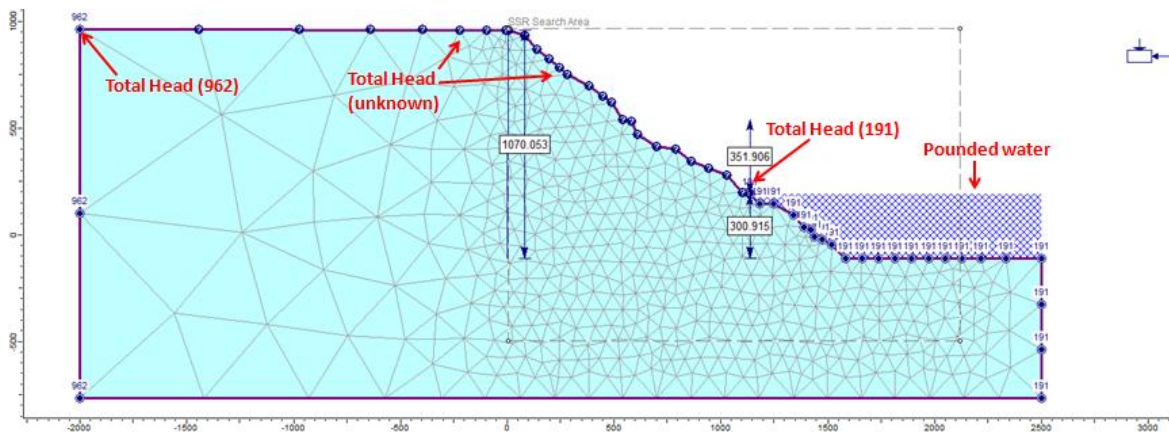


Figure 25: The Phase² model used for the stability analysis of the Håkåneset rockslide. The profile is constructed from the AA' profile in Figure 23

6.2 Analysis set up

General settings

For the numerical modeling in this study a plane strain analysis with *Gaussian* solver type is defined, as recommended by Rocscience (2014b).

Stress analysis set up

For the *Stress Analysis set up* the following settings are defined:

<i>Maximum Number of Iterations</i>	The default number of 500 was used.
<i>Tolerance:</i>	The tolerance of a model imply the point at which the calculations of the analysis should be considered as converged (Rocscience, 2014b). The stresses in the analyses of this study are simulated with a tolerance of 0.001, which is the default value in <i>Phase2</i> .
<i>Number of Load Steps:</i>	Auto (default)
<i>Convergence type:</i>	The convergence type defines the stopping criteria for the calculations. The default <i>Absolute Energy</i> is used as convergence criteria in this study.
<i>Tensile failure reduces shear strength to residual.</i>	This option was chosen because it implies that if tensile failure occurs at a point in a material (and shear failure has not already occurred), the shear strength of the material at that point will be automatically reduced to the residual shear strength parameters for that material. Rocscience (2014b) recommends this as a realistic assumption to make, particularly for brittle materials, thus it is considered as a representative condition for the metavolcanic rock masses

at Håkåneset. When defining this criterion it is required that the material is defined as plastic.

Joint tension reduces joint stiffness by a factor of 0,01 (default value): This setting specifies how the joint property stiffness is reduced if the joint element is subjected to tensile stress normal to the joint. The rock mass at Håkåneset is highly dissected by closed and open joints, and therefore it was considered that this condition is essential to include in the model.

Use effective stress analysis: Since the lake water and consequently groundwater is assumed as an essential part of the Håkåneset model, it is found reasonable to define that the analysis should be based on effective stresses in the slope. By the description given in Rocscience (2014b) this means that calculated deformation is a result of changes in effective stress due to pore pressure changes, assuming that changes in deformation or loading do not affect the pore pressure.

Groundwater seepage analysis set up

Due to lack of groundwater level measurements, it was decided to define a steady-state finite element ground water seepage analysis to be included in the modeling. To perform a groundwater seepage analysis the *Total Head boundary conditions* must be set to define the hydraulic boundary conditions of the model. For the Håkåneset model this corresponds to the elevation of the water level in the lake for the right boundary segments, which was already defined when constructing the lake in the model (see Chapter 6.1. *Pounded water*). By studying air photos it can be observed that several small lakes that do not have any open drainage channels, are located at the plateau above the unstable area. This observation can be interpreted as an indication that the water table in the slope is close to the surface at high elevations. Therefore, hydraulic conditions with a total head value of 962m, were assigned to all segments at the left vertical boundary of the model. The chosen value corresponds to the

elevation of the mountain at the left end point of the profile from which the model was constructed.

For simplification has infiltration conditions not been taken into account in the analysis of this study and boundary conditions at the free surface representing the mountain slope was assigned as Unknown ($P=0$, $Q=0$).

Since the hydrogeological conditions in the rock slope in this study are unknown, it must be emphasized that the groundwater seepage settings adds significant uncertainties to the model. A parameter study on the groundwater conditions will therefore be important to perform.

Shear Strength Reduction (SSR) analysis setup

The SSR analysis was defined with the default settings of "Initial Estimate of SRF" = 1 and "Tolerance"=0.001.

A SSR area is defined including the region where the slope is located, visible as a dotted square. Within the SSR-area the material is considered as brittle, and outside the area it behaves elastically (Rocscience, 2014b).

6.3 Input parameters for the Håkåneset rock mass

A slope stability analysis is undertaken in order to predict where the rock mass is most likely to fail based on the input parameters, i.e. the aim is to search for a feasible failure surface within the rock mass in the model. In most cases of large scale rock slope failures is the development of a failure surface not a uniform process, but rather a complex deformation in a combination of unfilled joints (rock-to-rock contacts), filled joints (gouge material) and bridges of intact rock (Grøneng et al., 2009). This is also assumed to be the case for the Håkåneset rockslide, which comprises a heavily jointed rock mass made up of hard brittle blocks separated by non-persistent discontinuity surfaces. The strength of such rock masses depends on the strength and deformability of the intact pieces and on their freedom of movement which, in turn, depends on the number, orientation, spacing and shear strength of the discontinuities (Hoek, 1983).

In Phase² a representative rock masses quality is assigned to the model by 1) defining materials with estimated parameters 2) defining joints with estimated properties. Estimation of material parameters for the rock mass at Håkåneset are discussed in Chapter 6.3.2 and estimated discontinuity properties are discussed Chapter 6.3.3.

6.3.1 MATERIAL MODEL AND STRENGTH CRITERION OF JOINTED ROCK MASS

A numerical model requires input parameters related to rock mass behavior and strength parameters. Necessary input parameters depend on what material model and strength criteria that are assumed to describe the rock mass.

Material models

Material models are idealized stress/strain relations that describes how the material behaves under variable stress conditions. Figure 26 is an illustration the different material models that are common to consider.

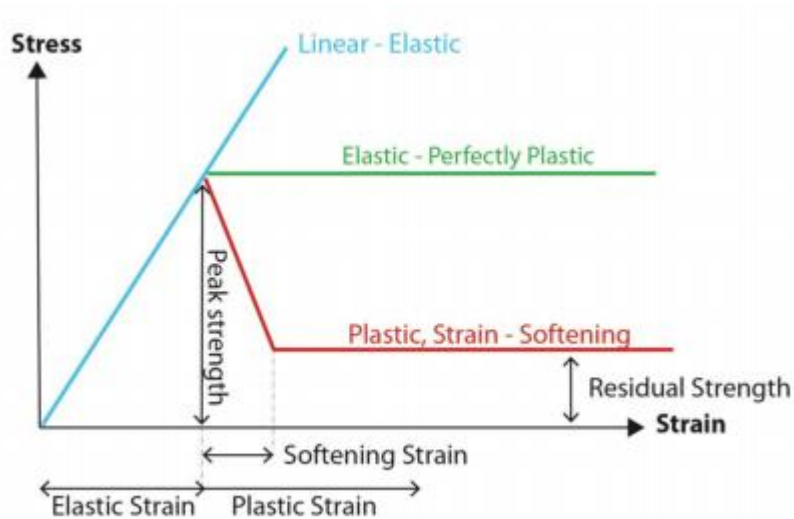


Figure 26: Stress-strain relations that represent the behavior of the rock mass when different material models are assumed. The residual strength relative to the peak strength describes the plastic strain-softening model of the material (ed. Hoek (2007)).

The elastic behavior of the material up to the level of failure (peak strength) is described by assuming a failure criterion. Failure criteria are discussed in the next section. The different material models describe how the strength of the material is assumed to change after the point of failure. The residual strength relative to the peak strength describes the plastic strain-softening model of the material due to failure.

Failure criteria

Mohr-Coulomb strength criterion

Mohr-Coulomb strength criterion is a traditional failure criterion, where the shear strength of a rock is represented by a linear relationship between the normal stress state, σ_n , and the material properties cohesion (c) and inner friction angle (φ) after the definition e.g. found in Hoek (2007):

$$\tau = c + \sigma_n \tan \varphi \quad (\text{Eq. 2})$$

Hoek-Brown empirical strength criterion

The mechanics behind a large landslide is complex because the rock mass failure is controlled by the characteristics of both intact rock material and discontinuities (Stead and Eberhardt, 2013). Due to this complexity, the failure in rock masses has a non-linear character that cannot be described with the linear Mohr-Coulomb criterion. Therefore, in order to describe the non-linear behavior of blocky rock masses, the empirical failure criterion *Generalized Hoek-Brown* was developed (Hoek et al., 2002).

The Generalized Hoek-Brown failure criterion for jointed rock mass is an empirical failure criterion that is defined by (Hoek, 2007):

$$\sigma_1' = \sigma_3' + \sigma_{ci}' \left(m_b \frac{\sigma_3'}{\sigma_{ci}} + s \right)^a \quad (\text{Eq. 3})$$

where:

σ_1' and σ_3' are the maximum and minimum effective principal stresses at failure,

m_b is the value of a Hoek-Brown constant m_i for the rock mass:

$$m_b = m_i \exp \frac{(GSI-100)}{28-14D} \quad (\text{Eq. 4})$$

s and a are constants which depend upon the rock mass characteristics

$$s = \exp \frac{(GSI-100)}{9-3D} \quad (\text{Eq. 5})$$

$$a = \frac{1}{2} + \frac{1}{6} \left(e^{-\frac{GSI}{15}} - e^{-\frac{20}{3}} \right) \quad (\text{Eq. 6})$$

and σ_{ci} is the uniaxial compressive strength of the intact rock pieces.

The factors m_b , s and a are included to reduce the properties of intact rock so that a strength estimate for jointed rock mass is obtained. These reducing factors are calculated on the basis of two factors that express the characteristic of joints in the rock mass and the rock mass quality:

- *Geological Strength Index (GSI) of the rock mass.*
- *Disturbance factor D , depending upon the degree of disturbance due to blast damage and stress relaxation. D varies from 0 for undisturbed in situ rock to 1 for disturbed rock mass.*

With this, Hoek-Brown is commonly used to describe the strength of jointed rock masses (Hoek and Brown, 1997). However, this criterion also assumes isotropic rock conditions and rock mass behavior. Therefore, it should only be used for rock mass which are dissected by a sufficient number of closely spaced discontinuities with similar surface conditions, so that isotropic behavior involving failure on discontinuities can be assumed. For the same reason, this criterion can only be applied when the block sizes are small compared to the overall object being studied (Hoek, 2007). With these restrictions, the Generalized Hoek-Brown strength criterion is favorable for describing the failure of big slopes with jointed rock masses like at Håkåneset

Equivalent Mohr-Coulomb parameters

Equivalent Mohr-Coulomb parameters are estimates for the shear strength parameters cohesive strength, c' , and the angle of friction, ϕ' , and is obtained by converting Hoek-Brown parameters to traditional Mohr-Coulomb parameters over a specified stress range (Hoek et al., 2002). This is a commonly used approach because even though Hoek-Brown failure criterion is assumed to best describe a jointed rock mass, most geotechnical software is still written in terms of the Mohr-Coulomb failure criterion (Hoek et al., 2002). As for finite element computation, finding estimates for the Hoek-Brown parameters require calculations that slow down the analysis considerably (Hammah et al., 2004). Therefore, it is favorable to use the *equivalent Mohr-Coulomb parameters* as input parameters in a numerical modeling. The conversion of the parameters can be undertaken with the software RocLab provided by

(Rocscience, 2011). Equivalent Mohr-Coulomb parameters have been used as input parameters in his study.

6.3.2 MATERIAL PARAMETERS

With the assumption of the rock mass as homogeneous, a single material model was constructed. Required parameters are properties that are related to unit weight of the rock and its strength and elastic properties. The results of field and laboratory test of rock samples from the particular study area (Chapter 5) supplemented empirical values and recommendations from Rocscience (2014b) have been used to obtain required Equivalent Mohr-Coulomb input values for the SSR-analysis in Phase².

Equivalent Mohr-Coulomb strength parameters was converted from the following Hoek-Brown parameters (Hoek et al., 2002) in RocLab (Rocscience, 2011):

- *Uniaxial compressive strength (σ_{ci}) of intact rock.*
- *Value of Hoek-Brown constant for intact rock (m_i).*
- *Geological Strength Index value (GSI-value) for the rock mass.*
- *Disturbance factor D .*
- *Deformation modulus of the intact rock, E*

Chosen values for the estimation are discussed below. Input and output of the conversion is summarized in Table 10

σ_{ci} (σ_{ci}) The uniaxial compressive strength of intact rock has been tested by uniaxial compressive strength test on specimens ($d = 50$ mm) that were cored from rock samples collected from the weakness zone, the possible rupture surface and from rock of good quality within the limits of the unstable rock masses in the study area. The rock sample from the weakness zone was taken from rock of the best quality within the zone. The laboratory work was undertaken and described in the project assignment, and the test results are summarized in Table 4 in Chapter 5. Due to the uncertainties related the obtained laboratory estimates (see Chapter 5) it was considered that an average value of all test results would be the most representative estimate for the uniaxial strength of the overall rock mass. Thus, the value of 98MPa for σ_{ci} was used as input in the estimation in

- RocLab.
- GSI During the field investigation the rock mass was given a GSI value of 60-80 for rough surfaces and 40-60 for smoother surfaces, see Chapter 5.2.2 and Appendix 3. Based on this, a GSI value of 60 was chosen as a representative input value for average rock mass.
- m_i This parameter was not tested during the laboratory work related to this study. Therefore, the guidelines given by Hoek (2007) have been the basis for assessing a representative value. Rocscience (2011) recommends a m_i in the range 25 ± 5 for a rhyolitic rock and 28 ± 5 for a gneissic rock. Therefore, the value 27 is chosen as a representative value for the rock masses at Håkåneset in this study.
- D According to Rocscience (2011) the disturbance factor should not be applied to the entire rock mass. In a natural rock slope, the GSI value takes account for the disturbance due to fracturing and weathering of the rock mass. Therefore, after discussion with the supervisor, a disturbance factor $D = 0$ was chosen for this modeling.
- E_i For the same reason that an average value of all valid tests was used to find an estimate of σ_{ci} , the average value of the performed deformability tests was used to find an estimate for Young's Modulus, E_i . The average of 12 deformability tests is 44300 MPa.

From the Hoek-Brown input parameters discussed above, the equivalent Mohr-Coulomb strength parameters cohesion, c , and friction angle, φ , are calculated. The strength of a material depends on the stress conditions, as can be read from the definition of shear strength in Eq. 2 (Hoek and Brown, 1997). Thus, the apparent cohesion and apparent friction angle have to be determined by taking the normal stress σ_n acting on the sliding surface into account. However, the software used in this study requires a constant input value of c and φ , which means it is necessary to first determine an assumed normal stress level for the material where a feasible failure surface is expected to form. The normal stress can be estimated from the overburden to a possible sliding plane, by the relation

$$\sigma_n = \gamma_{rock} \cdot h \cdot \cos\alpha_{slope} \quad \text{Eq. 7}$$

The major advantage by applying the FE-SSR technique in this study was that no prior assumption about a failure surface was needed. However, the normal stress dependent shear strength parameters bring up a limitation of the method if σ_n have to be calculated from the overburden of a feasible sliding surface that has to be assumed before the analysis. This highlights the importance of performing a parameter study of the shear strength parameters when investigating the slope stability. Based on the field observations the orientation of the J1-fault (described in Chapter 5.3) would a logical feature to use for determining a normal stress level that can be used to obtain a initial estimates for the materiel shear strength parameters. The calculation of the normal stress level is given in Appendix 5. Overburden ranges from 0 to approximately 75 m in the subaerial part of the slope and increases to approximately 200m at the level of the lake floor. 100 m overburden was chosen as a reasonable mean value. Further, the normal stress was calculated as an average normal stress according to the weight component of an overburden of $h=100\text{m}$ acting perpendicularly on the sliding plane with an average dip angle of 46° and a specific rock density of 30kN/m^3 (Table 4) after Equation 6. The input values give a normal stress of $2,1\text{MPa}$. The effective normal stress value is obtained taking the pore pressure acting on the plane into account. For simplification and for considering a worst case scenario with fully saturated slope materials, an average groundwater height of 100 m was assumed, resulting in an effective normal stress of $\sigma_n=1.4 \text{ MPa}$. (Hydrostatic stress calculated to be $0,7\text{MPa}$). The equivalent M-C parameters under a normal stress condition of 1.4 MPa can be determined by the Instantaneous MC sampler in RocLab, see Appendix 6. The results of the rock mass strength parameter estimations in RocLab are given in Table 10.

Table 10: Estimated material properties of the rock mass at Håkåneset. Conversion of Hoek-Brown parameters to equivalent Mohr-Coulomb parameters obtained in RocLab. M-C parameters are used as input in the Phase2 model.

INPUT (RocLab) Parameters:	Symbol	Mean Value	- 30%	+30%	Source
Strength criterion: Generalized Hoek-Brown					
Uniaxial compressive strength intact rock (UCS)	σ_{ci} [MPa]	98	67	127	Laboratory work undertaken in the project assignment
Geological Strength Index	GSI	60	42	78	Field observations during the project assignment work
Intact rock parameter	mi	27	19	35	Evaluated based on inbuilt RocData values in RocLab
Disturbance factor	D	0	0	0	Discussed with main supervisor Bjørn Nilsen
Young's Modulus	Ei [MPa]	44300	30100	57590	Laboratory work undertaken in the project assignment
Unit weight	[MN/m ³]	0,03	0,03	0,03	Laboratory work undertaken in the project assignment
OUTPUT (used as input in Phase2 models)					
Strength criterion: Mohr-Coulomb					
Parameters:		Initial ($\sigma_n=1,4$ MPa)	30 % reduced strength parameter input ($\sigma_n=1,4$ MPa)	30% increased strength parameter input ($\sigma_n=1,4$ MPa)	
Håkåneset model		Model 1	Model 2	Model 3	
Peak cohesion	C_{peak} [MPa]	1,5	0,8	3,6	RocLab estimation
Residual cohesion	C_{res} [MPa]	1,0	0,5	2,4	Assumed 2/3 of peak
Peak friction angle	φ_{peak} [°]	63	54	68	RocLab estimation
Residual friction angle	φ_{res} [°]	42	36	45	Assumed 2/3 of peak
Defomation modulus	E_m [MPa]	23036	5507	49357	RocLab estimation
Peak tensile strength	σ_t (peak)[MPa]	0,2	0,04	0,7	RocLab estimation
Residual tensile strength	σ_t (res)[MPa]	0,1	0,03	0,5	Assumed 2/3 of peak

Dilation angle

The shearing of rock induces a volume increase due to normal displacement in the rock (Rocscience, 2014b). Dilation angle increases with the rock shear strength, and ranges from zero to φ . According to Hammah et al. (2008) , the dilation angle does not have significant influence in the slope stability problems due to general low confinement stresses. Also for the rock mass at Håkåneset the confinement stress can be expected to be low, as the heavily dissected rock at the surface indicates significant stress relief have taken place. Based on this, dilation angle is set to zero in the undertaken modeling.

Tensile strength

Tensile strength reflects the interlocking of the rock particles when they are not free to dilate (Hoek and Brown, 1997). According to Stead and Eberhardt (2013) can tension cracking be interpreted as an early sign of instability. Consequently, the tensile strength is an essential parameter for slope stability. The applied tensile strength estimate in this study is obtained from the RocLab calculation of equivalent Mohr-Coulomb parameters (Table 10).

Table 11: Initial input material properties used for the SSR analysis in Phase²

Parameter			Source
Elastic type		Isotropic	
Unit weight	γ [MN/m ³]	0,03	Laboratory test in project assignment
Poisson's ratio	ν	0,18	Laboratory test in project assignment
Youngs modulus (rock mass)	E_m [MPa]	23036	RocLab estimation
Peak cohesion at 1,4MPa	c' [MPa] (peak)	1,5	RocLab estimation
Residual cohesion at 1,4MPa	c' [MPa] (resid)	1,0	(Trinh, 2014)
Peak friction angle at 1,4Mpa	φ ((peak)	63	RocLab estimation
Residual friction angle at 1,4Mpa	φ (resid)	42	(Trinh, 2014)
Peak tensile strength	φ_t' [MPa] (peak)	0,2	RocLab estimation
Residuak tensile strength	φ_t' [MPa] (resid)	0,1	RocLab estimation
Dilation angle	d	0	(Hammah et al., 2008)

Material type: Elastic and plastic

Required strength properties of a material in the Phase² model depend on whether the material is assumed as elastic or plastic. In order to perform a SSR-analysis the material has to be defined as plastic. A plastic strain-softening model is assumed for this study, and input of a residual strength of the material is required. By discussion and recommendation from Trinh (2014), the residual values are calculated as 2/3 of the peak values. This is considered as an reasonable estimate for the relative rough surfaces observed in field at Håkåneset.

6.3.3 DISCONTINUITY PARAMETERS

Barton-Bandis discontinuity shear strength parameters

When a rock mass is dominated by joints with no filling, the shear strength of the joint surface is critical for the stability due to the rock-to-rock contact (Wyllie and Mah, 2004). The frictional force at the joint surface depends on 1) the surface roughness, 2) the strength of rock at the discontinuity surface, 3) the normal stress acting on the discontinuity and 4) the amount of shear displacement (Grøneng and Nilsen, 2009). Barton and Choubey (1977) relates these properties to the three indices: joint roughness coefficient, JRC, the joint wall compressive strength, JCS, and the residual friction angle, φ_r , in addition to the normal stress, σ_n , action on the surface. The definition of the shear strength (τ) with the Barton-Bandis parameters is:

$$\tau = \sigma'_n \cdot \tan(JRC \cdot \log_{10} \left(\frac{JCS}{\sigma'_n} \right) + \varphi_r) \quad (\text{Eq. 8})$$

Barton-Bandis parameters for the rock mass at Håkåneset were obtained in the project assignment, following the methodology given by Grøneng and Nilsen (2009). Estimated JRC for the joint sets is given in Table 7, and JCS values are given in Table 8. Realistically will the strength of discontinuities be significantly lower than for intact rock. However, the Schmidhammer test results (Table 8) indicated significantly higher values for JCS, than respective USC values determined in the laboratory. Therefore, the Schmidt hammer values were considered as not reliable, and the empirical estimate of 25 MPa as a value for JCS have been used in the modeling (see Chapter 5.2.2.). As justified by Grøneng and Nilsen (2009) can φ_r be assumed equal the basic frictional angle φ_b determined by tilt test, thus the mean tilt test value of 28° (Table 4) was used.

In case of slip due to indicated development of a failure surface in the model, the joint shear strength parameters JRC and JCS will automatically be set to zero and the shear strength will depend only on the residual friction angle and the normal stress by to the following relation (Rocscience, 2014b):

$$\tau = \sigma_n \cdot \tan \varphi_r \quad (\text{Eq. 9})$$

When using Barton-Bandis slip criteria for a SSR analysis, the strength reduction is only applied to the material strength properties while the joints will retain their original strength properties during the SSR analysis.

Joint stiffness

Goodman et al. (1968) introduced normal stiffness (K_n) and shear stiffness (K_s) as two vital parameters that describes joint deformability by relating the normal and shear stress on the joint element to the normal and shear displacement. Joint stiffness is a parameter that is not well known and difficult to measure, and several methods for obtaining representative estimates have been developed. One of these are empirical formulas that estimates the joint stiffness based on the rock mass properties rock mass E-modulus (E_m), intact rock E-modulus (E_i), rock mass shear modulus (G_m), intact rock shear modulus (G_i) and joint spacing (L). The calculations are based on the assumption that that the deformability of the rock mass is due to the deformability of the intact rock and the deformability of the joints in the rock mass. The formulas are derived based on the average spacing of the joint set, assuming that the joint orientation is perpendicular to the loading.

Table 12: Estimated joint stiffness for each joint set. See Appendix 7a).

		Joint set values				
		J1	JF2	JF3	J4	SF
Normal stiffness	Kn [MPa/m]	47992	9598	47992	159972	479917
Shear stiffness	Ks [MPa/m]	20335	4067	20335	67785	203355

In the project assignment it was concluded that development of a failure surface along the foliation joint set SF should be investigated more in detail by the numerical modeling. Therefore, a sensitivity test on the joint stiffness of SF is undertaken, based on the values given in Table 13. The stiffness values are calculated by varying the mean spacing. Brideau et al. (2008) justifies that importance of schistose foliation in the development of a basal failure surface, therefore the chosen spacings used to obtain the stiffness estimates can be assumed realistic.

Table 13: Input for parameters study of joint stiffness of foliation joint set SF. See Appendix 7

PARAMETER STUDY SF					
Average spacing	L [m]	0,01	0,1	1	10
Normal stiffness	Kn [MPa/m]	4799167	479917	47992	4799
Shear stiffness	Ks [MPa/m]	2033545	203355	20335	2034

Justification of the stiffness parameters

An overview of empirical joint stiffness estimates is given in Sandøy (2012), Appendix 7b), suggesting that K_n is in the range 3000-10000 and K_s is in the range of 900-1000. The stiffness estimates for the Håkåneset joints are 10.000-500.000 for K_n and 5000-20.000 (Table 12) for K_s , thus significantly higher than the empirical data presented by Sandøy (2012)

The estimates obtained for the joint sets at Håkåneset is significantly higher than Sandøy (2012). The high stiffness calculated for the Håkåneset rock mass was found to be sensitive to the GSI value, as GSI is critical parameter for the ratio between E_i and E_m . Bandis et al. (1983) gives five factors which is expected to influence the normal stiffness of joints:

- i. initial actual contact area, relative amplitude and vertical distribution of the aperture between joint wall;
- ii. joint wall roughness, expecting that the small scale roughness is the most critical in controlling normal stiffness;
- iii. strength and deformability of asperities;
- iv. thickness, type and physical properties of the infilling material.

i., ii. and iv. are factors that are taken account of by the GSI when using estimating E_m based on the generalized Hoek-Brown failure criterion, which supports the assumption of GSI being the critical factor of the joint stiffness. Because of all uncertainties related to the calculations of stiffness in general, thus adding significant uncertainties to the background of the available empirical data, it was decided not to adjust the stiffness values obtained for the Håkåneset rock mass to the empirical data (after discussion with Nilsen (2014)).

Addition pressure inside joints

The *groundwater pore pressure* option is selected as an additional water pressure inside joints, and the model will take account for the water pressure within the joint due to groundwater in the joint analysis. This additional pressure is applied to both sides of the joint wall.

Initial joint deformation

Initial joint deformation refers to how the joint behaves in regard to the far field stresses (Rocscience, 2014b). This option is left on so that the joints in the model will deform based on both the defined far field stresses and the induced stresses due to external water load. As a result, the stress field in the vicinity of the joints will be altered from the initial far field distribution, which is assumed to give the most realistic conditions in the model.

Persistent structures: J1-Fault, JF3-fault and back scarp

The AA' profile (Figure 23) intersects with the prominent SW-NE trending JF3-fault, see Figure 21 (red line), which is interpreted to be a controlling factor for the slope stability by defining the northern lateral limit. Therefore, this structure is essential to include in the Phase² modeling. There have not been undertaken any test for obtaining material or discontinuity strength parameters specific for this fault zone. However, the geological investigation in the project assignment revealed that the fault zone is developed parallel to the defined JF3 joint set. Therefore, the JF3-fault has been added to the model as a continuous joint with JF3 joints properties. This is assumed as a valid simplification because field mapping indicate that there are no clear difference in the bedrock or surface characteristics in the fault zone relative to the overall rock mass in the slope. However, the fact that the JF3-fault can be mapped out on airphoto and DEM and in the field with a persistent ~km, while the JF3 joints only have persistence in the meter scale imply that there realistically are strength differences.

A second fault, J1-fault (see Chapter 5.3, Figure 21 and Figure 23) intersects with the AA' profile, and has orientation as suggesting it is developed along J1 joints. The thickness of this zone is estimated to be ~8m, comprising significantly damaged material and possible clay content. Because no exact testing has been undertaken on this weakness zone material for determining its shear strength, it was considered as a reliable simplification to define the J1-fault as a persistent J1 joint based on the accuracy of the undertaken model. A graph showing the estimated relation between J1 strength and the normal stress acting on the surface was obtained in the project assignment and given in Figure 20 in this thesis.

The profile also intersects with a back scarp, see Figure 21 (green line) and Figure 23. The orientation is measured to be congruent with the J1-fault set, and therefore added to the model as a persistent J1-fault.

The chosen values for the necessarily in put parameters in the Phase² model are summarized in Table 14:

Table 14: Initial joint strength input parameters for the Phase² modeling.

Parameter	Symbol	Joint set values					Source	
		J1	JF2	JF3	J4	SF		
<i>Barton-Bandis parameters</i>	JRS	14	5	20	10	5	<i>Field estimate</i>	
	JCS	25	25	25	25	25	$1/4\sigma$ <i>(Barton and Choubey, 1977)</i>	
	Basic friction angle	ϕ_b [°]	28	28	28	28	<i>Tilt test project assignement</i>	
	Residual friction angle	ϕ_r [°]	28	28	28	28	$\phi_r = \phi_b$ <i>(Barton, 1973)</i>	
<i>Joint stiffness</i>	Normal stiffness	Kn [MPa/m]	47992	9598	47992	159972	479917	<i>Formulas given in Rocscience (2014a)</i>
	Shear stiffness	Ks [MPa/m]	20335	4067	20335	67785	203355	<i>Formulas given in Rocscience (2014a)</i>

Ubiquitous joint model

"Ubiquitous joints" is an option in the *Interpret* mode in Phase² that display the regions in the model where the stresses generated from the SSR-analysis are sufficient to cause slip on a anticipated planes with a user defined orientation (Rocscience, 2014a). Hence, it is an efficient post-processing tool to investigate if failure can occur on a joint surface when only its estimated surface shear strength is known. It is fundamental to ubiquitous joints that the joints themselves do not influence the stress/displacement field. Based on experiences in Böhme et al. (2013) the introduction of ubiquitous joints in the strength factor calculations may lead to results that can help to explain the present days morphology. Because J1 and SF are the joint sets that are assumed to be most critical for the slope stability, these were included as ubiquitous joints with the properties given in Table 15.

Table 15: Ubiquitous joint Barton-Bandis properties for J1 and SF. Used in Analysis 1.2

	Joint set	Joint set	Source
	J1	SF	
Friction angle	28	28	Tilt test 5samples in project assignment
Inclination	-59	-19	Average all slope measurements from field investigation in project assignment
JRC	14	5	J1: Direct roughness measurement in field SF: Chart in Grøneng and Nilsen (2009)
JCS	25	25	1/4 σ_c recommended from Barton and Choubey (1977)

Joint network model

The rock mass at Håkåneset is observed as highly dissected and blocky, and the instability is assumed to be structurally controlled. Because of the non-persistency of the identified joint sets described in Chapter 5.2.2, a joint network models for each set was constructed which make it possible to construct the joints with orientation, spacing and persistence. In this way the model reflects realistic conditions by having sections that represent intact rock bridges. Several scenarios were analyzed by investigating different combinations of joint set in the model, i.e. different joint networks were assigned to the model. The different models are presented in Chapter 6.4.

Parallel Deterministic joint networks have been used in this study. This network model is defined by parallel joints with assumed constant spacing, length and persistence. This is a simplification of the reality as natural variation in joint orientation and extend are considerable. However, using the mean orientations as constant values is considered to be sufficient for the numerical modeling in order to get an impression of the stability of the slope.

Orientation

When constructing the joint networks the joint were defined with 3-dimensional orientation: dip and dip direction. Values are given in Table 5, which are the orientations obtained from the field measurements in the project assignment.

A 3-dimensional input requires a definition of a so called *Trace Plane*. A Trace Plane is the cross-sectional plane of the Phase² model, i.e. a vertically dipping plane. Its orientation is by definition given as the dip direction of this vertically dipping plane, where the dip direction is given by the normal vector (pointing into the screen) of the trace plane, measured clockwise from north (Rocscience, 2014b). When the trace plane orientation is entered in the model Phase² uses the 3-dimensional input to determine the 2-dimensional traces of the joint planes on the trace plane. Thus, when a trace plane is defined in the analysis it is not necessary to transform the measured joint orientations to apparent orientation relative to the model profile. The trend of the AA' profile, Figure 23, is 078. The AA' trend was determined from the DEM in ArcMap 10.1 (Esri, 2012). This gives a trace plane orientation of 348.

Spacing

Spacing is the perpendicular distance between the parallel joint planes. Since a trace plane is defined in the model of this study, then spacing value to enter is the actual, 3-dimensional spacing between the joint planes. This will be the true perpendicular distance between the parallel joint planes, i.e. the spacing after the correction of the orientation of the scan line. Table 6 gives values for true spacing of the joint sets identified at Håkåneset. In order to simplify the modeling the spacing values was exaggerated. Input values that are used as initial values are given in Table 16.

Length and persistence

Discontinuous joints in a joint network in Phase² are described with persistence and length.

Persistence defines the length of intact material between adjacent joint segments (Rocscience, 2014b). It is important to have in mind that the definition of persistence in Phase² as given in (Rocscience, 2014a) differs from the definition used during the geological mapping. The field investigation used the definition for persistence given by Wyllie and Mah (2004)m, where persistence is defined as the continuous length or area of the discontinuity, thus corresponding to the parameter defined as "length" in Rocscience (2014b). As illustrated in Figure 27 the persistence in the Phase² model is a measure of joint continuity represented as the ratio of joint length (L1) to total length along the joint planes (L2), thus having a value between 0 and 1. Input values in the model are given in Table 16.

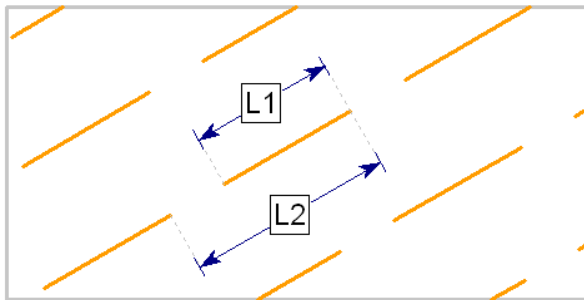


Figure 27: Length (L1) and persistence(L1/L2) of a joint after the definition used in the Phase2 model (Rocscience, 2014b).

Since the rock masses at Håkåneset is observed as highly dissected, where air photos indicate continuous joints of 10s of meters, see photo in Figure 18, a persistence value of 0.7 is chosen as representative for joint set J1, JF2, JF3 and J4, see Table 16. The schistose foliation is mapped out as less pronounced. Therefore a persistence value of 0,2 is considered as a representative average values. With this the model assumes that a significant have to be damaged in order to develop a failure surface.

The length defines the length of each individual joint in the network, as measured in the plane of the model (i.e. the trace plane). Input values for length are given in Table 16 based on the mapped persistence values given in Table 6.

Joint end condition

When a joint or joint set is added to the model, the end condition of the joint is specified as "open" or "closed". For the model of this study the end of the joints are defined as "Closed" where the joint terminates within the rock mass, and "Open" where the joint boundary terminates at the free ground surface. A "Closed" joint end condition means that relative movement (sliding or opening) cannot occur at the joint end, while "Open" joint end condition means that relative movement in the joint end is allowed. It is realistic that joints can open at the free surface. Down in the ground on the other hand, joints cannot open without inducing stresses in the surrounding, which is realistically represented with a "closed" end condition.

Summary of structural discontinuity parameters

In Table 16 the structural input parameters that have been discussed are summarized. These parameters are used to define the joint network properties for the different models used for the stability analysis in Phase².

Table 16: Chosen discontinuity input values in the Phase2 model. Spacing and length are exaggerated in order to exaggerate the modeling.

Joint model	<i>Parallel Deterministic</i>					
Trace plane orientation	348					
Joint set	Domain Lower-South (DipDir/Dip)	Domain Upper-South (DipDir/Dip)	Spacing	Length	Persistence*	Joint end condition
J1	076°/51° ± 19°	075°/63° ± 14°	30 m	100 m	0,7	Open at boundary, material and surface contact
JF2	355°/51° ± 14°	360°/67° ± 16°	60 m	100 m	0,7	
JF3	138°/79° ± 14°	140°/78° ± 8°	30 m	50 m	0,7	
J4	213°/76° ± 10°	207°/71° ± 15°	30 m	100 m	0,7	
SF	031°/16° ± 14°	277°/15° ± 18°	100 m	10 m	0,2	

* Determined after the definition in Rocscience (2014a) (different than the definition used in field for the field measurements in Chapter 5. In Table 6 persistence is defined as in Wyllie and Mah (2004)).

6.3.4 STRESSES

Strength properties depend on the stress conditions (Hoek, 2007). In Phase2 this is taken into account by defining a stress field. For surface models like a slope model a *Gravity stress field* is recommended (Rocscience, 2014a) to represent the in-situ stress conditions. Under this setting the stress are assumed to vary with depth. The depth was defined to be measured from the *Actual ground surface* of the model, which means that the initial vertical stress component at a given point is calculated using this measured depth and the actual unit weight of the overlying materials. The unit weight is defined in the *Define Material Properties* dialog. To use Actual Ground Surface is favorable for a slope stability study since the ground profile has a variable elevation. In addition, it is recommended by Rocscience (2014b) to use the Actual Ground Surface option when performing a SSR-analysis because experiences imply that it provides more reliable and accurate results with less computation, due to the more realistic estimate of the initial stress distribution.

The horizontal components of the gravitational field stress are given as Horizontal / Vertical stress ratios based on the vertical stress at any point in the model. On *In-Plane* and one *Out-Of-Plane* ratio is defined based on the directions of the mean principal stresses used for the calculations.

$$\text{Total stress ratio in plane: } \frac{\sigma_{\text{horizontal In-Plan}}}{\sigma_{\text{vertical}}} \quad \text{Eq. 9}$$

$$\text{Total stress ratio out – of – plane: } \frac{\sigma_{\text{horizontal Out-Of-Plan}}}{\sigma_{\text{vertical}}} \quad \text{Eq. 10}$$

Input values used for the estimation of the stress field at Håkåneset are based on values found in a database presented by (Hanssen, 1998). This is known as the last known data set of field stress measurements for Norway. The data set is a collection of data that is based on available information on three-dimensional rock stress measurements in NTH (NTNU) and SINTEF archives, dated from its initial development to 1992. Two boreholes in Rjukan, located 15,5 km west of the study site at Tinnsjø, can be used to get an impression of the field stresses in the region. Both have a quality ranking B (scale A-D) that should imply representative values. Note, near surface effects considerably affect the horizontal- and vertical stress components and lead to relative high compressive or occasionally tensile horizontal stresses at shallow depths (Hanssen, 1998). Data from Rjukan is given in Table 17 below:

Table 17: Overview of measured of vertical component (σ_v) and major (σ_H) and minor (σ_h) horizontal component of the measured 3D stress field. In addition the major orientation and the overburden of the measurements are given. The values are modified from Hanssen (1998).

	Overburden [m]	σ_v [MPa]	σ_h [MPa]	σ_h [°]	σ_H [MPa]	σ_H [°]
Rjukan 1	100	4,3	5,7	157	7,3	67
Rjukan2	25	2,8	1,9	148	6,8	58
Mean		3,55	3,80	153	7,05	63

The profile of the model of this study is trending in 078 direction, see Figure 23. Based on the given estimated mean stresses and mean stress orientations given in Table 17, the In-Plane and Out- of-Plane stress ratios, K, are calculated. The result is given in Table 18, showing that a reasonable stress field for the model of this study can be defined by an assumed In-Plan total stress ratio of 2,0, and a Out-of-Plane stress ratio of 1,1. Also, a "Looked In" stress can be defined. This component describes the horizontal stress at the ground surface. By recommendation from (Rocscience, 2014b) the "Looked In" stress was assumed as zero, which should be a reasonable value for the Håkåneset rock mass since it heavily dissected character imply stress relief.

Table 18: Estimated field stress for the study area based on empirical stress data found in

Parameter	Estimated value
Trend of profile	078
Mean σ_h -orientation	153
Mean σ_H -orientation	063
In-plane mean horizontal stress component	$\sigma_H = 7,05$ MPa
Out-of-plane mean horizontal stress component	$\sigma_h = 3,8$ MPa
Mean vertical stress component	3,55 MPA
Total stress ratio K ($=\sigma_{horiz.}/\sigma_{vert.}$) in -plane	2,0
Total stress ratio K ($=\sigma_{horiz.}/\sigma_{vert.}$) out-of-plane	1,1

6.3.5 HYDRAULIC MATERIAL PROPERTIES

Hydraulic properties are related to groundwater and saturated conditions, which influences the effective stresses in the rock mass. No groundwater borehole data exists for the study area. Therefore experiences from literature are used to give a reasonable estimate of the hydraulic parameters of the rock mass that are required for a Goundwater seepage analysis in Phase². The model set up is based on a *Simple* model type, which requires less input parameters. Required hydraulic parameters for the modeling are:

- A saturated permeability, Ks
- Anisotropic permeability, specified with a factor K2/K1 and a K1 Angle

In general, flow through intact rock is negligible for most rock types, thus in many studies it is common to assume that essentially all flow occurs along the discontinuities (Wyllie and Mah, 2004). Wyllie and Mah (2004) defines the term secondary conductivity, which refers to the flow in the rock mass, i.e. taking account for both the flow in the intact rock and in the discontinuities that are present. Thus, the term secondary hydraulic conductivity in Wyllie and Mah (2004) refers to the parameter saturated permeability, Ks, in Rocscience (2014b). Ks for a geologic material have a wide range of values due to its significant sensitivity to the persistence, width and infilling characteristics of the discontinuities. Typical ranges of Ks for a variety of rock types are given by Atkinson (2000). The rock masses at Håkåneset is best represented by the subgroup "*Fractured igneous and metamorphic rocks*", thus having a Ks in the range $2,5 \cdot 10^{-8}$ - 10^{-4} cm/s. The modeling was performed for both end values in order to test the significance of the hydraulic permeability parameter Ks. The rock mass in the model is assumed as homogenous and isotropic for simplicity, thus K2/K1 is 1 and the K1 angle is 0. With the *Simple* model type, an unsaturated permeability function is automatically determined by Phase2 based on the magnitude of the saturated permeability Ks and the selected Soil Type (Rocscience, 2014b). Soil type is set as General, which implies that the unsaturated permeability simply is assumed to decreases by an order of magnitude within the initial range of matric suction values, and then remains constant for higher values of suction (Rocscience, 2014b).

6.4 Parameter study

6.4.1 MODEL AND ANALYSES OVERVIEW

In numerical modeling it is essential to do simplifications of the reality. When the obtained result can be justified with actual geological conditions, the reliability of the model is increased and new factors can be added to see how they affect the result. In this study the complexity of the modeling was increased successively by adding new discontinuities. The following Model 2 are defined:

- Model 1: No discontinuities,
- Model 2: J1 joint set network
- Model 3: J1 and SF joint set network
- Model 4: J1, JF2, JF3, J4, SF joint sets networks. J1-fault, JF3-fault, and J1-back_scarp was added one at the time in the final analyses.

On each of the structural models different parameter studies was undertaken. The analyses performed with each of the models are given in Table 19, Table 20, Table 21, Table 22.

Table 19: Analyses overview on Model 1 (no joint sets)

MODEL 1		
Analysis	Sensitive parameter	Aim
Analysis 1.1	Groundwater seepage analysis for isotropic and anisotropic permeability conditions	Investigate the influence of high and low water table
Analysis 1.2	Effect of SSR-area	Investigate if the defined SSR-area influences on the resulting CSRF
Analysis 1.3	Effect of lake water	Investigate the stabilizing and destabilizing effect of the lake water in the model
Analysis 1.4	Effect of material model	Investigate how the modeled stability is depended on the material model in which the modeling is based on.
Analysis 1.5	±30% rock mass properties	Take account for the uncertainty related to the estimated input values for the rock mass in the model
Analysis 1.6	Ubiquitous joint sets (J1 and SF)	Investigate if the geomorphology that is mapped out can be explained by strength factor contour plots when random joints of J1 and SF are assumed to intersect the material in the model. Based on experiences of

Table 20: Analyses overview in Model 2 (J1 joint set)

MODEL 2		
Analysis 2.1	Model with J1 joint network. Two structural domains. Initial values.	Investigate how the stability in the rock mass changes when discontinuous joints dissect the material.
Analysis 2.2-2.5	Parameter study of friction angle in the rock mass	Investigate how the stability in the rock mass changes with decreased shear strength
Analysis 2.6-2.9	Parameter study of cohesion in the rock mass	Investigate how the stability in the rock mass changes with decreased shear strength
Analysis 2.10	1) 12% reduced φ 2) 48% reduced c.	Comparing two conditions of equal stability but different rock mass parameter values
Analysis 2.11	1) 50% reduced φ 2) 50% reduced c	Investigate contour plots for a unstable slope condition
Analysis 2.12	30% reduced φ and 50% reduced c a) high water table b) low water table	Investigate contour plots for a that is assumed to be the best reflection of the actual conditions in the slope
Analysis 2.13	Parameter study joint property, JRC, JCS and	Investigate the sensitivity of slope stability due to joint strength parameters of J1

Table 21: Analyses overview of Model 3 (J1 and SF)

MODEL 3		
Analysis 3.1	Model with J1 and SF discontinuities	Investigate the sensitivity of slope stability due to joint network properties of SF
Analysis 3.2-3.3	Parameter study on joint network property: persistence	
Analysis 3.4-3.7	Parameter study of joint property: stiffness	
Analysis 3.8-3.9	Parameter study of joint network property: length and persistence	

Table 22: Analyses overview Model 4 (all discontinuities)

MODEL 4		
Analysis 4.1	All joint sets added	Investigate the slope condition changes when all joint sets are added in the model
Analysis 4.2	J1-fault, JF3-fault, back scarp, all joints	Investigate the effect of adding major geological structures mapped in field

7 RESULTS

7.1 Results from structural analysis of TLS-data in Coltop

In order to reduce the uncertainty of the structural model obtained in the project assignment, a supplementary analysis of terrestrial lidar scan data (TLS) was performed in the 3D Lidar data analyzing software COLTOP. The aim with this supplementary structural analysis is to support the field orientation measurements and the reliability of the subdivision of joint sets defined in the project assignment, and to control if there are structures on the slope that were missed during field mapping.

7.1.1 RESULTS FROM DISCONTINUITY MAPPING IN COLTOP

Figure 28 show the point cloud model of the Håkåneset rock slide that was used for the structural analysis in COLTOP. The model is based on terrestrial laser scans from two directions, obtained by NGU in 2012. The software PolyWorks was used to clean, combine and georeference the scans before the model was exported to COLTOP.

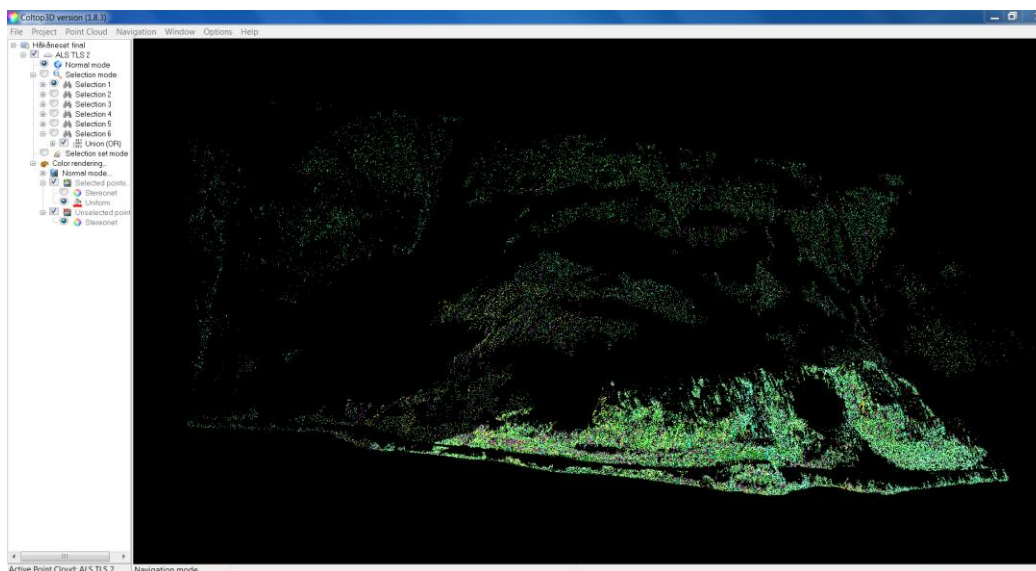


Figure 28: Print screen from the structural analyzing software COLTOP, showing the colored point cloud model of the study area at Håkåneset. The model is obtained by terrestrial laser scan from two directions in 2012.

The COLTOP-model reflects exposed surfaces as areas with homogeneous color in the point cloud, as described in Chapter 4.2.1 and Figure 12. The surfaces are interpreted to reflect the discontinuity sets that are present in the rock masses on the slope. In the Håkåneset model, six different colors were mapped out: green, yellow, turquoise, pink, purple and light yellow/green, see Figure 29.

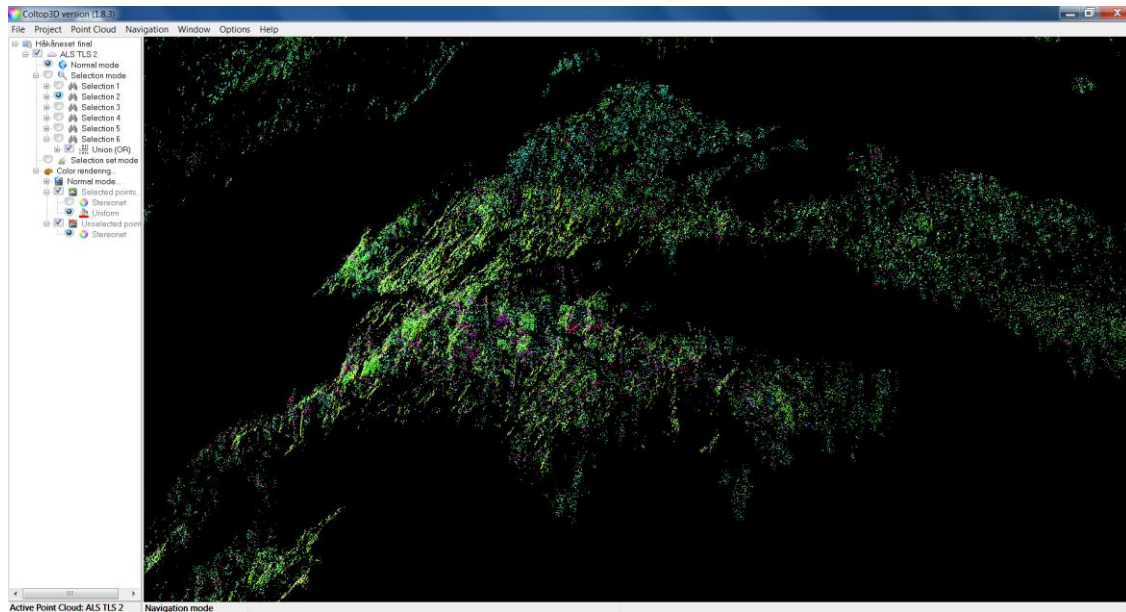


Figure 29: COLTOP displays exposed surfaces as areas with homogeneous color. The surfaces are interpreted to reflect the discontinuities that are present in the rock mass. Six color selections were defined and mapped out in the Håkåneset: turquoise, green, yellow/blue, light yellow/green, pink and purple.

10-30 surfaces of each color-selection were mapped out by drawing polygons. The output of these polygons is a high number of orientation (Dip direction/Dip) measurements. The number of measurements is referred to as *#Points* in Table 23. Some brief observations for each color-selection is listed in Table 23. Several of the selections are pronounced only as small surfaces that were difficult to define without including many scatter points, resulting in a relative wide standard deviation. Also, since the joint sets in Håkåneset in general are vertically dipping, points in one surface might have a 180 degree difference in dip direction, and consequently the color of the surface will not be homogeneous (Selection 4: yellow/blue is a good example).

Table 23: Surface selections mapped in the COLTOP-model. All data plotted in a stereographic projection pole plot.

Color	Selection	#Surfaces	#Points	Observation	Stereographic projection
turquoise	1	24	10336	<ul style="list-style-type: none"> — Mainly in the upper south domain. — Dominant systematic joints in the block area in the upper south domain. 	
green	2	30	22658	<ul style="list-style-type: none"> — Big slope parallel surfaces in the back wall. — The most pronounced color in the entire slope. 	
pink	3	30	4581	<ul style="list-style-type: none"> — Only small surfaces. — Visible in the whole model. — Variable density. 	
yellow/blue	4	19	7739	<ul style="list-style-type: none"> — Best pronounced in the road cut. — Often together with green color. 	
purple	5	11	3149	<ul style="list-style-type: none"> — Only pronounced in the Lower-South domain: in the block area and in the road cut directly under the block area. — Only small surfaces. — Often together with pink. 	
light yellow/green	6	20	25249	<ul style="list-style-type: none"> — Big slope parallel surfaces. — Dominant color in the lower part of the slope. — Not seen in the back wall. 	

The orientation of the six color-selections was determined by exporting the selected orientation data into the structural orientation analyzing software DiPS 6.0 (Rocscience). First the analysis was performed with data from the whole area. Second, data for each structural domain (North, Lower-South and Upper-South) were exported to DiPS separately and analyzed. The subdomains were defined in the project assignment, due to a systematic spatial structural variability in the slope, see Figure 19. Joint set orientations were determined by cluster analysis in contour plots (lower hemisphere, equal area, Fisher distribution). The

contour range was set to 2 -10 and 10 intervals, and the joint sets were defined by drawing a window covering all measurements within this contour range. Due to this setting some joint sets are not statistically significant, thus orientation data are not determined for these joint sets in the particular domains. The result is given in Table 24 as mean orientations (Dip direction/Dip) and its standard deviation. The same procedure has been performed on the orientations measurement data from the field mapping, given in Table 5.

Table 24: Results of structural analysis of TLS-data in Coltop, given as mean orientation (Dip direction/Dip) and standard deviation of identified surface color selections.

		<i>Domains</i>					
	<i>Colour</i>	<i>Entire study area</i>	<i>North</i>	<i>Lower-South</i>	<i>Upper-South</i>	<i>Back Wall</i>	
<i>Selection</i>	1	turquoise	15°/60° ± 19°	26°/47° ± 19°	11°/67° ± 18°	10°/56° ± 10°	17°/67° ± 15°
	2	green	66°/67° ± 16°	67°/65° ± 17°	71°/67° ± 17°	68°/65° ± 17°	63°/68° ± 13°
	3	pink	221°/79° ± 18°	232°/76° ± 15°	216°/79° ± 15°	211°/81° ± 15°	234°/79° ± 15°
	4	yellow/blue	122°/75° ± 19°	125°/69° ± 17°	123°/76° ± 17°	-	108°/76° ± 19°
	5	purple	260°/73° ± 18°	-	258°/74° ± 17°	-	-
	6	yellow/white	80°/44° ± 21°	77°/54° ± 23°	80°/43° ± 21°	89°/41° ± 19°	-

7.1.2 COMPARING STRUCTURAL ORIENTATION MEASUREMENTS: TLS VS. FIELD

The discontinuity orientations mapped in TLS-model, Table 24, was compared to the discontinuity orientations mapped in field, Table 5. It is clear that all selections from COLTOP can be related to one of the joint sets defined from the field measurements:

- Selection 1, turquoise surfaces, corresponds to the tectonic joint set JF2.
- Selection 2, green surfaces, corresponds to the slope parallel exfoliation joint set J1 in the steepest parts of the slope.
- Selection 3, pink surfaces, corresponds to joint set J4.
- Selection 4, yellow/blue surfaces, corresponds to the tectonic joints set JF3.
- Selection 5, purple surfaces, can be J1 or J4, see discussion in point 3) below.
- Selection 6, light yellow/green surfaces, corresponds to the slope parallel exfoliation joint set J1 in the shallowest part of the slope.

The structural analysis of TLS-data confirms that all dominant joint sets in the Håkåneset rock slope were mapped. Table 25 present the comparison between discontinuity orientations (Dip direction/Dip) derived from field data and from TLS-data. Data for each defined joint set is given for the entire study area and for

Table 25: Discontinuity orientations (Dip direction/Dip) obtain by structural analysis of field measurements compared to discontinuity orientations obtained by structural analysis of TLS-data in COLTOP-3D

Entire study area	Joint set: Discontinuity	J1-1 Exfoliation	J1-2 Exfoliation	J1-3 Exfoliation	JF2 Fault plane (conjugate)	JF3 Fault plane (conjugate)	J4 Joint	SF Schistose foliation
Field	TLS	74°/59° ± 20°	80°/44° ± 21°	260°/73° ± 18°	358°/65° ± 18°	133°/77° ± 20°	208°/76° ± 16°	237°/19° ± 21°
Field	TLS	66°/67° ± 16°	80°/44° ± 21°	260°/73° ± 18°	15°/60° ± 19°	122°/75° ± 19°	221°/79° ± 18°	-
Field	TLS	71°/62° ± 16°	77°/54° ± 23°	258°/74° ± 17°	359°/69° ± 18°	137°/72° ± 14°	237°/62° ± 13°	250°/23° ± 5°
Field	TLS	67°/65° ± 17°	80°/43° ± 21°	258°/74° ± 17°	26°/47° ± 19°	125°/69° ± 17°	232°/76° ± 15°	-
Field	TLS	76°/51° ± 19°	80°/43° ± 21°	258°/74° ± 17°	355°/51° ± 14°	138°/79° ± 14°	213°/76° ± 10°	181°/32° ± 12°
Field	TLS	71°/67° ± 17°	89°/41° ± 19°	258°/74° ± 17°	11°/67° ± 18°	123°/76° ± 17°	216°/79° ± 15°	-
Field	TLS	75°/63° ± 14°	89°/41° ± 19°	258°/74° ± 17°	360°/67° ± 16°	140°/78° ± 8°	211°/81° ± 15°	-
Field	TLS	68°/65° ± 17°	89°/41° ± 19°	258°/74° ± 17°	10°/56° ± 10°	-	-	-

each subdomain. Some important trends are observed when comparing the data sets:

1. Selection 2 (green) and Selection 6 (light yellow/green) can be distinguished as separate selections, but both are observed as slope parallel surfaces in the TLS-model, thus interpreted as an exfoliation joint. The orientations of Selection 2 and Selection 6 are labeled as J1-1 and J1-2, respectively in Table 25. For all domains the orientation of the field mapped data is approximately the average value of the TLS-data based joint sets J1-1 and J1-2.
2. J1-1 is oriented NE and dips with a steeper angle than J1-2. J1-2 is oriented more towards east than J1-1 in all domains. In addition, J1-1 is observed as most dominant in the Upper-South domain and J1-2 is observed as most dominant in the Lower-South domain. The latter can be seen visually in Figure 31, as the point cloud appear green and yellow in the upper parts, and more light yellow towards the lower part. Thus, it is reasonable to assume that the dip angle of the exfoliation joint in general is steeper in the upper part than in the lower part of the slope. The same trend that was observed in the structural analysis of the field measurements in the project assignment, and was the reason for the subdivision between the two southern structural domains (Lower-South and Upper-South). The results from the COLTOP analysis support this subdivision.
3. J1_3 is represented by the surfaces mapped out as Selection 5. This joint set could either be included in Selection 3, indicate that joint set J4 has a wide range of dip direction, or they can be included in Selection 2 as a variance of the steeply dipping exfoliation joint set J1. The latter has been assumed as most likely due to the following reason: The morphology on the slope in the study area is assumed to be defined by slow deformation along reactivated inherited structures. However, the dominant exfoliation joint set is by definition not a reactivated joint set, but rather a result of this reactivation due to stress relief during the deformation. Consequently, it is reasonable to include J1_3 surfaces in the exfoliation joint set, even though it is not surface parallel, because J1_3 can be assumed to reflect a steeply dipping inherited structure that defined the formation of exfoliation. Because the morphology on the slope of the study area reflects the dominance of the J1 structure, while J4 is not observed as a regional structure in the study area, the explanation of Selection 5 being a variance of J1 rather than a variance of J4 is assumed as most likely.

4. For JF2 and JF3 there is a consistent 10-20 degree bias between the dip directions of the field mapped data and TLS mapped data. For JF2 this bias is clockwise towards and for JF3 this bias is counterclockwise. An possible explanation of this bias is:

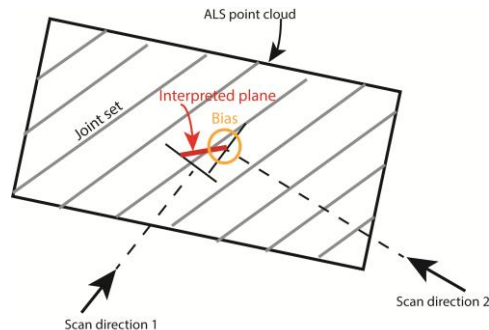


Figure 30: In Polyworks the colored surfaces are obtained by interpolation of a plane between two scan directions. This might cause a bias due to the scan direction This is likely to be the reason for the systematic difference between the field orientation measurements and the TLS orientations measurements of JF2 and JF3.

5. Foliation planes are not mapable in the TLS data model in COLTOP. This is as expected since the foliation seen in field was dipping with a low angle, and will therefore be approximately parallel with the laser beam. Consequently, foliation planes are not covered in the point cloud model. This highlights the importance of field mapping in order to detect all discontinuities that are present in a rock mass.

7.1.3 CONCLUSION

The structural analysis of LiDAR-data in Coltop support the reliability the field measurements, and indicate that all discontinuity sets that are dominant in the slope have been mapped in the field. There is no significant difference in the estimated orientation data derived with the two applied approaches. Therefore, the kinematic model obtained in the project assignment can be considered as representative for the Håkåneset rockslide, and is considered a good basis for further stability analysis of the rockslide.

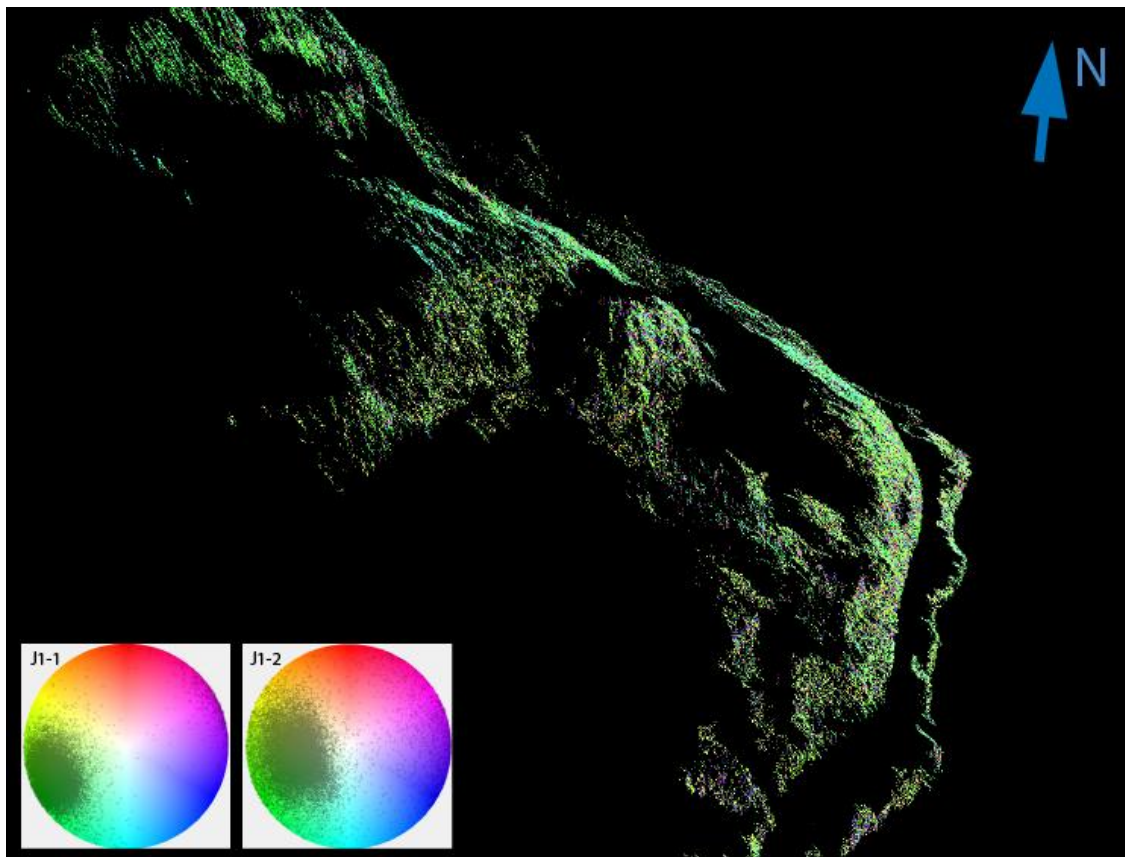


Figure 31: A systematic structural variability in the exfoliation joint set J1 is observed: the upper and central part is colored green and yellow, respectively, and the lower part is colored more light yellow. From the stereographic plots in the left corner this color trend indicate that the upper part of the slope is dominated by more steeply dipping surfaces than the lower part. The same trend was observed in the field mapped data in the project assignment.

7.2 Results from deformation analysis of TLS-data in Polyworks

A deformation analysis of the instability at Håkåneset was performed in order to identify displacements of rock masses and the volume of these. TLS-data models from 2012 and 2013 were compared to search for significant displacement.

No critical areas with significant displacement can be reported for the study area after the performed stability analysis in IMInspect, Polyworks. However, it is important to highlight that the data TLS-data models used for the analysis were limited. These limitations are due to vegetation cover, resulting in a model with decreasing points density for the southern part of the slope. Because of this the combination and comparison of the models was difficult, which lower the reliability of the results.

Figure 32 is the output model from the comparison of the 2013 model with respect to the 2012 model in IMInspect. The color codes are used to interpret the displacement activity in the slope. Note that grey color represents areas that have not been cleaned for vegetation in the 2013 TLS-data. The following conclusions can be interpreted from the performed analysis:

1. As a first step in the analysis the models from 2012 and 2013 was combined taking only the assumed stable areas, i.e. the northern part (right) and the upper most part of the slope into account. This procedure is undertaken by ignoring the points of the assumed unstable areas. Green color represents areas that have been nicely fitted, and by this it is seen that the fit alignment is good in the right part of the model. A green color would also be expected in the uppermost part of the slope, since this is defined as the back scarp of the instability. However, the error seems to increase towards the left of the model - indicated with more yellow and red colors. This is a clear indication of the limitations of the model that has been used for this displacement analysis, as regards insufficient point density of the left part of the model. This observation has to be remembered for further interpretation of the color codes within the limits of the unstable rock masses.
2. Blue color is pronounced in the parts representing the upper block area. The blue color indicates a negative rock mass volume, and could therefore be interpreted a sign of significant rock fall. However, when further investigating theses blue areas, it was revealed the 2012 scan has a limit in this part, see Figure 33. Consequently, large errors occur when the 2013 scan is compared to the reference scan in this region

because there are no points to be compared against in the 2012 data set. Thus, there is not sufficient evidence to conclude that there has been rock fall activity in the upper block area based on this analysis

3. The color codes along the road cut have a trend of increased error towards the left (south), where yellow and red colors correspond to increased rock mass displacement. This is the same trend observed for the upper part of the model in stable rock masses, as discussed in point 1, which means that this trend can be explained with the insufficient fit between the analyzed models. Because of this, the trend of a positive rock mass in this part of the slope cannot be interpreted as rock mass displacement.

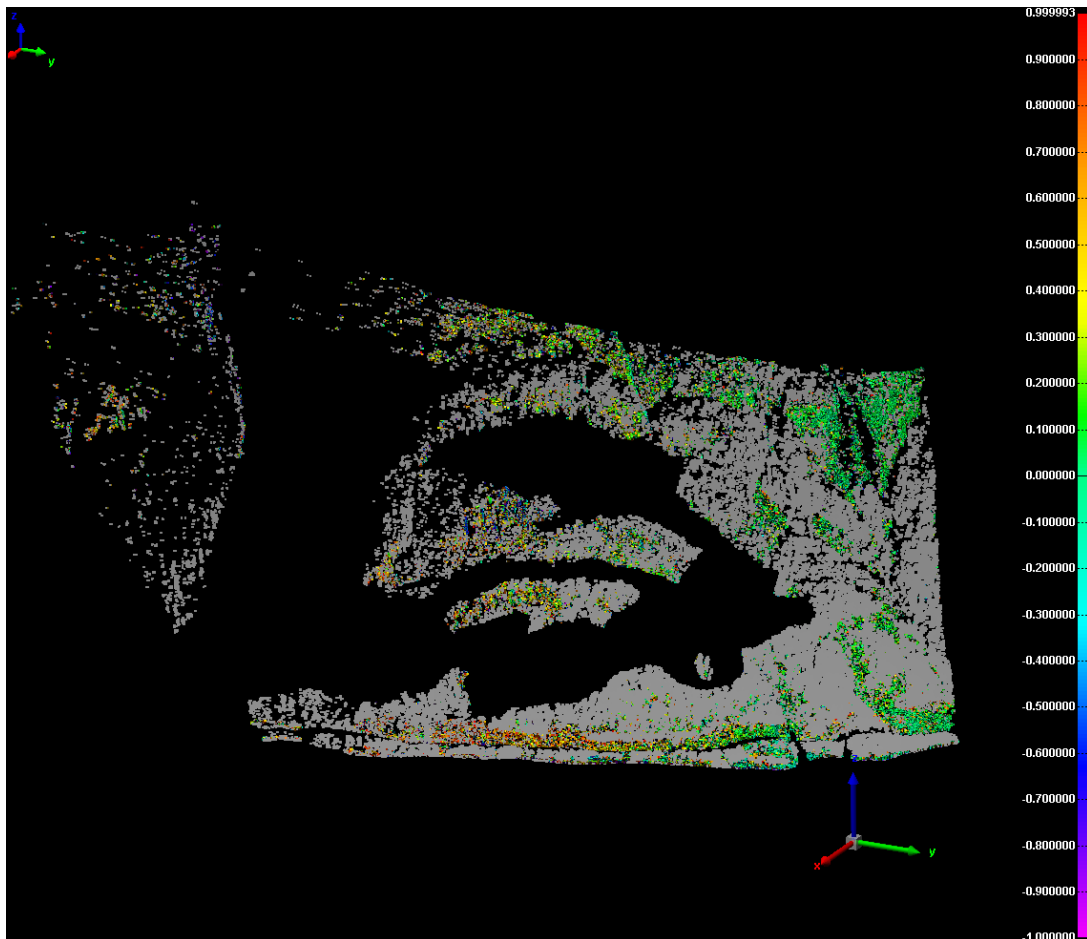


Figure 32: Output model from displacement analysis in IMInspect, Polyworks, by comparison of TLS-data models from 2012 and 2013. No critical displacement areas are revealed. Pronounced color cod

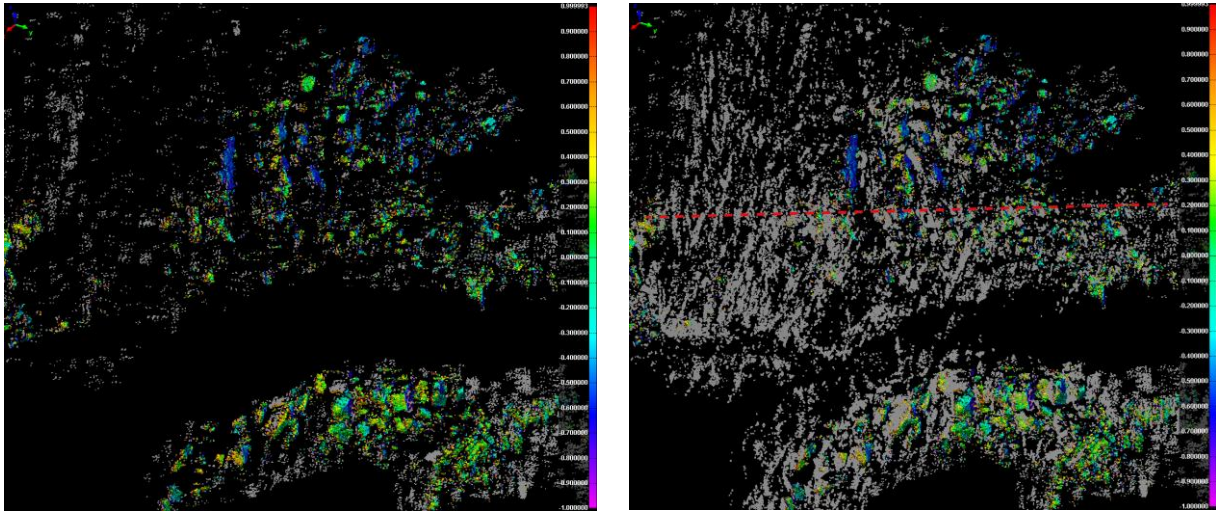


Figure 33: In the left figure both 2012 and 2013 data are displayed. In the right figure only 2013 data are visible. It is clear that the 2012 scan has a limit in the area, indicated with the red dotted line, that results in blue color (negative volumes). Thus, there is not sufficient evidence to conclude that there has been rock fall activity in the upper block area based on this analysis.

Conclusion of displacement analysis

Due to the quality of the data set the analysis is dominated by a systematic error because the fit alignment between the temporal models is bad. Thus, the results obtained by the analysis in this study cannot be used for further discussion of the slope stability condition at Håkåneset.

7.3 Results of stability analysis with numerical modeling in Phase2

This chapter presents the results obtained by numerical modeling using a finite element method (FEM) with a shear strength reduction (SSR) approach. Four structural models have been investigated by successively adding new discontinuities. The stability has been investigated by parameter sensitivity tests for different hydrogeological conditions and rock mass and joints properties, resulting in different critical strength reduction factor (CSRF). As a vital achievement of the stability analysis of the Håkåneset rockslide is to predict the most likely location and geometry of a potential sliding surface in case of a large-scale slope failure. This is done by visual analysis where maximum shear strain plots are used to interpret active-passive zones. According to Stead and Eberhardt (2013) will the failure surface geometry have a significant influence on the rock slope damage. With this, evaluation of shear strain at different slope conditions is justified as an efficient approach for indicating a probable sliding plane. Contour plots for total displacement, horizontal displacement and vertical displacement have also been interpreted in the study. When reading the results it is important to remember that the contour range values differs for each plot, and consequently the colors can only be used for interpreting relative changes within one plot and not for comparison of different analyses

An overview of performed analyses was given in Table 19, Table 20, Table 21 and Table 22.

When a model for numerical modeling is constructed, it is necessary to do significant simplifications of the reality. It must be emphasized that the result from a numerical modeling can never be of better reliability than the quality of the input data. Several uncertainties are discussed for the input values used in this study, related both to the model itself and to the rock mass input parameters. This must always be kept in mind when interpreting the results, and they should never be trusted as finite answers.

7.3.1 GROUNDWATER SEEPAGE ANALYSIS

This study uses a groundwater seepage analysis to model a groundwater table based on assumed hydraulic rock mass properties. Since there exist no hydraulic data and the

knowledge about the hydrogeological conditions in the jointed rock mass are limited, the obtained results are extremely uncertain.

A sensitivity study on the required hydraulic properties (K_s , K_2/K_1 and K_1 angle) has been performed. The aim with the sensitivity test is to model a groundwater table that is reasonable due to the field observations regarding the in situ water conditions, and to see how the location of the groundwater table affects on the stability conditions in the slope model. Chosen input values for the analyses are discussed in Chapter 6.3.5.

Analysis 1.1_1: Isotropic permeability conditions

1) Lowest hydraulic conductivity

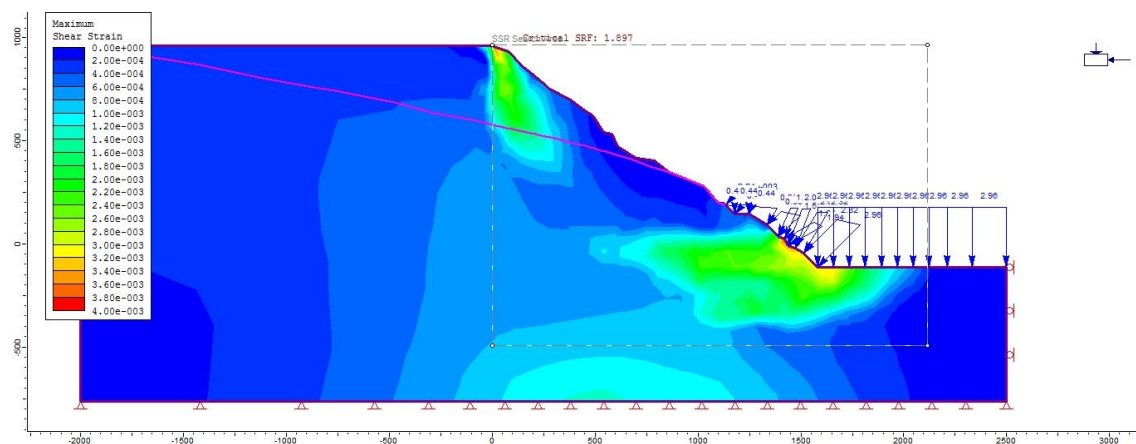


Figure 34: Maximum shear strain contours of Analysis 1.1. for isotropic permeability conditions and saturated permeability $K_s = 2.5 \times 10^{-8}$ the predicted groundwater table (purple line) is at surface for the area corresponding to the instability of this study. Critical SRF of 1.9 is obtained.

Figure 34 illustrates the maximum shear strain plot for a low value for saturated permeability, $K_s = 2.5 \times 10^{-8}$, and isotropic permeability conditions. The modeled groundwater table is represented as the purple line. The result is a groundwater table at the surface of the slope for the area corresponding to where the instability in this study is located. The shear strain contours indicate strain concentration in the toe and at the top of the slope. A critical SRF of 1.9 is obtained under the specified conditions.

Justifying the SSR-area

The dotted square in Figure 34 represents the defined SSR-area that is defined in order to get the most time effective model. Before the analysis of geological factors could start, it was considered necessary to investigate if the SSR-area influenced the result. When Analysis 1.1 was run without a SSR-area (referred to as Analysis 1.2 in Table 19) the CSRF and strain concentration zones were not significantly changed. Hence, the application of SSR-area in the model could be considered justified as not affecting the results of further modeling.

Analysis1.1_2: Highest hydraulic conductivity

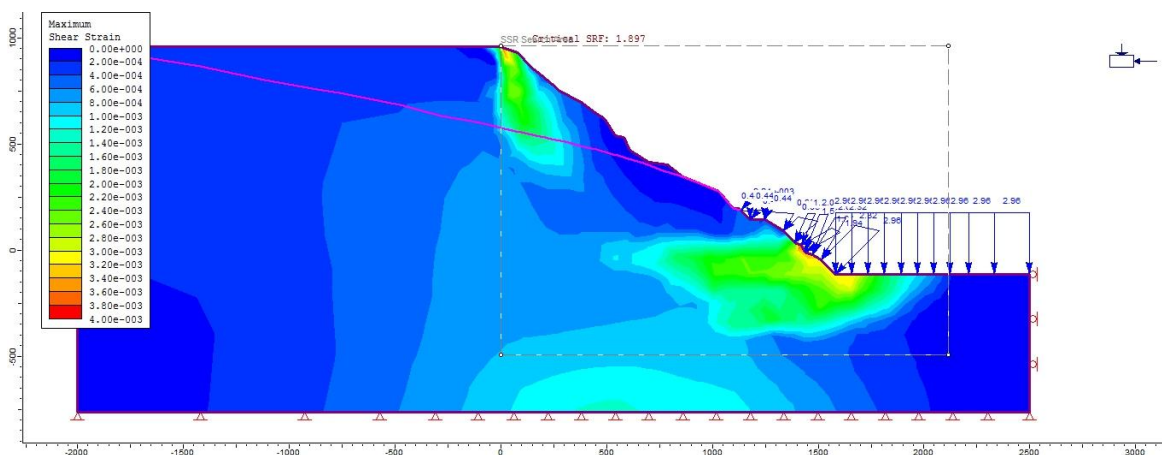


Figure 35: Maximum shear strain contours of Analysis 1.1 for isotropic permeability conditions and saturated permeability $K_s=1 \times 10^{-2}$. The predicted groundwater table (purple line) and CSRF are unchanged compared to Analysis 1.1_1.

Figure 35 illustrate the resulting shear strain conditions for Analysis 1.1_2 that assumes isotropic hydraulic conductivity that is a factor of 10^6 higher than assumed in Analysis 1.1_1. The groundwater table follows the slope surface in the area corresponding to the location of the Håkåneset instability, and the CSRF is unchanged 1.9 to the value obtained in Analysis 1.1_1. Strain concentration is predicted in the toe and at the top of the mountain slope. Thus, the result of Analysis 1.1_1 and Analysis 1.1_2 indicate that the magnitude of the hydraulic conductivity over the range that is assumed reasonable for the jointed rock mass at Håkåneset does not have a significant effect on the slope stability. Due to this observation it was decided to base further modelling on the mean hydraulic conductivity of $5.0 \cdot 10^{-5}$.

Analysis 1.1_3: Anisotropic permeability conditions

Figure 36 is the resulting shear strain plot when an anisotropic permeability condition is defined, assuming vertical groundwater flow with the horizontal permeability being a factor of 0.001 of vertical ($K_s = 5.0 \cdot 10^{-5}$). Under these settings a subsurface groundwater table (purple line) is predicted. Critical SRF is obtained for the value of 2.1. Strain concentrations are predicted in the same regions and of the same magnitude as in Analysis 1.1_1-2 where the groundwater table was at surface.

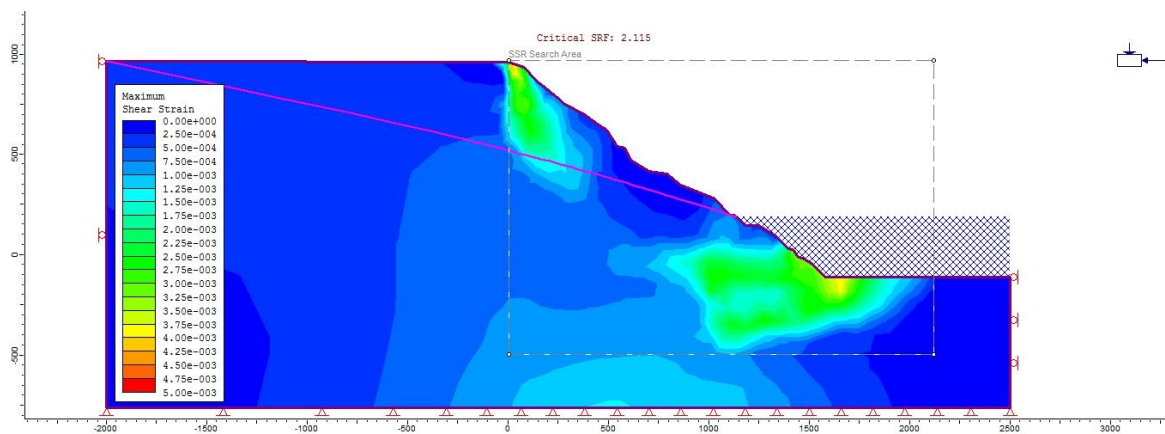


Figure 36: A subsurface groundwater table is predicted when an anisotropic permeability conditions with dominant vertical water flow is assumed. Vertical permeability defined as equal to $K_s = 5,0 \cdot 10^{-5}$ and horizontal permeability a factor of 0.001 to the vertical. CSRF of 2,1 is obtained.

7.3.2 EFFECT OF SUBMERGED-SUBAQUATIC INSTABILITY

Analysis 1.3 is conducted with the same settings as the anisotropic hydraulic model in Analysis 1.1_3, but with no lake water (pounded water and water load excluded). A critical SRF value of 2,1 is obtained. From Figure 37 show that strain concentrations are predicted at the top of the mountain slope and horizontally from the toe and into the slope.

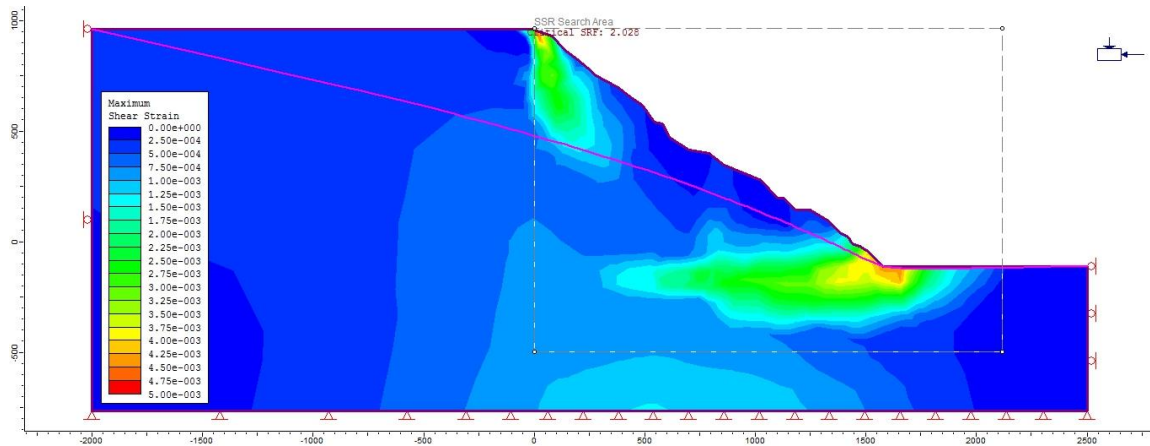


Figure 37: Maximum shear strain plot for a model without the lake water. Same model setting as in Analysis 1.1 with anisotropic conditions. CSRF value of 2.1 is obtained.

7.3.3 SHEAR STRENGTH REDUCTION (SSR) ANALYSIS

Model 1 is a topographic model with no discontinuities. A plot summarizing the resulting CSRFB for each analysis with Model 1 is given in Figure 38, and more detailed description is given in the following text. Also the results from the analyses regarding the hydrogeological conditions (Chapter 7.3.1-2) are plotted. The trend in Figure 38 indicates that the slope stability is most sensitive to factors that material properties are dependent on (material model, material strength).

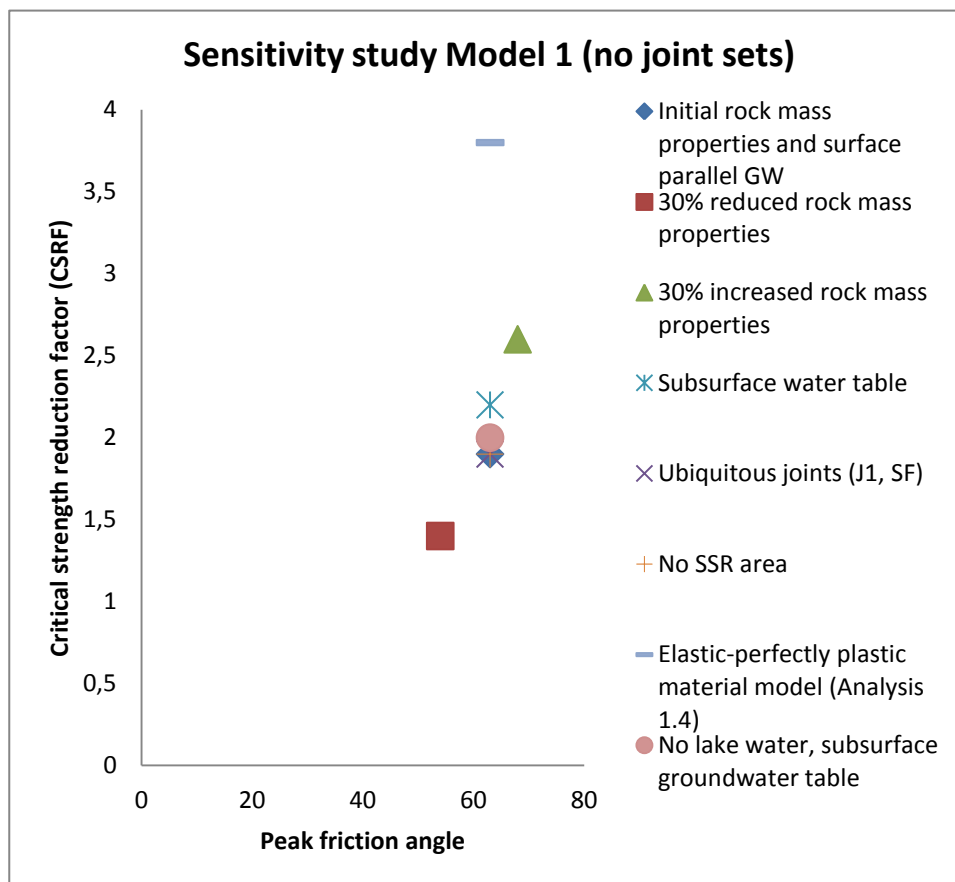


Figure 38: Summary of tested parameters with Model 1.

Influence of material model (Analysis 1.4)

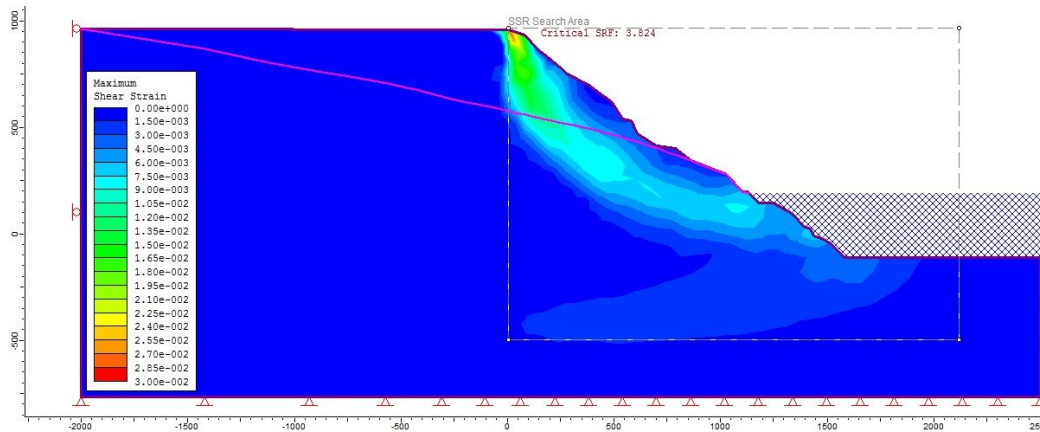
Analysis 1.1-3 assumes elastic-plastic softening material model. The choice of a material model is essential for the modeling result and therefore important to investigate.

In Analysis 1.4 an elastic-perfectly plastic (EPP) material model was assumed, that imply residual strength parameters equal the peak friction angle. Isotropic permeability was assumed to get the most conservative analysis. Compared to the model with elastic-plastic softening and isotropic hydraulic properties in Analysis 1.1, the CSRF was increased from 1.9 to 3.8 for the EPP model. The shear strain plot for the EPP model setup in Figure 39A indicates a continuous circular maximum strain concentration starting from the mountain plateau and daylighting at the level of the lake surface. In addition, maximum strain is expected in a small area at approximately 100 m depth. The total displacement plot in Figure 39B indicates a decreasing displacement from surface and into the slope, with maximum displacement at the top of the mountain slope, i.e. outside the area corresponding to the location of the Håkåneset rockslide. In Analysis 1.1 on the other hand, where residual strength was assumed to be $2/3$ of the peak value, most significant displacement was indicated in an area of the model that correspond to the submerged domain of the defined instability. The slope conditions indicated in Analysis 1.1 is to reflect the actual conditions in the slope in a better way than Analysis 1.4. Based on this it was decided to continue the further stability analysis in Phase² with an elastic-plastic softening material model, with residual material strength values assumed as $2/3$ of the peak values.

Model 1: No joints

Analysis 1.4: Elastic-perfectly plastic material model (residual strength 2/3 of peak value)

A)



B)

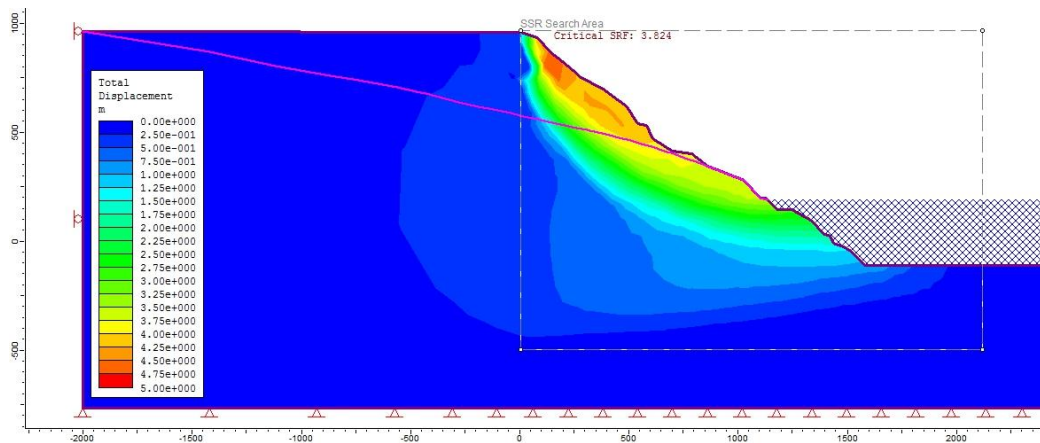


Figure 39: Elastic-perfectly plastic model setup. A) Maximum shear strain contours. B) Total displacement contours

Analysis 1.5: Parameter study of material strength properties

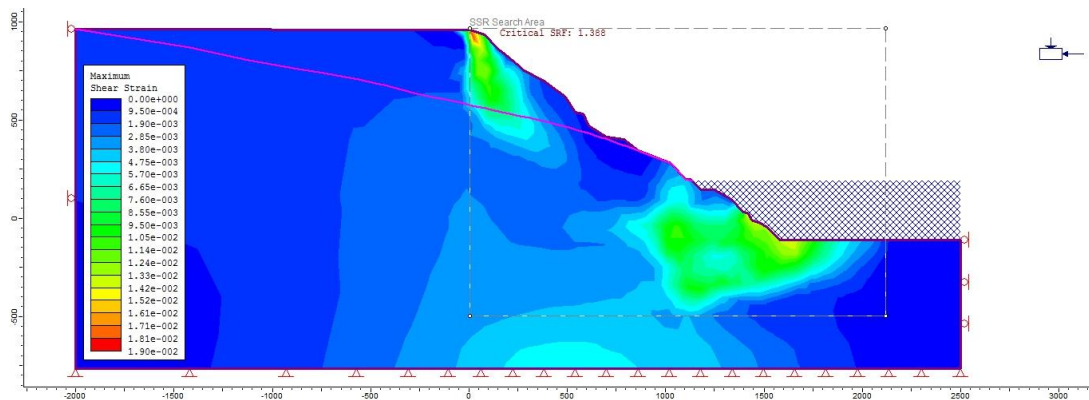
In Analysis 1.5 a parameter study on rock mass strength parameters was conducted. Groundwater table at surface is used in order to obtain the most conservative analysis. First all generalized Hoek-Brown parameters (σ_{ci} , GSI, m_i , D and E_i) used to calculate the Phase² input parameters were reduced 30% (input values given in Table 10). A model with reduced rock mass strength parameters resulted in a decrease of critical SRF from 1.9 to 1.4.

Maximum shear strain contours for this model setup is shown in Figure 40A), where strain concentration is indicated in the lower part of the slope, thus it coincides with the location of the unstable area. Figure 40B) show that maximum total displacement is indicated in the submerged component of the unstable slope.

Model 1: No joints

Analysis 1.5: 30% reduced rock mass strength

A)



B)

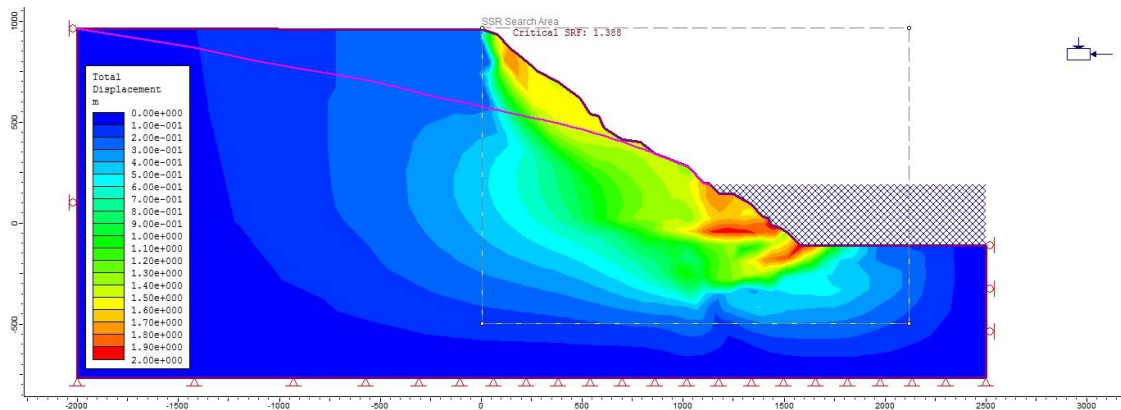


Figure 40: A) Maximum shear strain contour plot and B) Total displacement contour plot for 30%

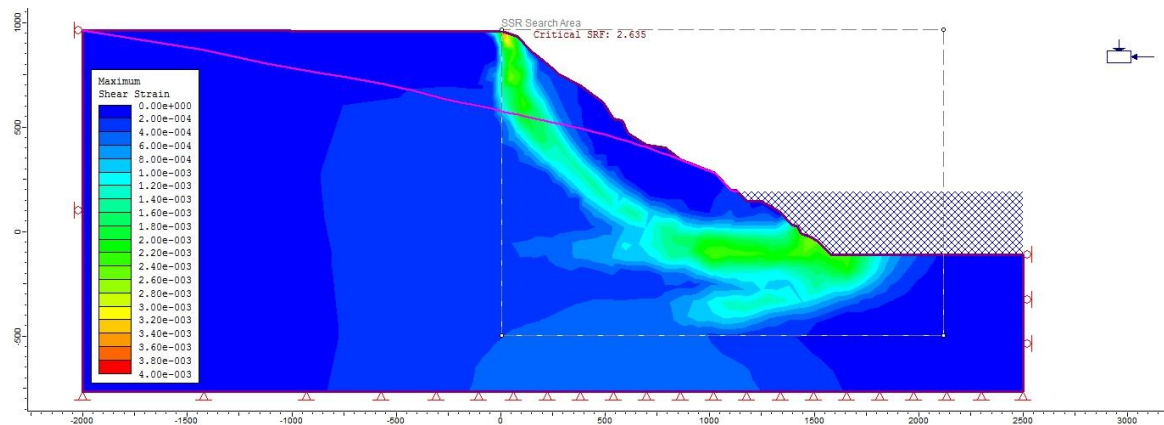
Secondly, the generalized Hoek-Brown parameters were increased with 30% (Table 10), resulting in increasing critical SRF from 1.9 to 2.6. Figure 41A shows that a model setup with

increased material strength properties predict a circular shaped maximum shear strain concentration area starting at the top of the mountain slope and continue down to the toe. Again the total displacement plot in Figure 41B indicates most displacement activity in the central part of the submerged slope component.

Model 1: No joints

Analysis 1.5: 30% increased rock mass strength

A)



B)

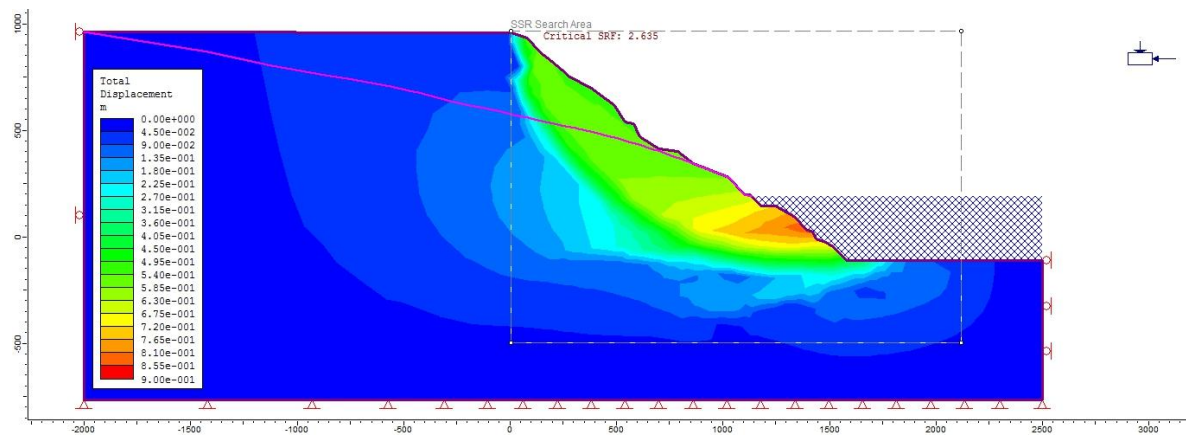


Figure 41: A) Maximum shear strain contour plot and b) Total displacement contour plot for 30% increased rock material properties (Analysis 1.5).

Model 1 with ubiquitous joints J1 and SF (Analysis 1.6)

In Analysis 1.6 J1 and SF joint sets were added to the Model 1 as ubiquitous joints. Groundwater table at surface is used in order to obtain the most conservative analysis. From

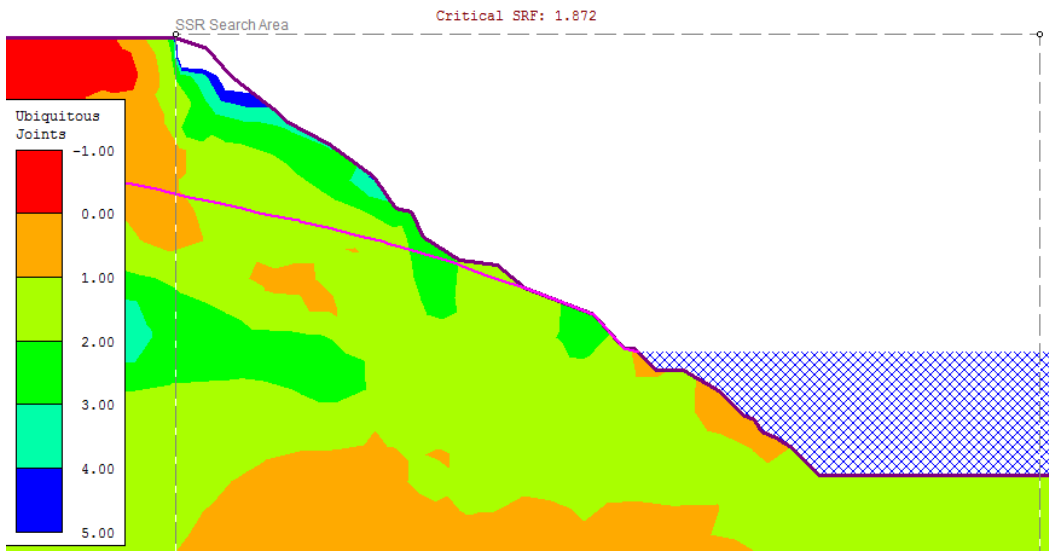
the kinematic feasibility test (see Chapter 5.4.2) it was concluded that the exfoliation joint set, J1, and the schistose foliation joint set, SF, are the most interesting joint sets for further investigation of the slope stability at Håkåneset regarding a massive slope failure. Therefore, these joint sets were included as ubiquitous joint sets in the stress calculations of Model 1, in order to get a first impression whether the stresses generated from the finite element analysis are sufficient to cause slip along planes with J1 and SF orientation based on the specified discontinuity strength parameters only. Barton-Bandis joint strength input parameters values is given in Table 14.

The resulting strength factor contour plot of Model 1 is presented in Figure 42. By definition, the factor of safety (strength factor) is the shear strength divided by the shear stress, implying that a FoS less than 1 indicate slip. In Figure 42A) only J1 is added as a ubiquitous joint in the model. The field estimate of JRC = 14 for J1 joint surfaces gave no critical FoS in the slope model. However, by reducing JRC to 5, the contour plot in Figure 42A) was obtained, indicating two critical areas in the submerged part of the slope. In Figure 42B) SF is added in addition to J1, resulting in expected FoS less than 1 in the region of Model 1 that corresponds to the limits of the instability of this study.

The result from the ubiquitous joint option supports the assumption of J1 and SF as critical structural factors regarding the slope stability at Håkåneset, thus the importance of J1 and SF properties was prioritized for the continuing numerical modeling .

Model 1: No joins

A) Analysis 1.6a: Ubiquitous joints J1



B) Analysis 1.6b: Ubiquitous joints J1 and SF

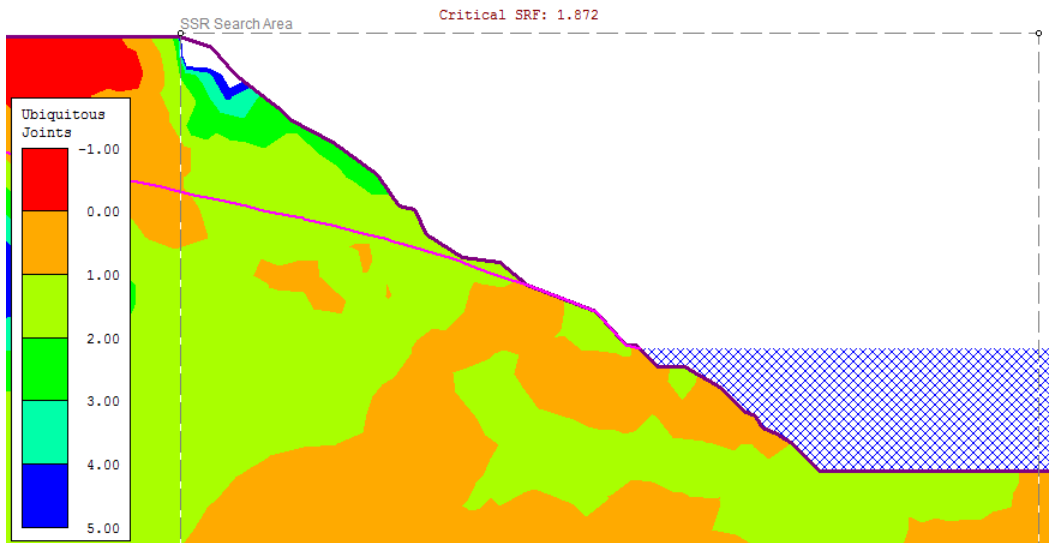


Figure 42: Strength Factor contour plots when A) J1 and B) J1 and SF are added as ubiquitous joints in Model 1. The area indicating critical conditions regarding failure (orange contour) increases from plot A) to B).

Model 2: The role of J1 on slope stability and sensitivity analysis of rock mass properties

Model 2 was constructed by adding the exfoliation joint set J1 as a joint network in the model. The spatial variation of the joint orientation of J1 in the lower part of the slope compared to the upper part (domain L-S and U-S, respectively (Chapter 5.2.2)) is taken account of. In Analysis 2.1-9 a parameter study of the rock mass properties friction angle (ϕ) and cohesion (c) were undertaken by successively reduction. Input discontinuity parameters are given in based on the Barin-Bandis slip criteria is given in Table 14. Groundwater table at surface is used in order to obtain the most conservative analysis.

Analysis 2.1: Adding J1 as a joint network in the model

Analysis 2.1 demonstrate that adding the J1 joint set to the model as a joint network had no effect on the predicted CSRf (1.9). On the contrary, the strain concentrations was significantly changed and clearly controlled by the presence of J1 joints, as can be seen from Figure 43.

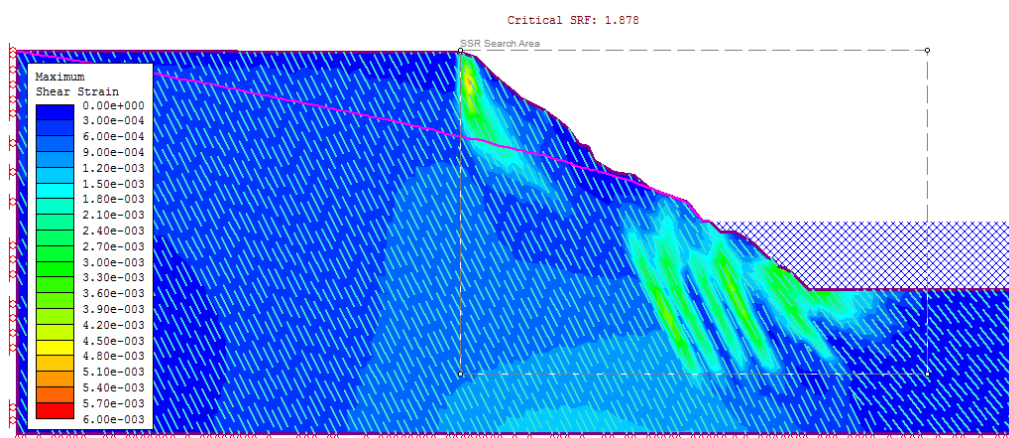


Figure 43: Maximum shear stain plot for Model 2 when initial values for rock mass and discontinuity strength are assumed. (CSRf = 1.9)

Analysis 2.2-9 Sensitivity study of rock mass strength parameters

The result form the sensitivity analysis of friction angle (ϕ) and cohesion (c) is plotted in Figure 44. The initial condition (0% reduction) correspond to the values $(\phi_{peak}, \phi_{res}) = (63, 42)$ and $(c_{peak}, c_{res}) = (1.5, 1.0)$ given in Table 11. A linear trend between safety factor (CSRf)

and parameter reduction is observed for both φ and c where CSRF is more sensitive to variations of φ than variations of c .

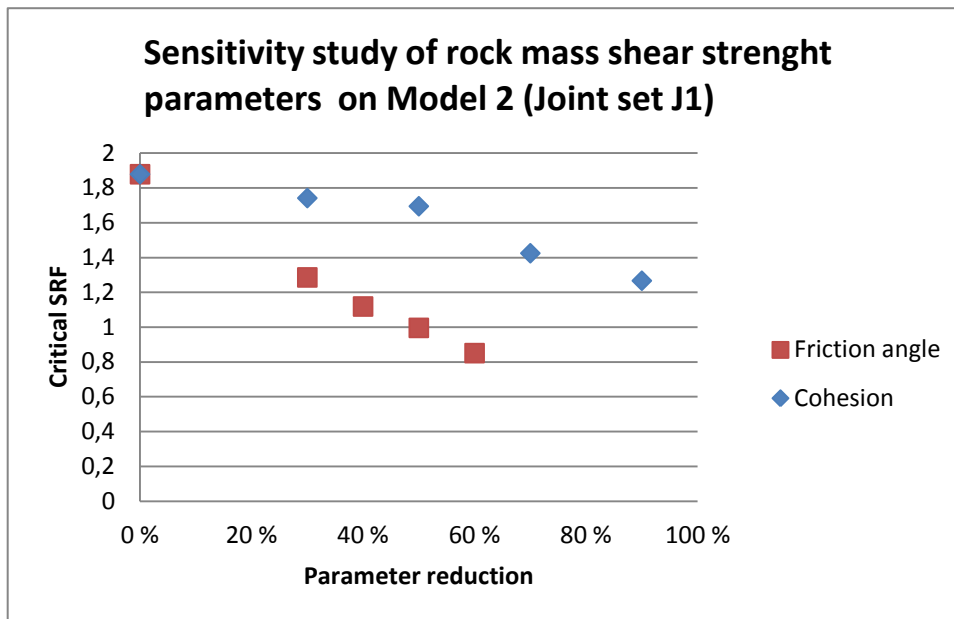


Figure 44: Result of parameter study of Model 2 by reducing friction angle and cohesion separately. CSRF appears as most sensitive to reduction in friction angle.

In Figure 45 rock mass parameter reduction is plotted in relation to the shear strength for a normal stress level of 1,4MPa. (Shear strength is calculated with Eq. 2).

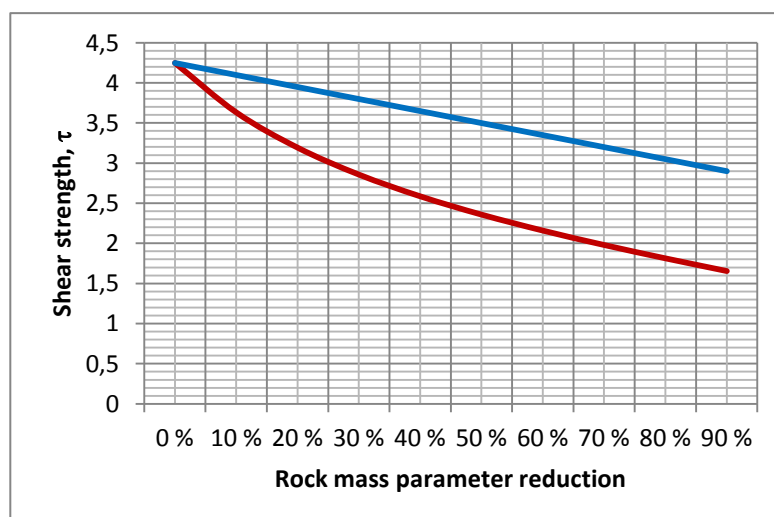
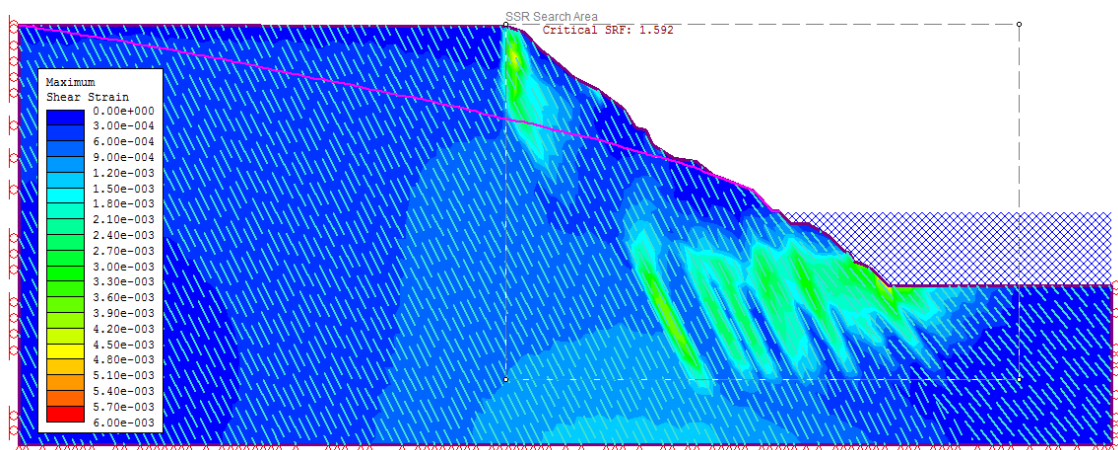


Figure 45: Shear strength sensitivity due to reduction of friction angle (red) and cohesion (blue). Calculations assumed that normal stress level is 1,4MPa.

From the relations in Figure 45 it can be read that a 12% reduction of friction angle should result in the same shear strength as 48% reduction of friction angle. Since CSRF by definition depends on the shear strength, it is expected that the two different models should indicate the same CSRF. This is confirmed in Analysis 2.10. On the contrary, the strain concentrations plots are significantly different in the case with 12% reduced cohesion compared to when only the friction angle is reduced 48%, as illustrated in Figure 46.

A) 12% reduced phi



B) 48% reduced cohesion

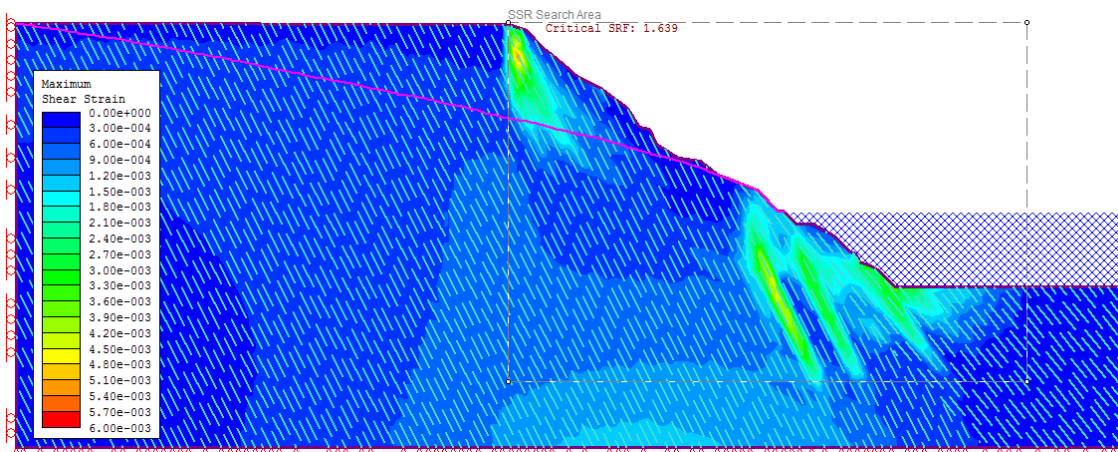


Figure 46: A) 48% reduced cohesion correspond to B) 12% reduced friction angle to obtain the same shear strength level and equal CSRF for both conditions. Even though the CSRF is equal, the strain concentration for the two conditions are significantly different.

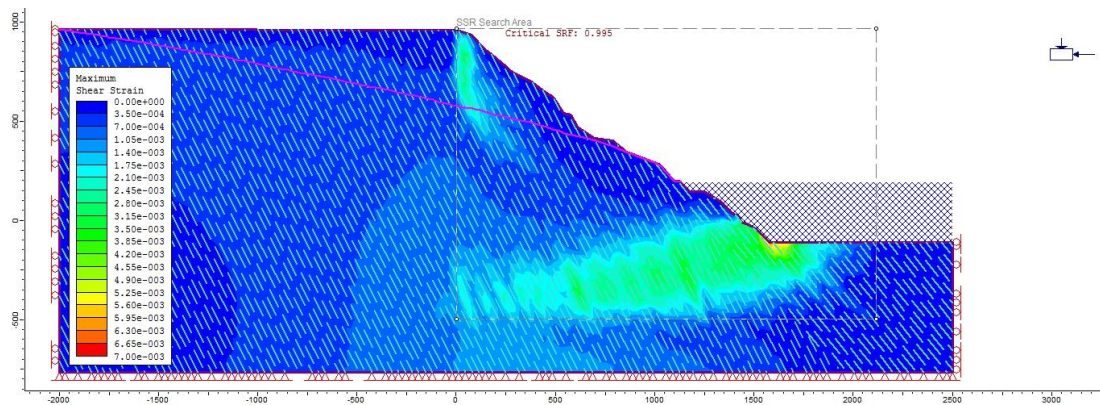
Analysis 2.11 demonstrates the expected slope conditions when a unstable condition with a safety factor less than 1 is indicated. According to the trend in Figure 44 a critical slope

condition with Safety Factor equal 1,0 should be obtained if the friction angle is reduced by 50% due to the initial values, Table 11. Figure 47A) shows maximum shear strain plot when the friction angle is reduced with 50% and a critical condition with CSRFB less than 1 is obtained. Most significant shear strain is expected from the central part of the submerged slope component and dipping into the slope. In Figure 47B) it can be seen that most significant total displacement is indicated from the level of the central part of the submerged slope.

Model 2: Joint set J1

Analysis 2.11_1): 50% reduced friction angle

A)



B)

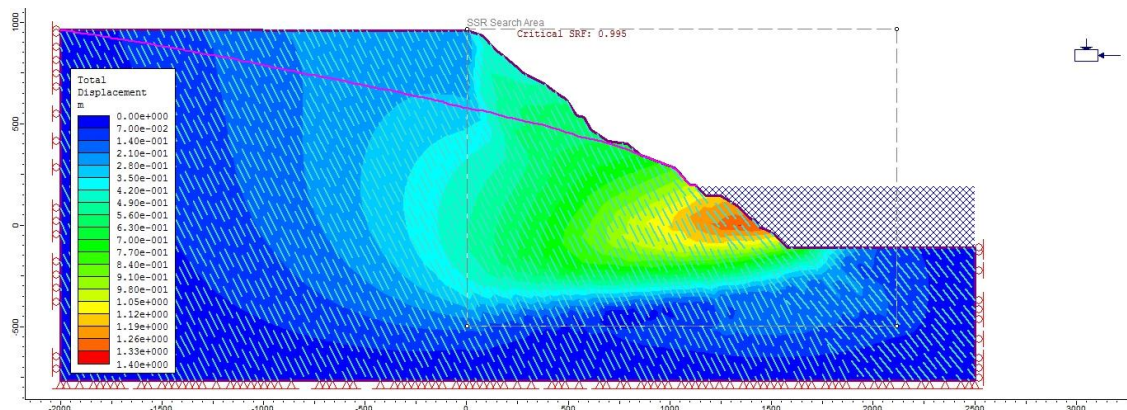


Figure 47: Model 2 with 50% reduced friction angle gives a safety factor of 1.0, which indicate unstable slope conditions. A) Maximum shear strain contour plot and B) Total displacement

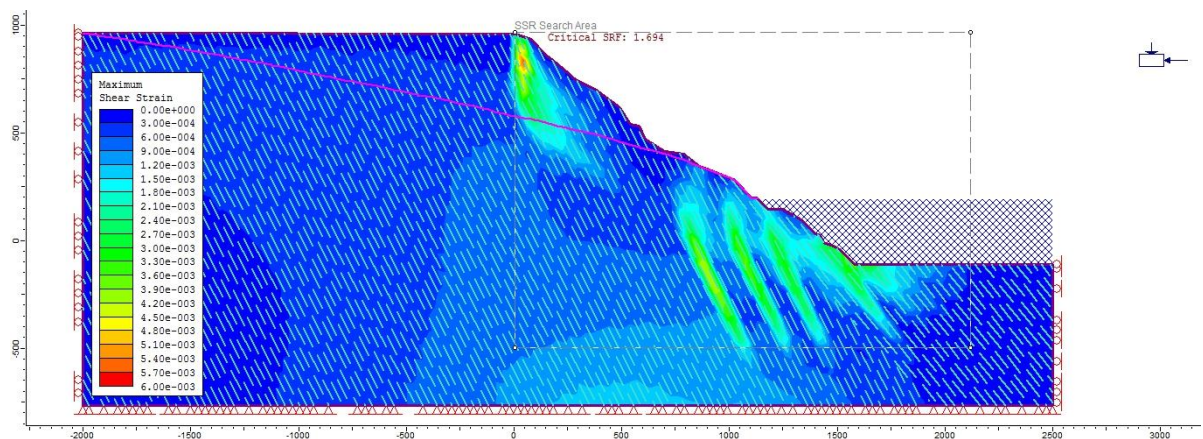
To compare, a model set up with 50% reduced cohesion was conducted, resulting in the contour plots seen in Figure 48. The shear strain plot in Figure 48A indicate maximum strain concentration in four zones that are dipping parallel with the J1 joints. Most significant

displacement, Figure 48B, is indicated in the part of the slope that is at the level of the lake level.

Model 2: Joint set J1

Analysis 2.11_2): 50% reduced cohesion

A)



B)

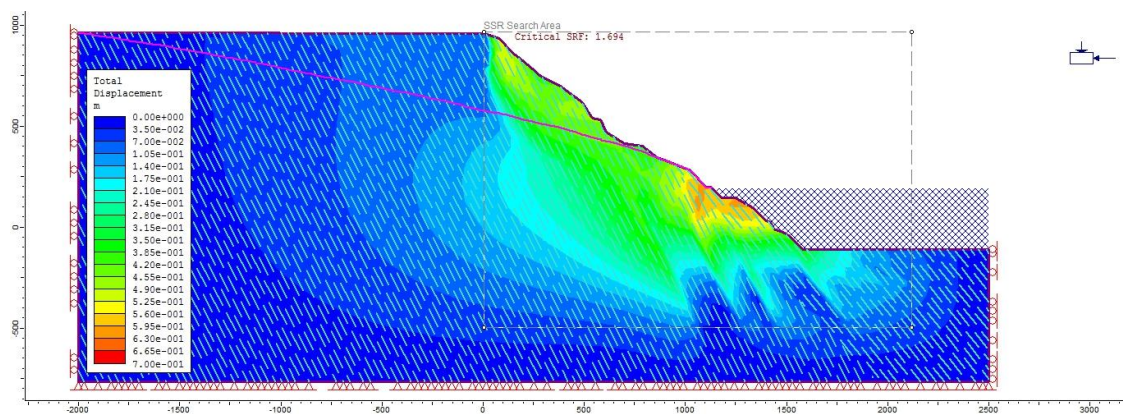


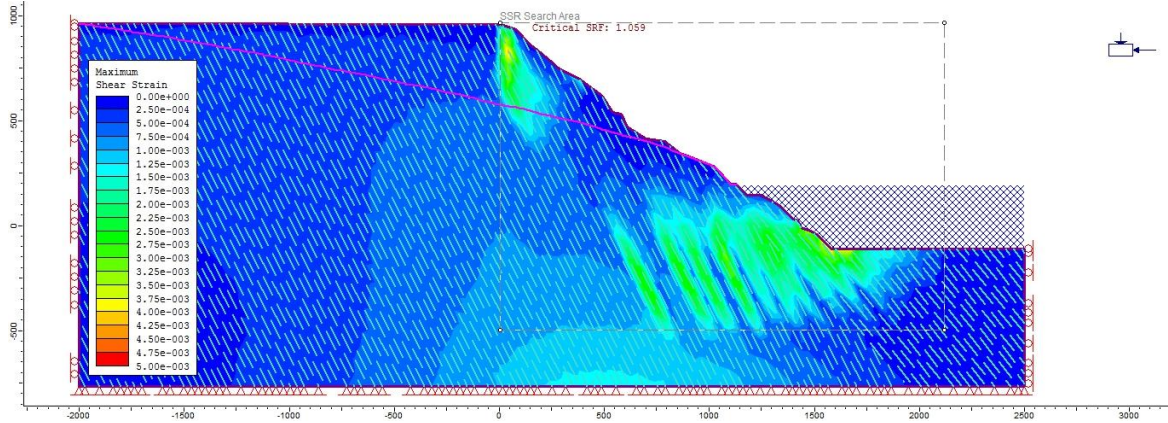
Figure 48: Model 2 with 50% reduced cohesion gives a safety factor of 1.7, which indicate stable slope conditions. A) Maximum shear strain contour plot and B) Total displacement contour plot. In this case the most active zone is indicated closer to lake surface level.

Based on the results presented above, it was concluded that conditions that bring the slope towards a critical state of failure can be obtained by reduction of friction angle, while reduction of the cohesion gives a strain condition that best describes the mapped morphology in the slope. By combining these experiences, Analysis 2.12a was conducted with a material

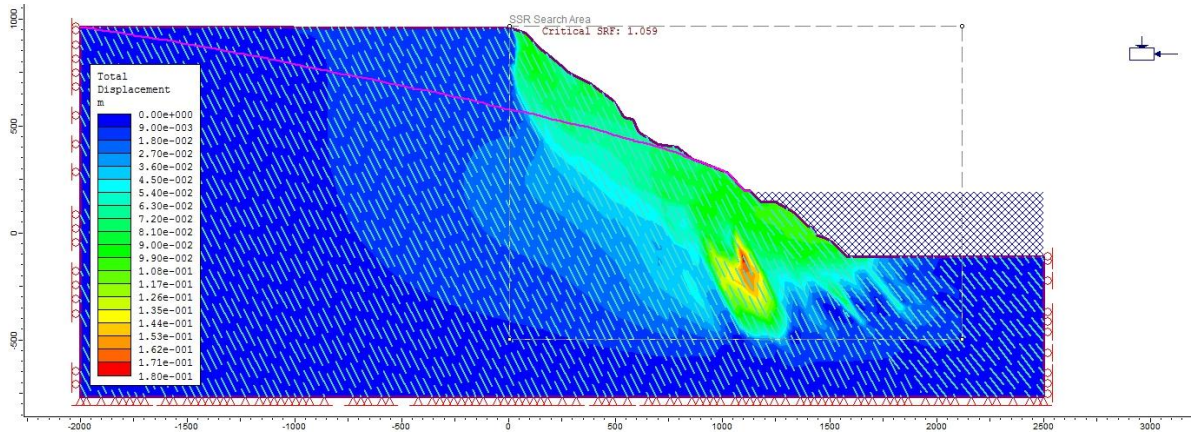
model with 30% reduced friction angle and 50% reduced cohesion to initial values. Groundwater conditions were set as conservative with groundwater table at surface. This material model setup was found by trial as the condition that brings the SRF close to the critical state at 1 and at the same time is closest to reflect the observed geomorphology in the slope. However, it is important to remember that this visual analysis is also fully dependent on other input parameters (tensile strength, E-modul, joint surface strength, hydraulic properties etc.) that are not tested for, thus the obtained values for ϕ and c that leads to a model condition that indicate failure cannot be taken as true critical values. The result of the model setup in Analysis 2.12 is illustrated in Figure 49. For this model set up a CSRF 1.06 was obtained when a high water table is assumed for a conservative analysis. Maximum shear strain zones in Figure 49A) are parallel to J1 orientation in the lower part of the model. In addition, strain condition is indicated at the top of the entire mountain slope. Figure 49B) indicate that most significant total displacement should be expected in a subsurface area (red/yellow contours) at a lake bottom level, while the horizontal displacement (abs) plot in Figure 49C) indicate most significant displacement (relative to CSRF=1) in the submerged component of the instability from the central area and up to the lake surface level.

Analysis 2.12b assumed anisotropic permeability and a subsurface ground water table a CSRF of 1.1 was obtained. The contour ranges for the anisotropic hydraulic condition is presented in Appendix 8.1, showing that the contour are only slightly different to the isotropic hydraulic condition.

A)



B)



C)

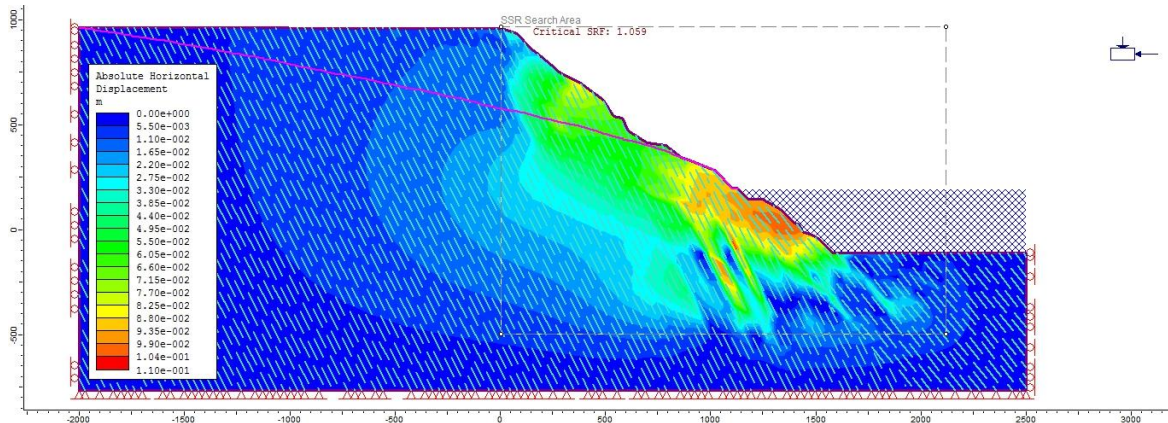


Figure 49: Analysis 2.12 on Model 2 assuming $(\phi_{peak}, \phi_{res})=(44, 29)$ (30% to initial) and $(c_{peak}, c_{res})=(0.75, 0.5)$ (50% to initial) (Table 11). A) Maximum shear strain. B) Total displacement relative

Discontinuity strength parameter sensitivity test (Analysis 2.11-13)

Joint set J1 is defined with Barton-Bandis strength parameters JRC; JCS and friction angle. The sensitivity of these parameters regarding the slope stability was investigated by reducing the JRC and JCS with 50% and the friction angle with 30% (Analysis 2.13) one at the time. For all three analyses the CSRF was constant at 1.06 and the investigated contour ranges was equal for all conditions. Thus the J1 joint shear strength properties cannot be investigated more in detail with the accuracy of the model set up in this study.

Model 3: J1 and the role of schistose foliation on slope stability

In analysis 3.1 Model 3 is conducted by adding the schistose foliation joint set SF into the model together with J1. A sensitivity test on SF strength parameters (Barton-Bandis parameters and stiffness) was considered as important because SF has been interpreted as essential in the development of a basal sliding plane. The analysis results obtained with Model 2 indicate that the rock mass strength properties are important, and varying the discontinuity parameters of J1 did not affect the result under the defined conditions. To investigate this observation further, Model 3 is constructed with the 30% increased rock mass strength properties so that the strength contrast between the intact material and the weaker joint planes is increased. In that way, the effect of varying the joint properties should be strengthened.

The result from the parameter study of SF joint set is summarized in Table 26. First the persistence of SF in the joint network model was increased from 0,2 to 0,5 and 0,8 in Analysis 3.1-3. CSRF is constant for all analyses. Joint stiffness is an uncertain parameter that is important to investigate. The joint stiffness is calculated from the average spacing (field value in Table 6) of the joint set, see Appendix 7. Because the foliation was difficult to identify in field, a parameter study is performed by assuming different spacing in Analysis 3.4-7, see Table 13. The result from varying the spacing/stiffness indicates that the critical SRF is not affected by the stiffness of the SF joint set. In Analysis 3.8 and 3.9 the length of SF was increased to 50 m in order to test if the lack of influence of SF stiffness could be because the length of the SF joints was small (10 m in Analysis 3.4-7) compared to the length of J1 (100 m). Analysis 3.8 assumes a persistence of 0.2, while Analysis 3.9 assumes persistence of 0.5. Again the CSRF was unaffected.

Table 26: Parameter study of joint stiffness and joint geometric properties of the foliation joint set (SF).

Analysis	Tested parameter	Value	CSRF
Analysis 3.1	Persistence	0,2	2,6
Analysis 3.2		0,5	2,6
Analysis 3.3		0,8	2,7
Analysis 3.4	Average spacing: <i>normal stiffness/shear stiffness</i>	0,01: 4799167/2033545	2,7
Analysis 3.5		0,1: 479917/203355	2,6
Analysis 3.6		1: 47992/20335	2,6
Analysis 3.7		10: 4799/2034	2,7
Analysis 3.8	Length/persistence	50/0,2	2,7
Analysis 3.9		50/0,5	2,6

Model 4: Investigate in the effect of adding all joint sets to the model

In Analysis 4.1 Model 4 is constructed with all joint sets and initial rock mass properties are assumed. In Analysis 4.2-3 the complexity of Model 4 is increased successively by adding continuous joints that represents mapped geological structures (see Chapter 5.3): In Analysis 4.2 the JF3-fault and the J1-fault is added as persistent joints, assuming JF3 and J1 Barton-Bandis joint strength properties, respectively. In Analysis 4.3 also the back scarp is included as a persistent joint with J1 properties. Analysis 4.4 investigates the influence of reduced rock mass when all discontinuities (joints and tectonic structures) are added in the model. Anisotropic permeability conditions are assumed for all analyses. Investigated scenarios and the CSRF obtained for each are plotted in Figure 50. Again it is observed that the most critical factor for reducing the CSRF is the rock mass properties: Analysis 4.1-3 all results in a CSRF at approximately 2, while CSRF drops to approximately 1.1 when the rock mass strength is reduced in Analysis 4.4. Analysis 2.12a and b) are also plotted in Figure 50 for comparison with other analysis modeled with reduced rock mass properties.

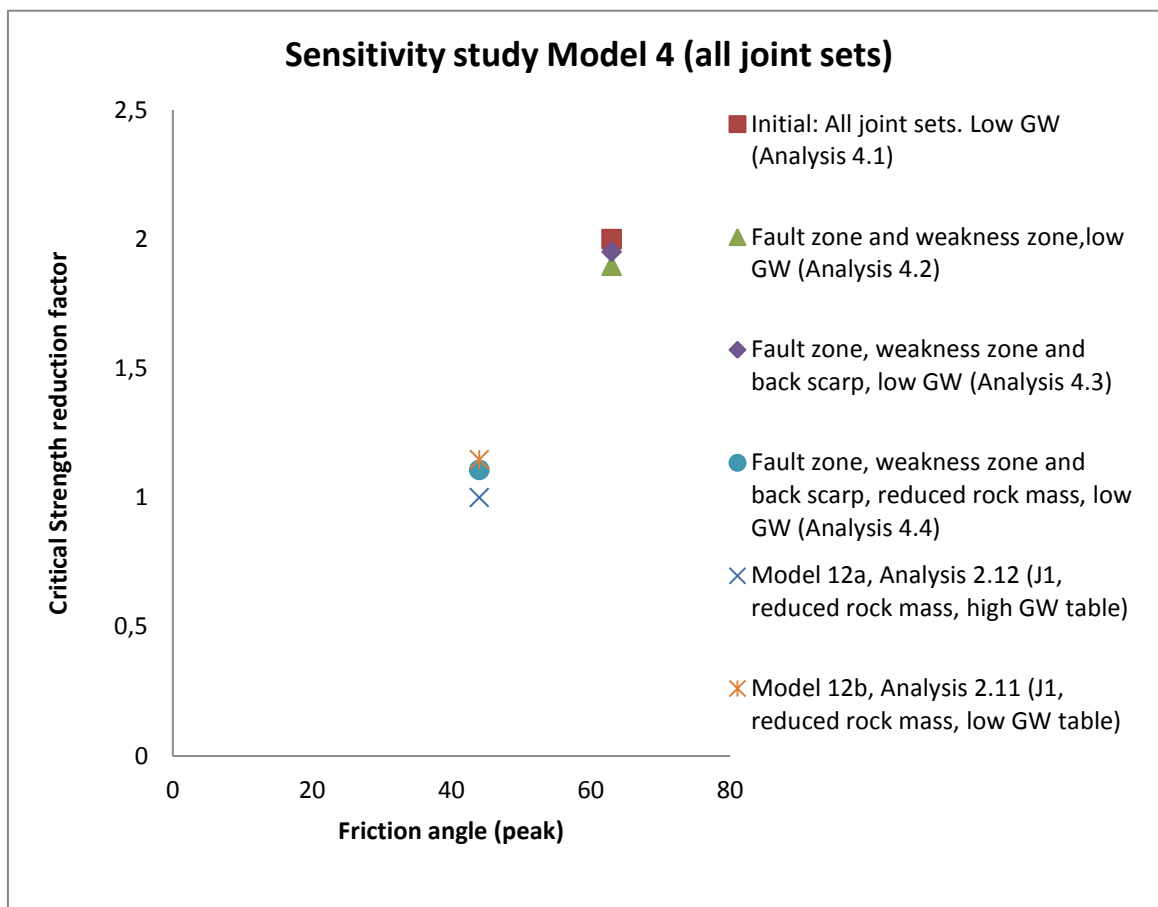


Figure 50: Sensitivity study of Model 4. Investigate the effect of adding mapped geological structures in the Model 4.

The model in Analysis 4.4 has the model set up that is closest to reality, as it includes all major geological structures that are mapped as important for the slope stability (J1, JF2, JF3, J4, SF, back scarp, J1-fault, JF3-fault and groundwater table below the surface). A CSRF of 1.1 is obtained under the specified settings. The Maximum Shear Strain plot in Figure 51A) indicates most significant strain concentration in the toe of the slope and in several steeply dipping zones in the area of the model that coincide with the assumed limits of the Håkåneset instability. In addition, a minor strain concentration area is indicated subsurface in the upper part of the mountain slope.

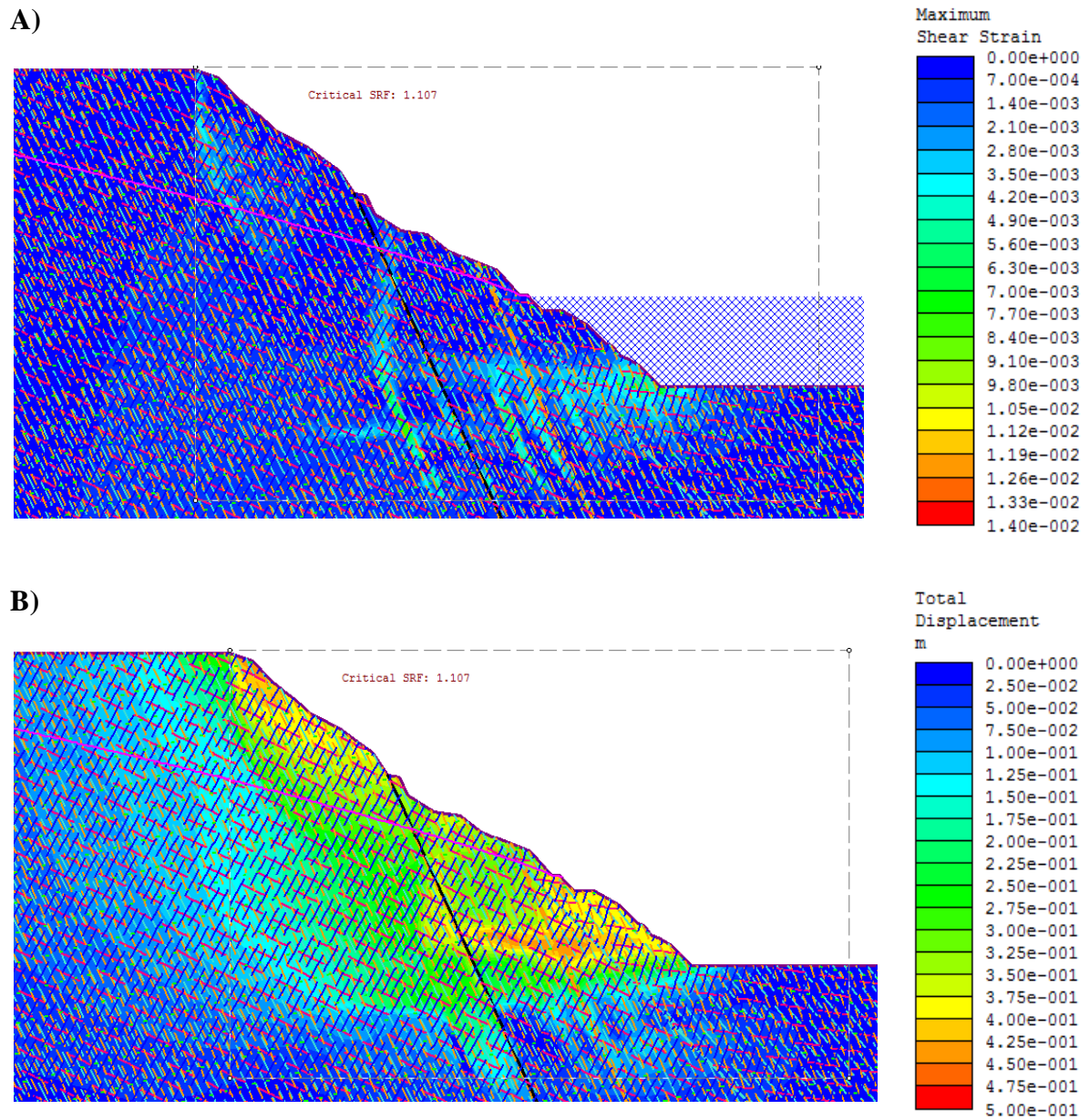


Figure 51: Subsection of Model 4. Analysis 4.4 is the most complex model constructed in this study and includes: All joint sets (J1, JF2, JF3, J4, SF), the back scarp, J1-fault zone, JF3-fault and the weakness zone that intersect the profile. When 30% reduced rock mass properties (peak $\phi = 44$, peak $c = 0,75$) and anisotropic permeability conditions are assumed the CSRF is calculated to 1.1.

8 DISCUSSION

8.1 Geological investigation of the Håkåneset rockslide

8.1.1 STRUCTURAL ANALYSIS OF FIELD AND TLS-DATA

Geological site investigation of the unstable rockslope at Håkåneset, revealed that unstable rock mass is heavily dissected by five discontinuity sets J1, JF2, JF3, J4 and SF. Supplementary structural analysis of TLS-data in COLTOP confirms that all dominant joint sets in the study area was mapped in field. A consistent bias between the orientations determined by field measurements and by TLS-analysis can be explained with the overlap in the scan direction of the TLS survey. The foliation planes of SF were not visible in the TLS-analysis, which can be justified due to its shallow dip perpendicular to the scan direction.

J1 ($075^{\circ}/63^{\circ}$, $076^{\circ}/51^{\circ}$) dips in the direction of the slope and has been interpreted as a exfoliation along preexisting joints. JF2 ($360^{\circ}/67^{\circ}$, $355^{\circ}/51^{\circ}$), JF3 ($140^{\circ}/78^{\circ}$, $138^{\circ}/79^{\circ}$) and J4 ($207^{\circ}/71^{\circ}$, $213^{\circ}/76^{\circ}$) are interpreted as inherited tectonic structures that has been gravitationally reactivated. Factors indicating that the mountain slope is heavily affected by tectonics are:

- A persistent fault zone is a reactivated tectonic structure with JF3 orientation that cuts through the study area. Hence, the JF3 joints can be considered as gravitational reactivated inherited tectonic structure.
- Mineral lineations formed by muscovite sheets, observed on a JF2 surface (described in the project assignment) support the interpretation of tectonic activity.
- JF2 and JF3 orientations fit to a conjugate strike-slip fault system that appears regionally in Telemark.
- Joint surfaces with mineralization are dominant in the entire slope. Mineralization of joint surfaces may occur by tectonic activity.
- The rock mass in the J1-fault zone that daylight in the road cut (at Location 6 in Appendix 1) is dissected by lenses structure. Lenses forms by tectonic movement.

In field the foliation SF ($277^{\circ}/15^{\circ}$, $031^{\circ}/16^{\circ}$) was observed as variable both in development and orientation. Based on analyses of oriented thin sections of in situ rock from the road cut in the study area a distinct foliation was identified with N-NE trend. Thus the direction of the foliation in the lower-south domain determined in field is supported by the thin section

analysis. The thin section analysis confirms that foliation is defined by biotite and muscovite sheets oriented in a preferred orientation parallel to deformed grains of other minerals in a fine grained matrix.

J1, JF2, JF3 and J4 are all steeply dipping, and a kinematic test indicate that the orientation of these joint sets make planar sliding, wedge sliding and toppling feasible:

1. Planar sliding is feasible in steep parts of the slope along planes of minimum dipping values of the exfoliation plane (J1) dipping 50-65 degree in NE direction towards Tinnsjø.
2. Wedge sliding formed by the intersection of the conjugate joint sets JF2 and JF3 is feasible where the slope is steeper than 50-60 degrees.
3. Toppling of small blocks is feasible due to the closely spaced joint sets J4 that dips 50-90 degrees into the slope.

The failure mechanisms described above are limited to steep slope sections only, and can only occur for small rock volumes. This is confirmed with field observations, where significant rock block toppling and wedges formations was observed in the road cut.

Large scale rock slope deformation can only be justified by assuming deformation along a combination of several anisotropies. J1 and SF have been considered as the most critical joint sets to make massive slope feasible:

1. Because J1 is steeply dipping (50-65 degree) and SF is shallowly dipping (up to 19 degree) and both with the approximately same dip direction towards NE they can form a compound sliding surface characterized as bi-planar sliding.
2. A possible back scarp and a weakness zone formed by tectonic activity are oriented like J1.
3. Mineral lineations and groove marks were observed in field on a J1 surface. These are indicators of displacement along J1, even though their presence is not statistically significant.
4. Thin section analysis indicates that microfracturing is strongly affected and develops parallel to the foliation (not statistically significant).

Due to prominent subaquatic bedrock structures on the bathymetric map (see Figure 21) it is considered reasonable to assume the same rock mass characteristics in the subaquatic component of the instability as in the subaerial. A distinct cut off in the relief of the bathymetric structures is interpreted as evidence that the two distinct SW-NE striking faults in

the central part of the studied area form the northern lateral release surface of the Håkåneset rock slide. Such clear release surface does not occur in the south and the bathymetric data rather suggest that the limit of the unstable area in the south is transitional. No systematic decrease of degree of damage of the rock mass towards the south in the subaerial slope component can be interpreted as an indication that the fracturing of the rock mass mainly have taken place before an assumed sliding process started. This is also supported by the fact that the orientations of all joint sets appear consistent also outside the defined lateral limits of the instability. According to Stead and Eberhardt (2013) is release surfaces an essential component of kinematic release for a landslide. Obviously, the missing distinct lateral limit in the south is a factor that reduces the likelihood of a massive failure of the slope. The buttress observed in the bathymetric image in the south of the study area can be the sufficient stabilizing feature that has prevented a southern lateral limit to be developed.

8.1.1 RECORDED SLOPE DEFORMATION ACTIVITY

SW movement trend in the differential GNSS analysis is consistent with the direction of toppling failure along J4. Notwithstanding, the dGNSS measurement is based on only one year's interval and from one rover point only, thus being far from statistically significant. The annual scale rate (9 mm horizontally and 2 mm vertically) is however supported by traditional GPS displacement measurements undertaken by SSV from 2003 to 2006 that revealed an annual average displacement of 10 mm horizontally and 2 mm vertically in at the exposed location called Gvålvikknatten in the central area of the Håkåneset rockslide (see Appendix 1). In both of the geodetic measurement approaches that have been undertaken the horizontal displacement is higher than the vertical. According to Wyllie and Mah (2004) is horizontal displacements greater than vertical displacements characteristics for toppling behavior. This support that the small scale displacements that are recorded can geologically be explained as toppling activity of smaller rock volumes.

The displacement analysis performed on TLS-data did not reveal any reliable results due to limited quality of the data set. However, frequent rock fall recorded along the road by SVV (see also Figure 8 and Figure 9) can be interpreted as evidence that there are activity in the slope due to large slope deformation. Although this is true, external factors like road construction effects, erosion, freeze and thawing etc. will likely be a significant factor for triggering rock fall.

8.1.2 FINDINGS FROM SSR-ANALYSIS

Impact of topography on slope stability

Stead and Eberhardt (2013) mention tension cracking in the slope crest and heave/bulging at the toe as early indicators of slope instability, where slope topography is one of the essential factors controlling the spatial distribution of such damages in a rock slope. The analysis result presented in this study (Chapter 7) seem to indicate that the topography is a vital factor also for the presence of the Håkåneset instability, because active zones in the maximum shear strain plots area are concentrated in majority in the toe of the slope model and in a smaller area in the upper region in the mountain slope for all analyses. Since the topography in the model is the only factor that is kept constant in all analyses, its importance as a dominating factor to the strain concentration is justified.

The induces active zone in the toe is also clearly seen on displacement contour plots that indicate that most significant displacement out of the slope can be expected at approximately 100 m depth in Lake Tinnsjø. This is supported by prominent geological structures on bathymetric map. The buttress in the south of the study area is located at approximately the same elevation as the indicated active zone, and strengthens the assumption of the buttress being a vital stabilizing feature.

Sensitivity of hydrogeological conditions

According to Wyllie and Mah (2004) there are in particular two essential water pressure properties that reduces stability: 1) the diminishing of the shear strength of potential failure surfaces and 2) increasing the forces that induce sliding when present in tension cracks and near vertical fissures.

A subsurface groundwater table was obtained from the groundwater seepage analyses when anisotropic permeability with vertical permeability significantly greater than the horizontal permeability was assumed. Because the rock mass at Håkåneset is heavily dissected by steeply dipping joint sets (> 50 degree for both J1, JF2, JF3 and J4) this anisotropic permeability condition is assumed as realistic. By assuming isotropic permeability in the material the groundwater seepage analysis resulted in a surface near groundwater table. According to Wyllie and Mah (2004) can a surface parallel groundwater table in strong rock with widely spaced joints be justified by the fact that the a low porosity rock imply that the

water flow will rapidly fill the joints close to surface and increase the water pressure in the slope in periods of increased precipitation. Therefore, in order to take account for periods of heavy rain fall and snow melt as a worst case scenario a surface near groundwater table can be assumed realistic to use in a numerical modeling.

Obviously, a lower groundwater table will have a positive effect on the CSRF due to increased effective stresses when the pore pressure decreases, which is confirmed in Analysis 1.1_2 (Figure 34) and Analysis 1.1_3 (Figure 35) and illustrated in Figure 38. However, by studying Figure 50 it is seen that the outcome of this analyses indicates that the sensitivity of slope stability to groundwater table location under the defined hydraulic conditions is negligible compared to the effect of varying the material properties. The importance of material properties to slope stability is discussed in the next section.

Excluding the constructed lake water (pounded water and water load) in the Model 1 had no effect on the predicted CSRF, as can be seen from the result of Analysis 1.3 and 1.1_3. Also the maximum shear strain contours for each analysis, Figure 36 and Figure 37 respectively, were only slightly changed. This can be interpreted as an indication that the stabilizing effect of a water load from the lake is negligible compared to the major effect of the topography to induce unstable areas in the Håkåneset mountain slope. On the contrary, it is well known that the presence of groundwater and the associated water pressure on a potential sliding plane is crucial in rock slope stability (Nilsen et al., 2000). Therefore, the lack of sensitivity in the model by excluding such an essential factor as the water highlights the importance of interpreting numerical modeling results with caution. Essential hydrogeological factors and their effect on the stability of the Håkåneset rockslide are further discussed in Chapter 9.3.

Material strength as a controlling factor for massive slope failure

The numerical modeling undertaken in this study highlights the rock mass strength as the most critical factor to slope stability. This is experienced both from the sensitivity study of Model 1, 2 and 4 where CSRF is significantly changed when rock mass parameters are varied, as illustrated by the plots in Figure 38 and Figure 50. Figure 38 shows the results obtained by sensitivity test with Model 1 (J1 joints included as the only discontinuities), where it is clear that the rock mass strength is the fare most controlling factor in comparison the other tested factors, i.e. the groundwater level. From Figure 50 it become visible that the dominance of the rock mass strength as the controlling factor to slope stability also is supported by the

sensitivity study of Model 4. Realistically, Model 4 should represent a more unstable slope than Model 1-3 since the material is broken up by the discontinuities that represent the rear release surfaces. Still, the CSRF appears not to be affected by the discontinuities and is only changed significantly when the rock mass strength is reduced.

The vital importance of rock mass strength to rock slope stability is easily justified by the fact that the joint sets at Håkåneset are non-persistent, implying that damage of intact rock is necessary in the development of a basal sliding surface. A basal sliding plane is an essential structure in a rockslide. Bjerrum (1967) defines progressive failure as the process where a continuous sliding surface is developed by damage of intact material. Furthermore, Eberhardt et al. (2004) justify degradation of rock mass strength as the vital factor for progressive failure in a natural rock slope. Progressive failure and degradation means that the rock mass strength is reduced over time due to the propagation of fractures through intact rock between existing discontinuities. Obviously, this damage controlled failure mechanism is developed by a through-going step path failure, involving tension failure by microcracking and shear failure of intact rock (Stead and Eberhardt, 2013). The foliation parallel microfractures seen in thin the sections of insitu rock from the study area can be used as supporting indicators of progressive failure.

Terzaghi (1962) emphasize that shear failure is controlled by two parameters: 1) the shearing resistance represented by the friction angle (φ) and 2) the cohesion (c) of intact rock bridges between discontinuous joints. The sensitivity test results of friction angle and cohesion undertaken in this study, plotted in Figure 44, indicate that the stability of the slope is most sensitive to changes in friction angle. Slope stability is quantified by the CSRF, which by definition depends on the shear strength. When shear strength is plotted to percentage value reduction of friction angle and cohesion separately, see Figure 46, the same trend with shear strength being more sensitive to changes of friction angle than changes of cohesion, is observed. Analysis 2.12 investigates how friction angle and cohesion influences the slope differently for a specific CSRF condition. Figure 46A illustrate the reduction of friction angle, indicating that the J1 discontinuity is important due to the distribution of the strain concentrations. In Figure 46B) on the other hand, is the cohesion reduced, and J1 seems to be less important as the strain concentration appears in a smaller region but with higher magnitude of the maximum induced strain. The result of Analysis 2.12 indicates that the strain concentration in the slope is significantly affected by the magnitude of friction angle relative to the cohesion. A possible explanation to this observation is: Because the cohesion is

related to the shearing of intact rock in rock bridges it is reasonable to assume that rock damage becomes easier when the cohesion is reduced, implying that more rock bridges in a smaller area can be sheared. The friction angle is related to the frictional restraint in the rock, and consequently sliding along J1 surfaces can be assumed to be easier when friction angle is reduced. To summarize, when the rock is less cohesive the development of a failure surface is less affected by pre-existing joints because rock bridges between sub parallel joints are more easily shared, while for a rock with reduced friction angle the weakness defined by pre-existing joint become even more pronounced because the strength contrast between the joint and the rock bridges become even stronger. The J1-fault and the J3-fault are mapped out with as with a persistence in the km scale and have several indicators suggesting they are essential for the development of the instability in the Håkåneset rockslope. Both of these structures have orientations that correspond to a joint set. In addition, the interpreted back scarp, which is the third persistent structure that is essential for the slope stability, also has a orientation the correspond to a existing joint set (J1). The fact that the persistent faults and the back scarp are developed along pre-existing joints, suggest that the model that strengthens the importance of the joints in the model, i.e. a model with a frictional angle reduce compared to the initial value, best describes the reality.

The role of the J1 discontinuity set on the slope stability

As discussed above does the result from the rock mass sensitivity test in Analysis 2.12 highlight the pre-existing joints as essential for the stability in the slope. As described in Chapter 9.1.1. is the exfoliation joint set J1 considered as vital for the slope stability due to field observations and its control on the kinematics of the rockslide. In the FEM-analysis the importance of J1 regarding slope stability was first confirmed by adding J1 as ubiquitous joints in Analysis 1.6, where the resulting Safety Factor plot, Figure 42A, indicate most critical parts in the region of the model where the instability is located in nature. Active zones indicated with ubiquitous joints have also been justified by Böhme et al. (2013) for the Stampa rockslide in western Norway. Adding J1 to the Phase² model as a joint network in Analysis 2.1 did not change the CSR_F value, but had a significant effect on where strain concentrations were induced: with J1 joints in the model several steeply dipping strain concentration zones parallel to the orientation of J1 joints became dominant. These strain concentrations were induced mainly in the lower part of the constructed mountain slope and fit well to the where the back scarp and the fault zones would intersect the profile that the

model in constructed from. The trend of back scarp and the fault zones in the profile can be seen on Figure 54. These observations clearly highlight the importance of the J1 joint set as a crucial structure for the stability of the rock slope at Håkåneset.

The J1-fault and the back scarp is interpreted as two possible rear release surfaces. As mentioned, adding J1 in the model indicates several steeply dipping strain concentrations with J1 orientation. With this observation, the feasibility for the development of new rear release surfaces in addition to J1-fault and the back scarp cannot be excluded. The varying topography and graben morphology in the upper part of the slope are observations that support that several more active sliding zones are present in the deforming rock slope. However, in case of a basal failure surface is developed and allow for sliding it would be reasonable to think that the back scarp and fault zones would be critical as rear release surfaces because of their persistent character and reduced strength due to earlier damage. With this, the importance of the exfoliation joint set regarding the stability of the Håkåneset rockslide is clearly supported by the results from the undertaken numerical modeling in this study.

The role of the foliation on the slope stability

By field observations and kinematic feasibility test, the foliation joint set SF was identified as important for the formation of a basal sliding surface. By numerical modeling this interpretation was first supported when most active zones corresponding to the instability came out clearly in the ubiquitous joint strength factor plot of Model 1, as illustrated in Figure 42B. By comparing Figure 42A and Figure 42B it can be observed that a larger of area of the instability in the Håkåneset rock slope is indicated as critical in the plot when SF is included (Figure 42B). This strengthens the importance of SF to the instability of the slope. Furthermore, was SF included in Phase² model as a joint network of non-persistent joints, defined with shorter length and less persistent than J1 (see Model 3 Appendix ??). As observed when J1 was included in the modeling, adding SF did not have any effect on the CSRFB either. The shear strain contours plots for Model 2 and Model 3, given in Appendix ??, indicate only minor differences. Still, with SF present in the model the strain concentrations seem to appear more distinct, and a likely basal sliding plane is reasonable to interpret to develop with SF direction, daylighting at approximately 100m depth in Lake Tinnsjø. On the contrary, the mean dip angle of SF (19°) is less than the assumed friction angle of the

discontinuities (28°), thus sliding along foliation planes alone is unlikely. This supports the interpretation of a retrogressive step path failure as the most likely failure mechanism in the development of a basal sliding surface for the Håkåneset rockslide. In the field were the foliation planes mapped out as purely developed, which further supports progressive failure as failure mechanism. Identified microfracturing parallel to the foliation in thin sections of the insitu rock can also be used to justify the likelihood of stepped failure along foliation joints. With this, the development of a basal sliding plane have to be assumed to require significant rock damage, thus confirming the previous interpretation of the rock mass as the most controlling factor for this instability. The lack of sensitivity in the modeling when varying important joint parameters like persistence, spacing and stiffness, as seen from the results presented in Table 26 can be justified with the dominance of rock mass strength in the development of a sliding surface.

8.2 Influence of Lake Tinnsjø on the stability of the Håkåneset rockslide

In particular two important factors are evaluated as essential regarding the presence of Lake Tinnsjø and the instability at Håkåneset: 1) the stabilizing effect due to hydraulic pressure from the water column and 2) the depth of the groundwater table on which the induced pore water pressure in the rock masses is strongly dependent. Some reflections regarding these effects are discussed in the following text. In addition, a buoyancy effect must be expected to influence on the stability in a negative way, as seen in the study of the Hochmais–Atemkopf rockslide by Schneider-Muntau and Zangerl (2005)

Following the definition given by Born et al. (1979) Lake Tinnsjø can be classified as a discharge lake due to its location with respect to the surrounding topography. The groundwater table in this environment will always communicate with the lake level and raises close to the surface along the mountain slope as seen in Figure 52. In a temperate climate like in southern Norway, precipitation and consequently the groundwater table level is variable. Figure 53 illustrates how a fluctuation of the groundwater table due to variable precipitation periods will affect a combined subaerial-subaquatic rock slope instability differently than a fully subaerial instability. The fact that the groundwater table always will communicate with the lake surface implies that the groundwater table variations only will affect the upper part of the instability, while for the subaerial rock slope the hydrogeological conditions in the unstable rock mass can change from almost dry to fully saturated conditions. Based on this it should be reasonable to expect that lake Tinnsjø is favorable as regards stabilizing the deforming rock mass at Håkåneset because its presence contributes to less variations in the groundwater table, and consequently negative effects due to induced seepage forces are prevented. This interpretation is however strongly dependent on that the lake surface level can be constant, so that seepage forces due to a fluctuating lake level can be considered as negligible.

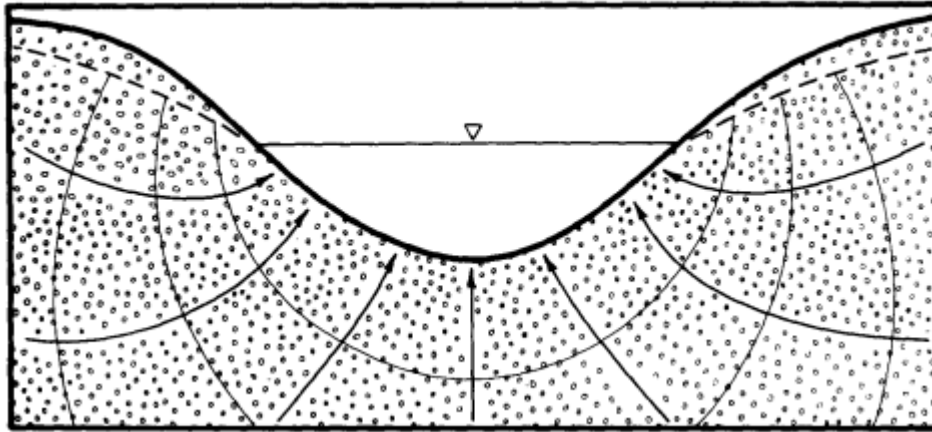


Figure 52: Typical groundwater flow (black arrows) in a discharge lake like Tinnsjø. The groundwater table (dotted line) communicate with the lake level and raises subsurface along the mountain slope (Born et al., 1979)

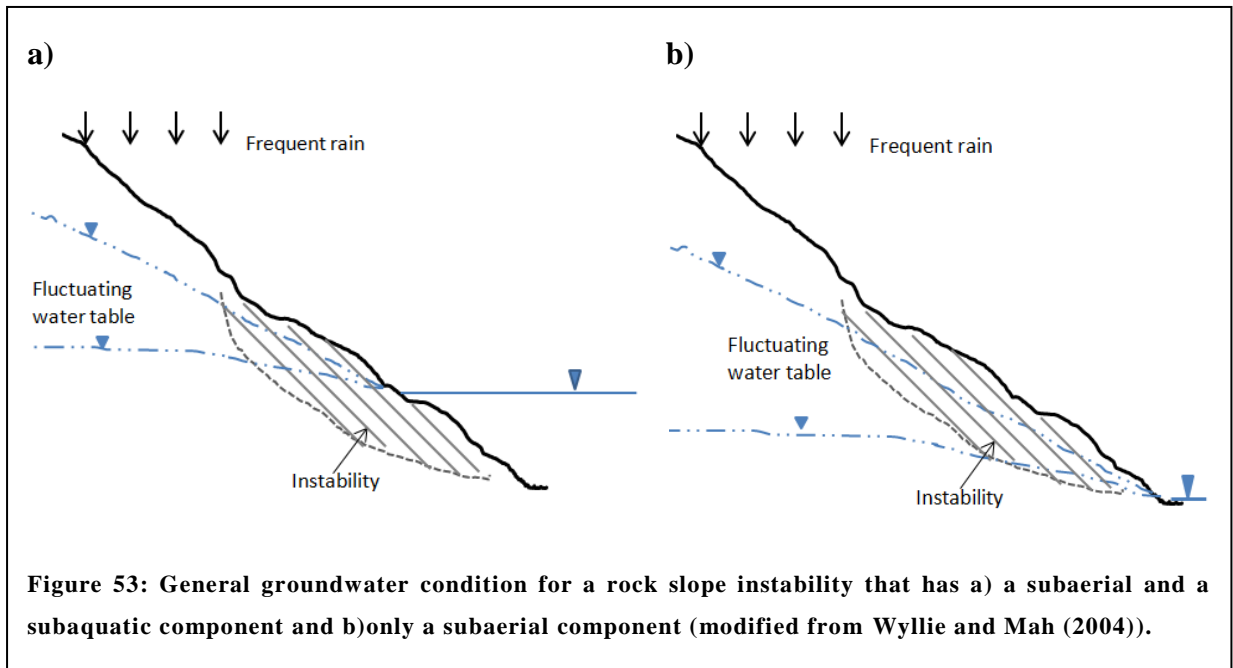


Figure 53: General groundwater condition for a rock slope instability that has a) a subaerial and a subaquatic component and b) only a subaerial component (modified from Wyllie and Mah (2004)).

8.3 Volume estimation of the deforming mass in the Håkåneset rockslide

Figure 54 show the result from Analysis 4.4 on Model 4 and illustrate the location of the failure surface that is interpreted as most likely due to the numerical modelling obtained in this study. Justification of the interpretation is given in the following text.

A bi-planar failure mechanism is interpreted as likely for the Håkåneset rock slope. Model 4 is the model in this study that is constructed to reflect the most of the actual structures in the slope. In Analysis 4.4 a condition close to the critical state (CSRF ~ 1) obtained in, thus the contour plots from this analysis is reasonable to use for indication of the failure surface in case of a massive slope failure.

The failure plane is interpreted to be compound of 1) a steep rear release surface developed along J1 joints and 2) a shallow basal failure surface developed by retrogressive failure along the schistose foliation. These interpretations are based on visual analysis of shear strain and displacement contour plots. The reliability of the results can be justified due to the fact that:

- a. the location of the most active zones is approximately consistent for all analyses.
- b. the active zones are indicated in areas of the model that coincide with the location geological structures (back scarp, two fault zones) that was interpreted as important for the slope stability during the geological investigation.
- c. the interpreted basal sliding plane daylight the slope at a location that coincide with a topographic step in the topography. This step may be interpreted as a bulging toe. According to Stead and Eberhardt (2013) is a bulging toe considered as a pre-indicator of slope instability.

Due to the persistent character of the mapped back scarp and the J1-fault zone these are considered to define the most likely rear release surfaces. In addition, during the field investigation the material in the J1-fault zone was observed as significantly disturbed and with clay content. Based on this it is reasonable to assume that the shear strength along the J1-fault is significantly reduced compared to other J1-joints. These observations support a scenario with the J1-fault as rear release surface in combination with the basal sliding plane daylighting at approximately 100 meters depth in Lake Tinnsjø. Worst case scenario is induced if failure takes place along the back scarp.

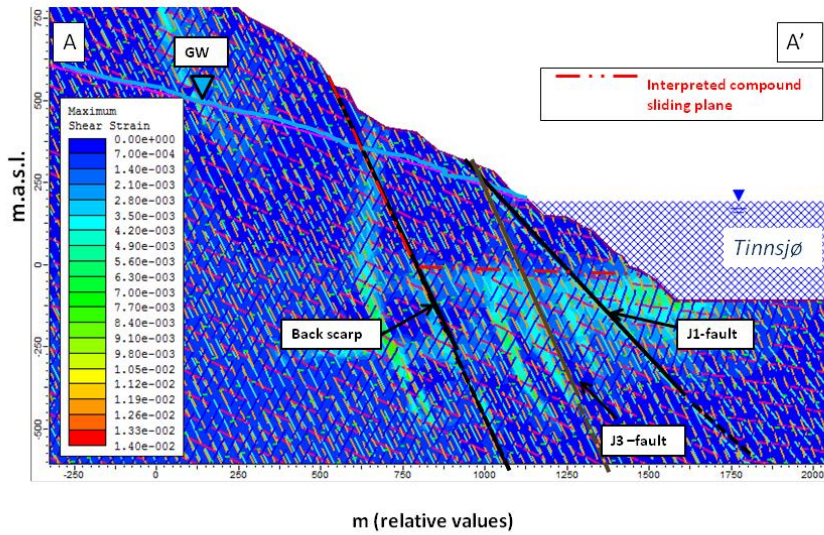
The geometry the Phase2 profile in Figure 54 of each of the rear release surface scenarios described above is used for the volume calculation. The extend of the instability at surface

was estimated in ArcMap 10.1 (Esri, 2012). Because the southern limit of the rockslide is assumed to be translational, two scenarios were calculated: 1) the buttress limits the instability and 2) the topographic gully is the limit (worst case). The calculations are given in Appendix. Assuming the J1-fault as rear release predict a deforming volume from 17 to 33 million m³ if the southern limit controlled by the buttress or the gully, respectively. Worst case scenarios with the back scarp as rear release surface predict that the instability involves a rock mass in the range of 74 to 144 million m³.

From the conclusions about the effect of Tinnsjø on the slope stability, it is interesting to consider a scenario where the basal surface daylight at the lake level, where hydrostatic pressure from the lake is not affecting the slope. Under these conditions the unstable mass is estimated to be in the range from 2 - 4 million m³ with J1-fault as release surface and 26-50 with the back scarp as rear release surface.

A)

Håkåneset rockslide
 Analysis 4.4: Model 4 (all discontinuities), low GW
 Critical SRF = 1,1



B)

Håkåneset rockslide
 Analysis 4.4: Model 4 (all discontinuities), low GW
 Critical SRF = 1,1

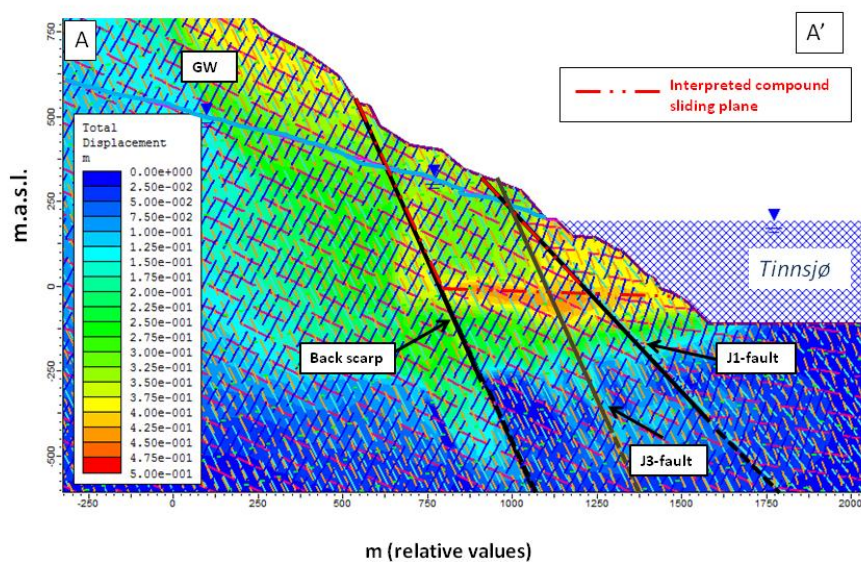


Figure 54: A) Maximum shear strain and B) Total displacement in Model 4, Analysis 4.4. A compound sliding surface is indicated (red dotted) by visual interpretation.

8.4 Uncertainties in the slope stability assessment of Håkåneset rockslide

In this slope stability assessment of the Håkåneset rockslide several techniques are applied, which require a great amount of input parameters. The quality of modeling results is impossibly better than the input parameters. Obtaining representative values for the required parameters on which the modeling is based is challenging and the result can never be concluded as completely true. In addition are significant simplifications of the reality necessary when constructing the model. While this is true, when the modeling results show reasonable patterns that can be related to observations in the field the reliability of the model is increased. Because of this possibility of visual justification numerical modeling is well accepted as an efficient tool in slope stability assessment for getting an impression of what can be considered as most likely critical factors and conditions. Several of the obtained results for this study of the Håkåneset rockslide can be justified with field observations, which adds reliability to the constructed model. However, it is important to be aware of the most important limitations and uncertainties related to the undertaken stability assessment. This will be discussed in the following text.

By nature geology is complex and anisotropic, thus the isotropic rock mass assumption which the numerical modeling is based on is unrealistic.

Induced stresses and the resulting strains depend on the field stress in the rock mass, thus the strain contour plots obtained in the numerical model should realistically be dependent on the defined stress field. The stress field values used as input in this study are empirical values, which means their representativeness for the in situ conditions at Håkåneset is questionable. Nonetheless, since Phase² is a 2D-program it is difficult to obtain stress distribution parameters that take into account the natural three dimensional stress fields. While this is true, in the case of the undertaken modeling the reliability of the assumed field stress can be justified because the shear strain patterns obtained by the undertaken modeling can be related to major structures mapped in the field and on the DEM. In addition, experience from previous rockslope stability studies indicate that field stress only have minor influence on the SSR analysis (Loftesnes, 2010; Sandøy, 2012).

The results from the undertaken numerical modeling highlight the rock mass strength parameters (friction angle and cohesion) as a critical factor for driving the slope towards a disequilibrium conditions.

Estimations for the rock parameters in this study are obtained by field and laboratory results on in situ rock. Representative rock samples are in general difficult to obtain. The rock samples used in this study were collected from the road cut and were partly detached, thus their representativeness for intact in situ rock is highly questionable as strength reduction due to the influence from the road construction might be significant. The uncertainty related to the rock strength is further supported by the unrealistic relationship with the laboratory estimate for UCS as lower than the field estimate for JCS. In addition, significant uncertainties related to scale effect when obtaining rock properties with different approaches will always be present even though the scale are accounted for by empirical based conversions.

The numerical setup requires initial rock mass input parameters for friction angle and cohesion determined as instantaneous strength parameters under an assumed normal stress condition. The normal stress condition is determined by assuming that the basal failure surface develops in rock mass with 100 m overburden. The location of a possible basal plane for a massive failure of the Håkåneset rockslide is unknown, thus the assumed overburden of 100 m is a major simplification of the reality and add uncertainty to the modeling. In addition, since the predicted failure plane geometry of the Håkåneset rockslide is bi-planar and due to topography, the overburden of the failure surface will be variable, implying that normal stress level and consequently the rock mass strength also will be variable.

Retrogressive failure is concluded as the most likely failure mechanism for the Håkåneset rock slope. This mechanism involves tension cracking, thus the tensile strength of the rock will be essential in the development of the sliding plane. In the undertaken numerical parameter study the significance of the tensile strength due to strain concentrations have not been tested for, which is an important limitation of the undertaken parameter study

The importance of joint spacing and persistence on rock slope kinematics are well documented, e.g. by (Brideau et al., 2008). Still, the performed parameter study of SF joints in the model had negligible effect on the safety factor and strain estimation. This is not realistic and is a significant limitation of the numerical model in this study. A possible explanation to the lack of influence might be that because the joints are constructed to be non-persistent the

importance of rock mass properties masks the influence of varying joint characteristics. Also, the dominant topographic effect might contribute to this.

Because the Håkåneset rockslide extends both over and under water and a groundwater table will naturally be an essential component to include in the model. In addition, the rockslide is located in a climate region where frequent rainy periods are common, thus a fluctuation groundwater table and induced seepage forces will be part of the reality. Seepage forces has not been taken into account in this study, neither have infiltration conditions. Water conditions are complex and introduce significant uncertainties and limitations to the modeling. Some important uncertainties related to the Håkåneset modeling are:

- seepage forces and infiltration conditions
- the permeability of the rock mass
- the hydrogeological conditions of joints
- the influence of the fault to the groundwater table location

A detailed description of groundwater conditions related to slope stability is given by Wyllie and Mah (2004).

8.5 Recommendations for further investigations

Based on the described uncertainties regarding both geological factors and hydrological conditions there is still need for increased knowledge about the Håkåneset rock slide. In particular it is important to obtain better dataset to detect the ongoing deformation. Therefore, it is important that dGNSS measurements are continued for several years in order more comparable data. The measurements should be optimized by installing additional rover points in order to detect whether the observed displacement is a result of massive slope deformation or minor scale block toppling. Also, to continue to with the TLS survey is considered important for detecting rock fall activity. For further TLS surveys it must be emphasized to focus on increasing the quality of the data, as the data set used in this study was not sufficient to obtain reliable results.

The numerical modeling suggests the J1-fault as a likely rear release surface, and obtaining more reliable material strength properties for this zone would be important for further predicting the likelihood of sliding along this zone. Test material can be easily obtained, since this structure is daylighting in the road cut. Shear box test can be used to determining the shear strength of such weakness zone material. In the field clay filling on discontinuities surfaces within the damaged rock mass in this weakness zone was observed. It is recommended that this material is tested for swelling clay, because swelling effect is a critical phenomenon regarding rock stability. Identification of swelling clays can be obtained with a X-ray diffraction (XRD) analysis in the laboratory of NTNU/SINTEF.

9 CONCLUSION OF THE STUDY

Structural analysis on TLS data validated the previously obtained structural field measurements and the kinematical model of the Håkåneset rock slide. The undertaken FE-SSR analysis in Phase² supports that bi-planar failure mechanism involving development of a basal failure surface by retrogressive failure is feasible.

The stability assessment suggests that:

- The steeply dipping exfoliation joint set (J1 (075°/63°, 076°/51°)) can be confirmed essential for defining a rear release surface. A fault and a back scarp visible in the subaerial slope are persistent structures with J1 orientation that justify the importance of J1 in case of a massive slope failure. The presence of multiple sliding surfaces is supported by strain concentration contours obtained by numerical modeling, and can also be justified by the variable topography in the rock slope.
- Due to topographic influence it is reasonable to expect that the most active zone is in the submerged part of the slope even though hydrostatic forces from the lake will act as a stabilizing factor. This is justified by prominent bedrock structures on bathymetric map. Visual analysis of strain concentrations plot suggests that a basal failure surface can daylight at approximately 100 m depth in the lake. In addition this adds reliability to the interpretation of a subaquatic buttress being a significant stabilizing factor and the reason for the lack of a clear southern lateral limit.
- A basal failure surface can be developed by step-path retrogressive failure. This requires significant rock damage, as the field observations indicate that schistose foliation planes are poorly developed. Thin section analysis revealed that the rock is strongly anisotropic and have indicators that justify shear deformation, which supports that development of a basal sliding surface is feasible.
- With retrogressive failure as a likely failure mechanism, the rock mass shear strength properties are crucial to investigate to predict the likelihood of large scale failure to occur.
- Volumes in the range 2 - 50 million m³ is estimated for failure involving only subaerial material, and 17-144 million m³ if the basal failure surface is assumed to daylight at the submerged toe. These calculations are indeed very uncertain and further stability assessment of the Håkåneset rockslope is highly recommended before predicting the likelihood of a massive failure of the slope.

10 REFERENCES

- Revista de la Asociación Geológica Argentina: Buenos Aires, Asociación Geológica Argentina.
- Abellán, A., Oppikofer, T., Jaboyedoff, M., Rosser, N. J., Lim, M., and Lato, M. J., 2014, Terrestrial laser scanning of rock slope instabilities: *Earth Surface Processes and Landforms*, v. 39, no. 1, p. 80-97.
- Atkinson, L. C., 2000, The role and mitigation of groundwater in slope stability: *Slope Stability in Surface Mining*, p. 89.
- atlas.nve.no, The National Catchment Database (REGINE), Volume 2014, Norwegian Water Resources and Energy Directorate
- Bandis, S., Lumsden, A., and Barton, N., Fundamentals of rock joint deformation, *in* Proceedings International Journal of Rock Mechanics and Mining Sciences & Geomechanics Abstracts 1983, Volume 20, Elsevier, p. 249-268.
- Barton, N., 1973, Review of a new shear-strength criterion for rock joints: *Engineering geology*, v. 7, no. 4, p. 287-332.
- Barton, N., and Choubey, V., 1977, The shear strength of rock joints in theory and practice: *Rock mechanics*, v. 10, no. 1-2, p. 1-54.
- Bitelli, G., Dubbini, M., and Zanutta, A., 2004, Terrestrial laser scanning and digital photogrammetry techniques to monitor landslide bodies: *International Archives of Photogrammetry, Remote Sensing and Spatial Information Sciences*, v. 35, no. Part B 5, p. 246-251.
- Bjerrum, L., 1967, Progressive failure in slopes of overconsolidated plastic clay and clay shales: *Journal of Soil Mechanics & Foundations Div.*
- Blikra, L., Longva, O., Braathen, A., Anda, E., Dehls, J., and Stalsberg, K., 2006, Rock slope failures in Norwegian fjord areas: examples, spatial distribution and temporal pattern, *Landslides from massive rock slope failure*, Springer, p. 475-496.
- Born, S., Smith, S., and Stephenson, D., 1979, Hydrogeology of glacial-terrain lakes, with management and planning applications: *Journal of Hydrology*, v. 43, no. 1, p. 7-43.
- Brideau, M.-A., Yan, M., and Stead, D., 2008, The role of tectonic damage and brittle rock fracture in the development of large rock slope failures: *Geomorphology*, v. 103, no. 1, p. 30-49.
- Bunholt, H., Nordahl, B., Hermanns, R. L., Oppikofer, T., Fischer, L., Blikra, L. H., Anda, E., Dahle, H., and Sætre, S., 2013, Database of unstable rock slopes of Norway.: In: Margottini C, Canuti P, Sassa K (eds) *Landslide science and practice*, Springer, Berlin, v. 3, no. Spatial analysis and modelling., p. 423-428.
- Böhme, M., Hermanns, R. L., Oppikofer, T., Fischer, L., Bunholt, H. S., Eiken, T., Pedrazzini, A., Derron, M.-H., Jaboyedoff, M., and Blikra, L. H., 2013, Analyzing complex rock slope deformation at Stampa, western Norway, by integrating geomorphology, kinematics and numerical modeling: *Engineering Geology*, v. 154, p. 116-130.

- Dons, J. A., and Jorde, K., 1978, Berggrunnskart Skien: Norges geologiske undersøkelse (NGU), scale 1:250000.
- Eberhardt, E., Stead, D., and Coggan, J., 2004, Numerical analysis of initiation and progressive failure in natural rock slopes—the 1991 Randa rockslide: *International Journal of Rock Mechanics and Mining Sciences*, v. 41, no. 1, p. 69-87.
- Eiken, T., 2013, Deformasjonsmålinger i potensielle fjellskred, Telemark: Institutt for geofag, Universitetet i Oslo.
- Eilertsen, R., 2013, Personal communication, Bathymetric data Tinnsjø.
- Esri, 2012, ArcGIS ArcMap, Esri
- Frivold, T., 2006, Gvålviknatten rasovervåkningsprosjekt, Tinn kommune 2002/2003.
- , 2007, Gvålviknatten rasovervåkningsprosjekt, Tinn kommune. 2006.
- geo.ngu.no, Nasjonal berggrunnsdatabase, Berggrunn N250 med fjellskygge, Volume 2104: Kontaktadresse: Postboks 6315 Sluppen, 7491, The Norwegian Geological Survey.
- Goodman, R. E., Taylor, R. L., and Brekke, T. L., 1968, A model for the mechanics of jointed rock: *Journal of Soil Mechanics & Foundations Div.*
- Griffiths, D., and Lane, P., 1999, Slope stability analysis by finite elements: *Geotechnique*, v. 49, no. 3, p. 387-403.
- Gruber, S., and Haerberli, W., 2007, Permafrost in steep bedrock slopes and its temperature-related destabilization following climate change: *Journal of Geophysical Research: Earth Surface* (2003–2012), v. 112, no. F2.
- Grøneng, G., and Nilsen, B., 2009, Procedure for determining input parameters for Barton-Bandis joint shear strength formulation, Trondheim, Instituttet, NTH, 21 bl. :
- Grøneng, G., Nilsen, B., and Sandven, R., 2009, Shear strength estimation for Åknes sliding area in western Norway: *International Journal of Rock Mechanics and Mining Sciences*, v. 46, no. 3, p. 479-488.
- Hammah, R., Yacoub, T., Corkum, B., and Curran, J., The practical modelling of discontinuous rock masses with finite element analysis, *in Proceedings Proceedings of the 42nd US Rock Mechanics Symposium–2nd US-Canada Rock Mechanics Symposium*, San Francisco, US2008.
- Hammah, R., Yacoub, T., Corkum, B., Wibowo, F., and Curran, J., Analysis of blocky rock slopes with finite element shear strength reduction analysis, *in Proceedings Proceedings of the 1st Canada-US Rock Mechanics Symposium2007*, p. 329-334.
- Hammah, R. E., Curran, J. H., Yacoub, T., and Corkum, B., Stability analysis of rock slopes using the finite element method, *in Proceedings Proceedings of the ISRM regional symposium EUROCK2004*.
- Hanssen, T. H. D. I., 1998, Rock stresses and tectonic activity: *Fjellsprenngskonferansen*, Oslo 1998, no. Norsk Jord- og Fjellteknisk forbund, p. 29.29 - 29.10.
- Harbitz, C., Pedersen, G., and Gjevik, B., 1993, Numerical simulations of large water waves due to landslides: *Journal of Hydraulic Engineering*, v. 119, no. 12, p. 1325-1342.
- Hermanns, R., Hansen, L., Sletten, K., Böhme, M., Bunkholt, H., Dehls, J., Eilertsen, R., Fischer, L., L'Heureux, J., and Høgaas, F., 2012a, Systematic geological mapping for landslide understanding in the Norwegian context: *Landslide and engineered slopes:*

- protecting society through improved understanding. Taylor & Francis Group, London, p. 265-271.
- Hermanns, R., and Longva, O., 2012, Rapid rock-slope failures: Landslides (types, mechanisms and modeling). Cambridge University Press, Cambridge, p. 59-70.
- Hermanns, R., Oppikofer, T., Anda, E., Blikra, L., Böhme, M., Bunkholt, H., Crosta, G., Dahle, H., Devoli, G., Fischer, L., Jaboyedoff, M., Loew, S., Sætre, S., and Yugsi Molina, F., 2013, Hazard and Risk Classification for Large Unstable Rock Slopes in Norway: Italian journal of engineering geology and environment.
- Hermanns, R. L., Oppikofer, T., Anda, E., Blikra, L. H., Böhme, M., Bunkholt, H., Crosta, G. B., Dahle, H., Devoli, G., Fischer, L., Jaboyedoff, M., Loew, S., Sætre, S., and Molina, F. Y., 2012b, Recommended hazard and risk classification system for large unstable rock slopes in Norway: Norwegian Water and Energy Directorate (NVE).
- Hermanns, R. L., Oppikofer, T., Molina, F. Y., Dehls, J., and Böhme, M., 2014, Approach for Systematic Rockslide Mapping of Unstable Rock Slopes in Norway: Springer, v. 3, no. , p. 129-134.
- Hoek, E., 1983, Strength of jointed rock masses: Geotechnique, v. 33, no. 3, p. 187-223.
- Hoek, E., 2007, Practical Rock Engineering, Rock Mass Properties: Toronto, Ontario, Canada, Rocscience Inc.
- Hoek, E., and Brown, E., 1997, Practical estimates of rock mass strength: International Journal of Rock Mechanics and Mining Sciences, v. 34, no. 8, p. 1165-1186.
- Hoek, E., Carranza-Torres, C., and Corkum, B., 2002, Hoek-Brown failure criterion-2002 edition: Proceedings of NARMS-Tac, p. 267-273.
- Holtedahl, O., and Andersen, B. G., 1960, Glacial map of Norway: The Norwegian Geological Survey (NGU) scale 1:2000000.
- <http://www.nve.no/>, The National Lake Database (Innsjødatabasen), Volume 2014: Middelthunsgate 29, Postboks 5091 Majorstua, 0301 Oslo Norwegian Water Resources and Energy Directorate.
- Hungr, O., Leroueil, S., and Picarelli, L., 2012, The Varnes classification of landslide types, an update: Landslides, p. 1-28.
- InnovMetric, 2014, PolyWorks: 3D scanner and 3D digitizer software, InnovMetric Software Inc.
- ISRM, 2007, Suggested Methods for Determining the Uniaxial Compressive Strength and Deformability of Rock Materials in: Ulusay, R., Hudson, J.A. (Eds.), The Complete ISRM Suggested Methods for Rock Characterization, Testing and Monitoring:1974-2006., ISRM & ISRM Turkish National Group p. 137-140.
- Jaboyedoff, M., Metzger, R., Oppikofer, T., Couture, R., Derron, M.-H., Locat, J., and Turmel, D., New insight techniques to analyze rock-slope relief using DEM and 3D imaging cloud points: COLTOP-3D software, in Proceedings 1st Canada-US Rock Mechanics Symposium 2007, American Rock Mechanics Association.

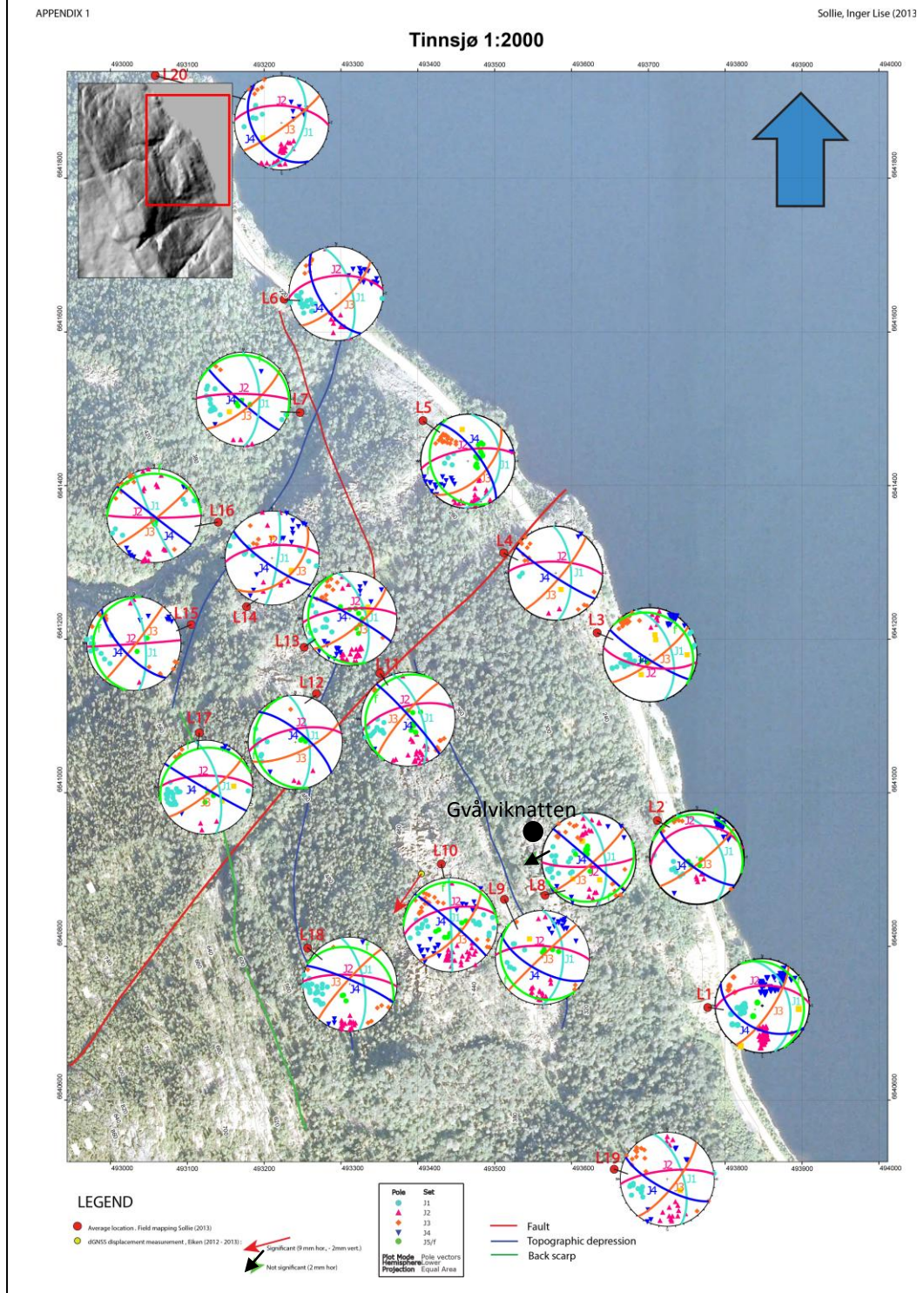
- Jansen, I. J., 1986, Telemark Kvartærgeologi. Jord og landskap i Telemark gjennom 11 000 år. , Institutt for naturanalyse.
- Langelid, A., 2013, Gvålviknatten rockfall monitoring project.
- Loftesnes, K., 2010, Svaddenipun, Rjukan: Stability analysis of potentially unstable mountainside.
- Myrvang, A., 2001, Bergmekanikk, Institutt for geologi og bergteknikk, NTNU.
- Nilsen, B., 2014, Discussion related to this master thesis: *Håkåneset, Tinnsjø - Stability analysis of potentially rock slope instability*. .
- Nilsen, B., Palmström, A., and Bergmekanikkgruppe, N., 2000, Engineering Geology and Rock Engineering: Handbook, Norwegian Group for Rock Mechanics.
- Oppikofer, T., Bunkholt, H., Fischer, L., Saintot, A., Hermanns, R., Carrea, D., Longchamp, C., Derron, M., Michoud, C., and Jaboyedoff, M., Investigation and monitoring of rock slope instabilities in Norway by terrestrial laser scanning, *in* Proceedings Landslides and Engineered Slopes. Protecting Society through Improved Understanding: Proceedings of the 11th International & 2nd North American Symposium on Landslides, Banff, Canada2012, p. 3-8.
- Ramberg, I. B., 2008, The Making of a Land: Geology of Norway, Geological Society Publishing House.
- Rocscience, 2011, RocLab, Rocscience Inc., p. Rock mass strength analysis using the Hoek-Brown failure criterion.
- , 2013, DiPS, Rocscience Inc., p. Structural orientation analysis software.
- , 2014a, Phase2 v8.02: Finite Element Analysis for Excavations and Slopes., Rocscience Inc.
- , 2014b, Phase2 v8.02: WebHelp 5.50, Rocscience Inc.
- Sandøy, G., 2012, Back-analysis of the 1756 Tjellefonna rockslide, Langfjorden.
- Schneider-Muntau, B., and Zangerl, C., Numerical Modelling of a Slowly Creeping Landslide in Crystalline Rock—a Case Study, *in* Proceedings Impact of the human activity on the geological environment. Proceedings of the fifth ISRM regional symposium Eurock. Brno, International Society for Rock Mechanics, Czech Republic2005, p. 535-540.
- Skempton, A., and Hutchinson, J., Stability of natural slopes and embankment foundations, *in* Proceedings Soil Mech & Fdn Eng Conf Proc/Mexico/1969.
- Sollie, I. L., 2013, Håkåneset, Tinnsjø - Geological investigation of potentially rockslide.
- Stead, D., and Eberhardt, E., 2013, UNDERSTANDING THE MECHANICS OF LARGE LANDSLIDES: Italian Journal of Engineering Geology and Environment - Book Series (6).
- Stead, D., Eberhardt, E., and Coggan, J., 2006, Developments in the characterization of complex rock slope deformation and failure using numerical modelling techniques: Engineering Geology, v. 83, no. 1, p. 217-235.
- Sørensen, B. E., 2014, Thin section analysis of in-situ rock, Håkåneset: The Norwegian University of Science and Technology (NTNU).
- Terranum, 2013, Coltop3D - LIDAR data processing and analyzing software for geologists.

- Terzaghi, K., 1962, Stability of steep slopes on hard unweathered rock: *Geotechnique*, v. 12, no. 4, p. 251-270.
- Trinh, Q. N., 2014, Personal Communication.
- Viola, G., Ganerød, G. V., and Wahlgren, C.-H., 2009, Unraveling 1.5 Ga of brittle deformation history in the Laxemar-Simpevarp area, southeast Sweden: A contribution to the Swedish site investigation study for the disposal of highly radioactive nuclear waste. : *Tectonics*, v. 28.
- www.nve.no, Geohazard database of Norway (Skredhendelsesdatabasen) Volume 2104: Middelthunsgate 29, Postboks 5091 Majorstua, 0301 Oslo Norwegian Water Resources and Energy Directorate.
- www.senorge.no, seNorge, Volume 2014, Norwegian Water Resources and Energy Directorate
- Norwegian Meteorological Institute
- Norwegian Mapping Authority.
- Wyllie, D. C., and Mah, C., 2004, *Rock slope engineering*, CRC Press.
- Zangerl, C., Eberhardt, E., and Perzmaier, S., 2010, Kinematic behaviour and velocity characteristics of a complex deep-seated crystalline rockslide system in relation to its interaction with a dam reservoir: *Engineering Geology*, v. 112, no. 1, p. 53-67.
- Østhus, N., 2012, Regulation lisençe of Lake Tinnsjø, Øst-Telemarks brukseierforening.

APPENDIX

A1: Map: Structural orientations, lateral limits, locations (Project assignment)

Appendix 1 Structural orientation plot map of the Håkåneset rockslide site. Geological investigation was undertaken by the candidate in the project assignment, 2013.



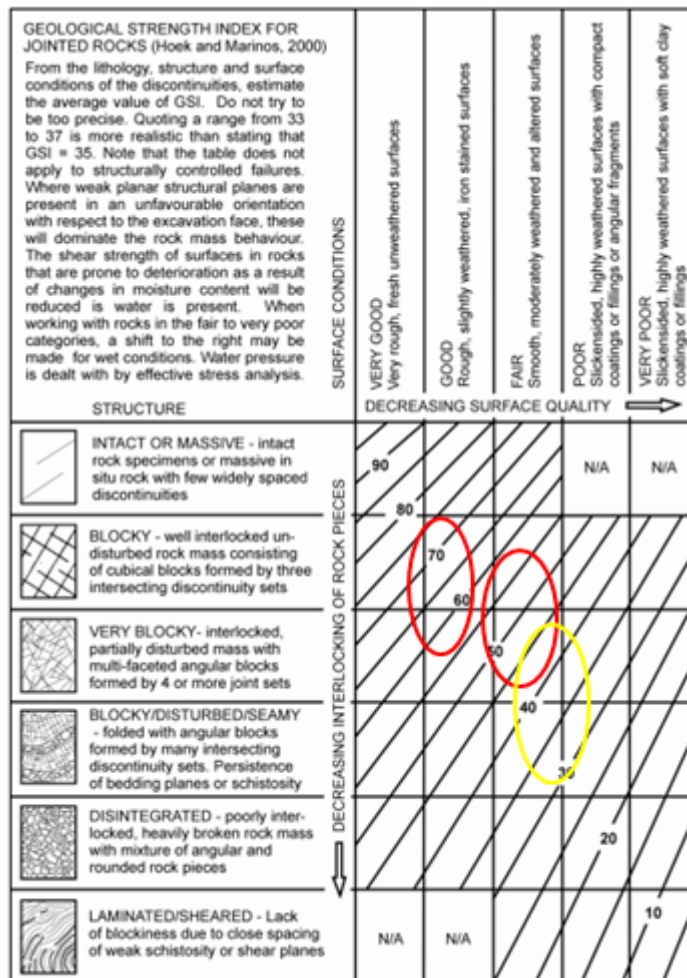
A2: dGNSS measurements (2012,2013), NGU, UiO

Appendix 2: dGNSS displacement results for measurements from 2012 and 2013. This is a modified table of the result table in Eiken (2013)

Rover point	Year	N	E	H	Horizontal displacement (m)	Horizontal displacement direction (360)	Vertical displacement (m)
TIN-1	2012	6640912,1708	493537,2837	438,1888			
TIN-1	2013	6640912,1702	493537,2814	438,1890	0,002	255,38	0,000
TIN-2	2012	6640928,5981	493425,3752	501,1442			
TIN-2	2013	6640928,5904	493425,3698	501,1422	0,009	215,04	-0,002

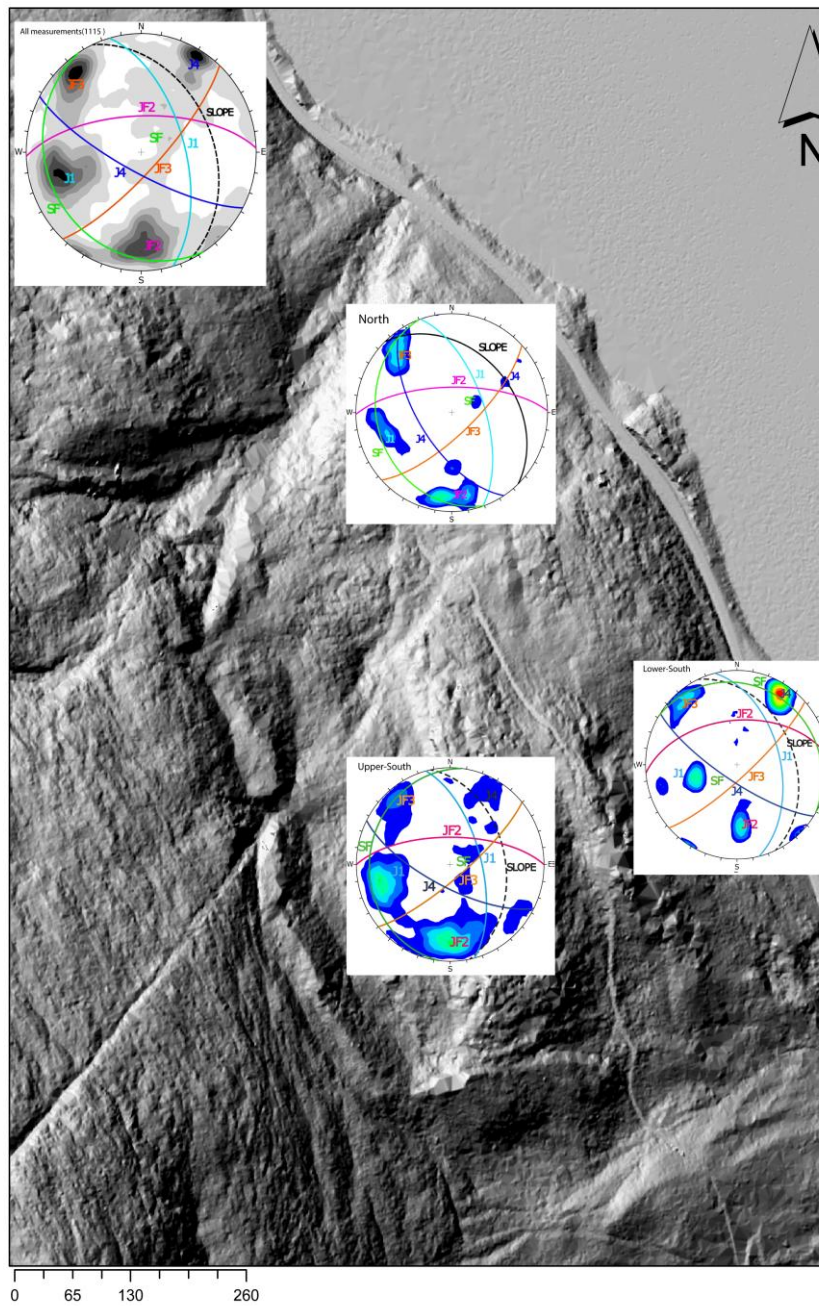
A3: GSI estimate of the rock mass at Håkåneset

Appendix 3:GSI estimate of the for the Håkåneset rock mass obtained by field investigation during the project assignment. Red: General rock mass. Yellow: J1-fault zone (ed. Hoek (2007))



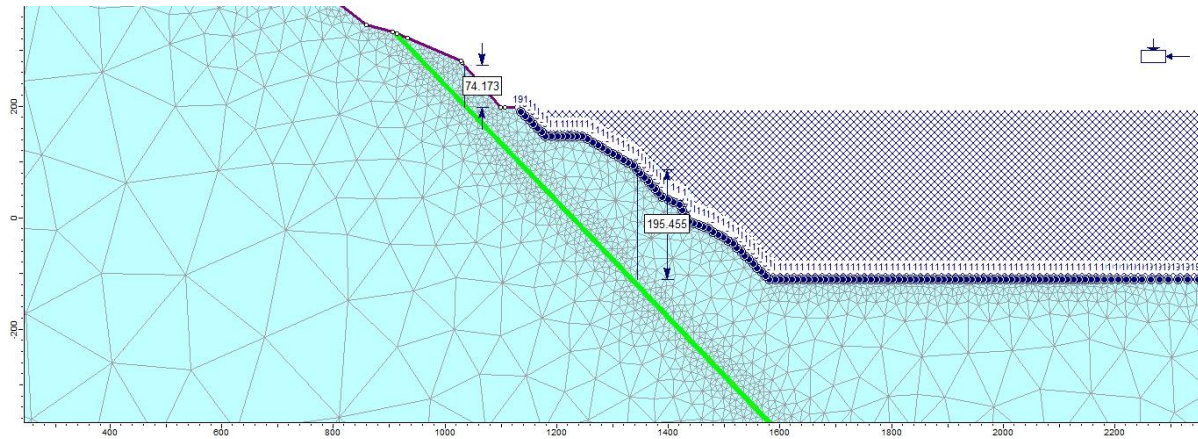
A4: Stereographic pole plots of structural domains

Appendix 4: Contour plots (lower hemisphere, equal area, Fisher distribution) for each subdomain and of all field measurement obtained in the project assignment.



A5: Normal stress calculation to potential failure surface

Appendix 5: Subsection of Phase2 model for estimation of overburden down to an assumed potential failure surface (green line). The overburden is used to determine the normal stress dependent material shear strength parameters cohesion and friction angle as instantaneous values in RocLac (Rocscience, 2011).



$$\overline{\text{Overburden}} \sim 100 \text{ m}$$

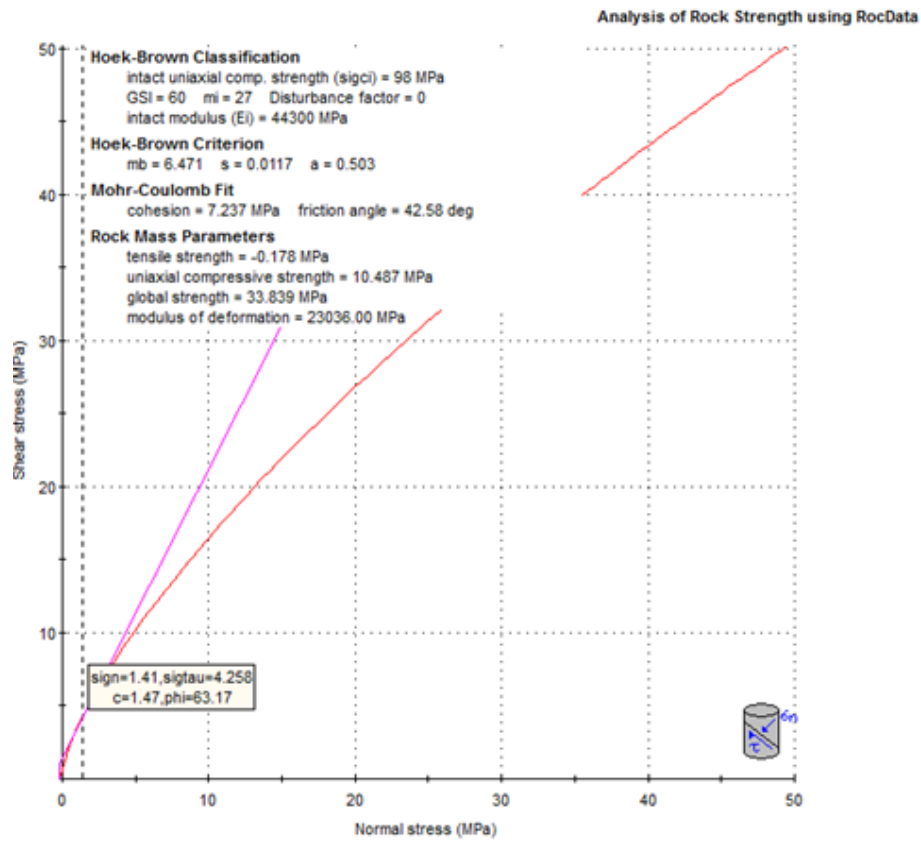
$$\sigma_n = \gamma_{rock} \cdot h \cdot \cos \alpha_{slope} = \frac{30 \text{ kN/m}^3}{\text{m}^3} \cdot 100 \text{ m} \cdot \cos 46^\circ = 2,1 \text{ MPa}$$

$$\sigma_p = \gamma_w \cdot h \cdot \cos \alpha_{slope} = \frac{10 \text{ kN/m}^3}{\text{m}^3} \cdot 100 \text{ m} \cdot \cos 46^\circ = 0,7 \text{ MPa}$$

$$\bar{\sigma} = 2,1 - 0,7 = 1,4 \text{ MPa}$$

A6: Rock mass strength conversion in RocLab

Appendix 6: Output in RockLab. Instantaneous Samples for normal stress at 1,4MPa assumed.



A7: Calculation of joint stiffness

Formulas for the calculations can be found in (Rocscience (2014b))

$$k_n = \frac{E_i E_m}{L(E_i - E_m)}$$

$$k_s = \frac{G_i G_m}{L(G_i - G_m)}$$

k_n = normal shear stiffness

k_s = shear stiffness

E_i = deformability modulus intact rock

E_m = deformability modulus intact rock

L = mean joint spacing

G_m = rock mass shear modulus

G_i = intact rock shear modulus

Appendix 7a: Input values and results of joint set stiffness calculations

Rock parametes	Symbol	Value	Source
Deformation modulus, intact rock	Ei [MPa]	44300	Laboratory estimate obtained in project assignment
Deformation modulus, rock mass	Em [MPa]	23036	RocLab (Rocscience, 2011)conversion, assumed Generalized H-B failure criterion
Poisson ratio	Poissons	0,17	Laboratory estimat
Shear moduls, intact rock	Gi [MPa]	18771	Formulas given in Myrvang (2001)
Shear modulus, rock mass	Gm [MPa]	9761	Formulas given in Myrvang (2001)

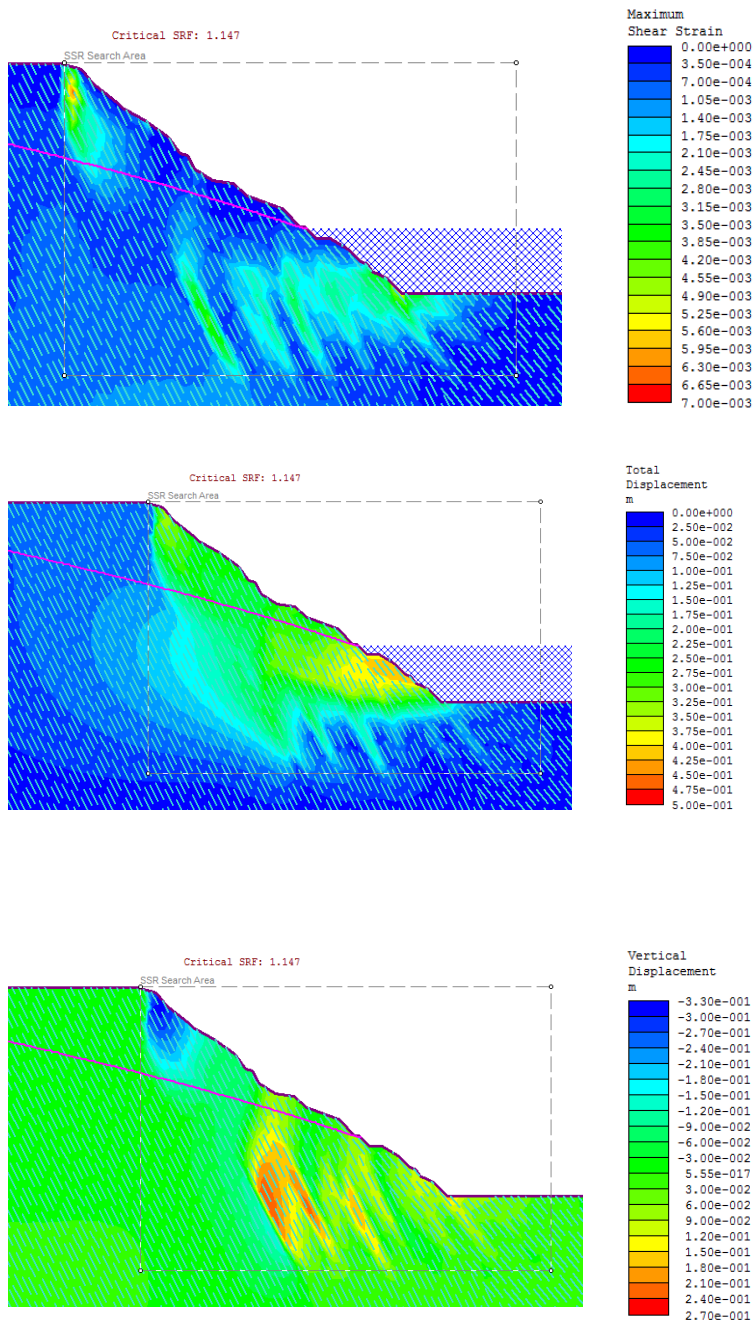
Parameter	Symbol	Joint set values					Source
		<u>J1</u>	<u>JF2</u>	<u>JF3</u>	<u>J4</u>	<u>SF</u>	
Joint set character	Average spacing L [m]	1	5	1	0,3	0,1	Field estimate
Joint stiffness	Normal stiffness Kn [MPa/m]	47992	9598	47992	159972	479917	Formulas given in Rocscience (2014a)
	Shear stiffness Ks [MPa/m]	20335	4067	20335	67785	203355	Formulas given in (Rocscience, 2014a)

Appendix 7b: Epirical joint stiffness data given in (Sandøy, 2012)

K_n (MPa/m):	K_s (MPa/m):	Rock type:	Sources:
10 000	1000	Diorite	Fischer et al. (2010)
5000	1000	Paleozoic-Mesozoic sedimentary rocks	Brideau et al. (2010)
6000	2600	Meta-rhyolite	Loftesnes (2010)
7235	2170	Granitic- granodioritic gneiss	J1: calculated from laboratory work and RocLab
2989	897		J5: calculated from laboratory work and RocLab
100	100	Faults	Böhme (2012), Wines and Lilly (2003).

A8: Phase² contour plots

Appendix 8.1: Analysis 2.12b (Model 2): 30% reduced friction angle 50% reduced cohesion for anisotropic hydrological conditions.(Initial values given in Chapter 6). Location of the groundwater table is highly uncertain.

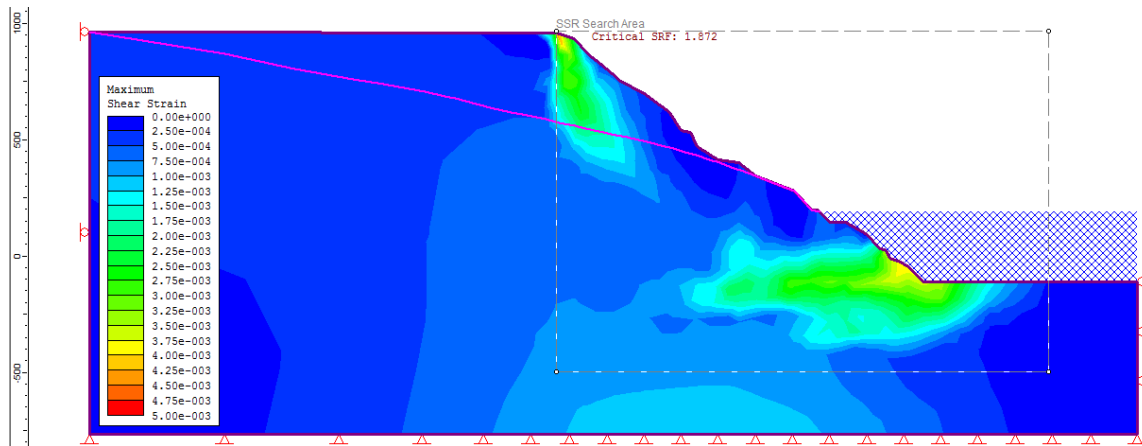


Appendix 8.2

Shear strain plot Model 1

Analysis 1.1: Initial rock mass

CSRF:1.9

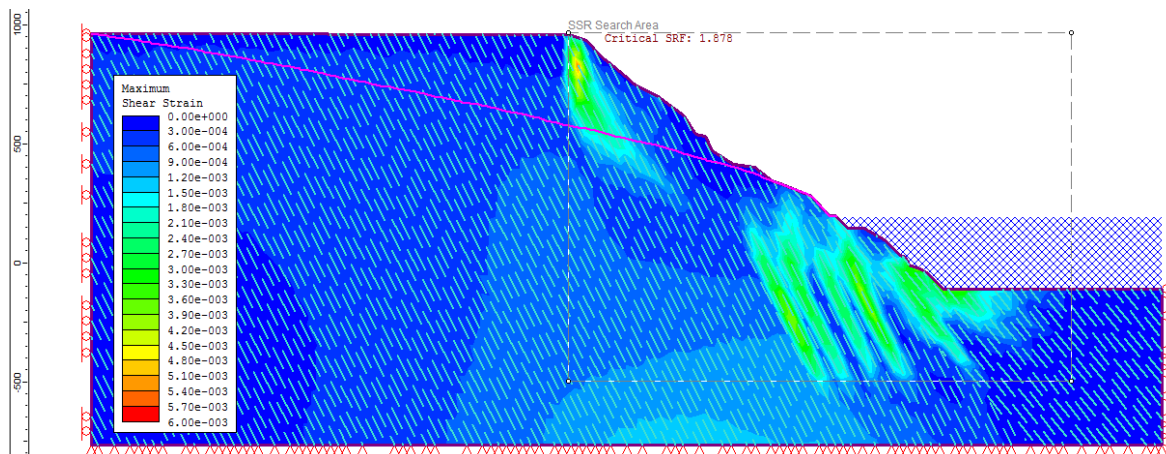


Appendix 8.3:

Shear strain plot Model 2: J1

Analysis 2.1: Initial rock mass

CSRF: 1.9

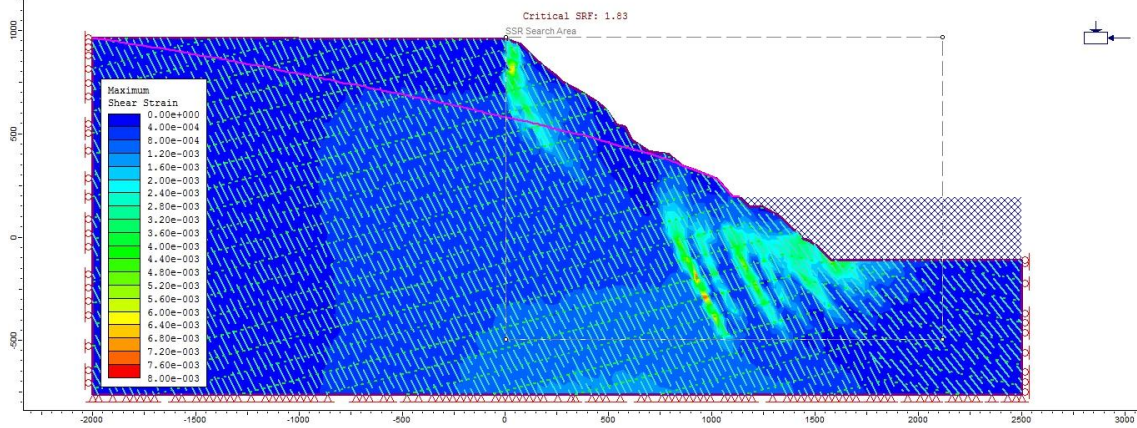


Appendix 8.4:

Shear strain plot Model 3: J1 and SF

Analysis 2.1: Initial rock mass

CSRF: 1.8

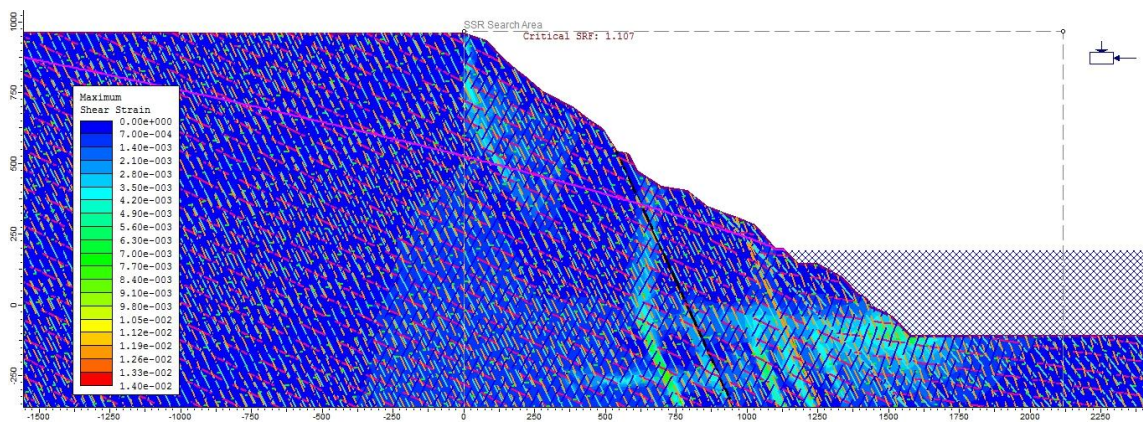


Appendix 8.5:

Shear strain plot Model 4: All discontinuities

Analysis 4.4: Initial rock mass

CSRF: 1.1

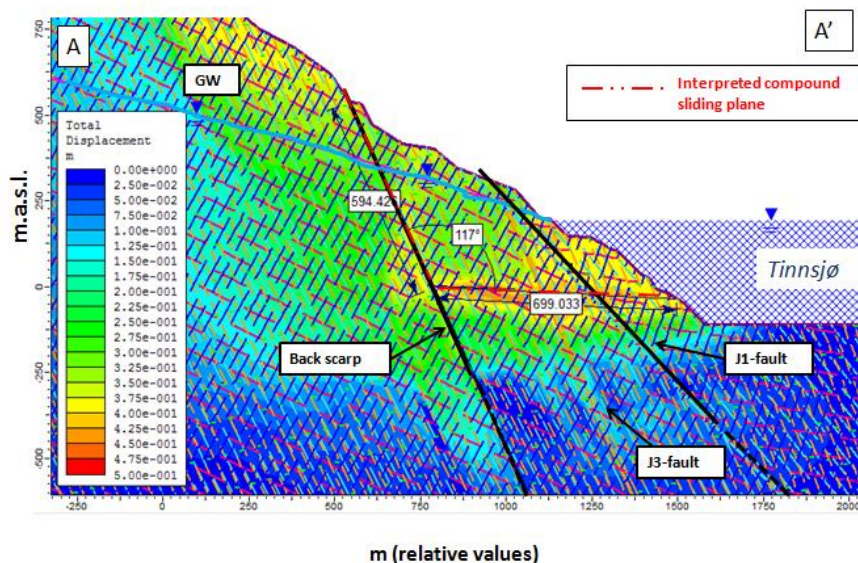


A9: Geometry for volume calculations

Appendix 9.1

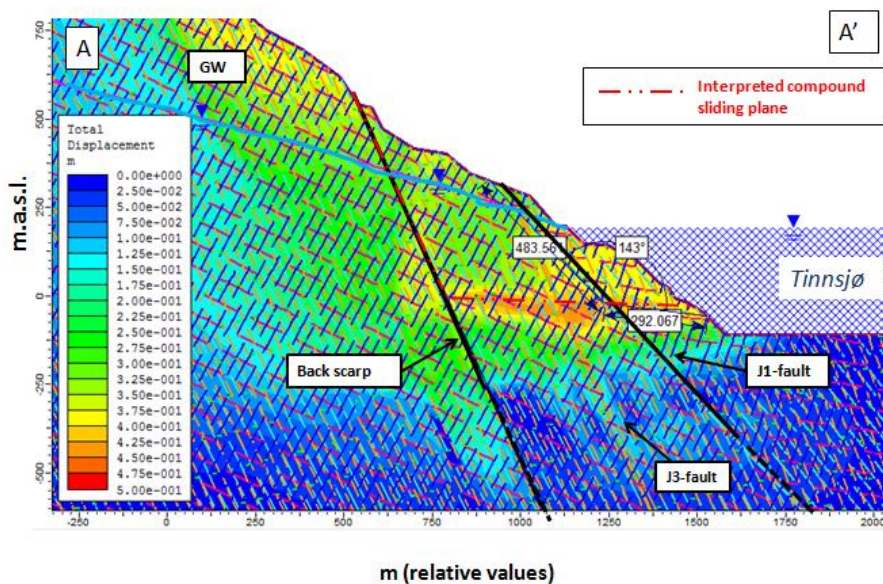
Appendix 9.1a

Håkåneset rockslide
 Analysis 4.4: Model 4 (all discontinuities), low GW
 Critical SRF = 1,1

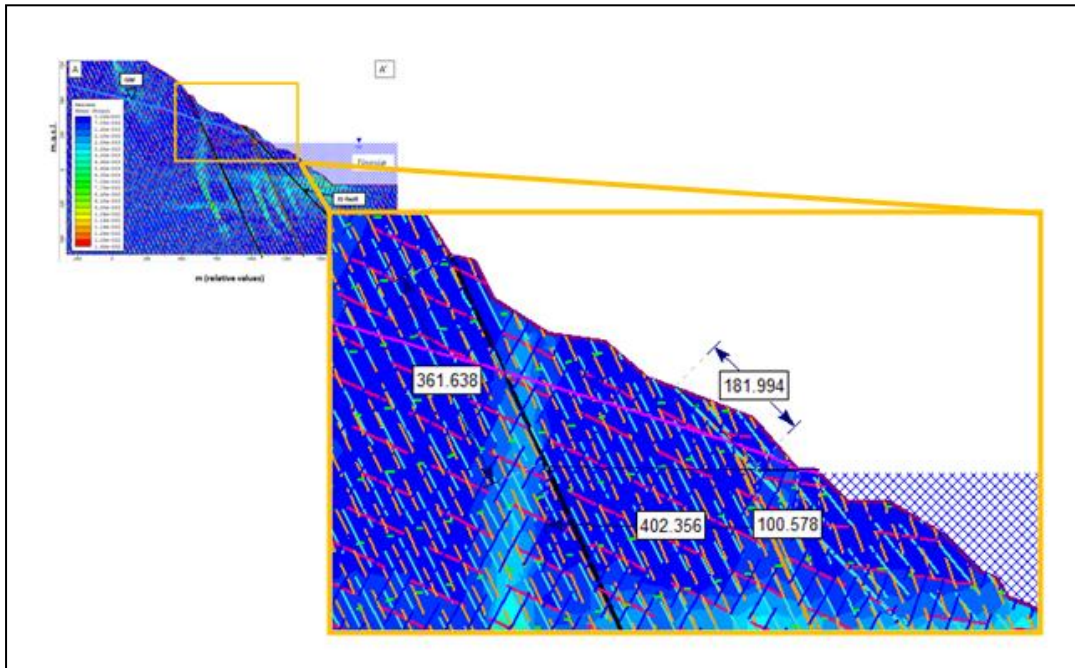


Appendix 9.1b

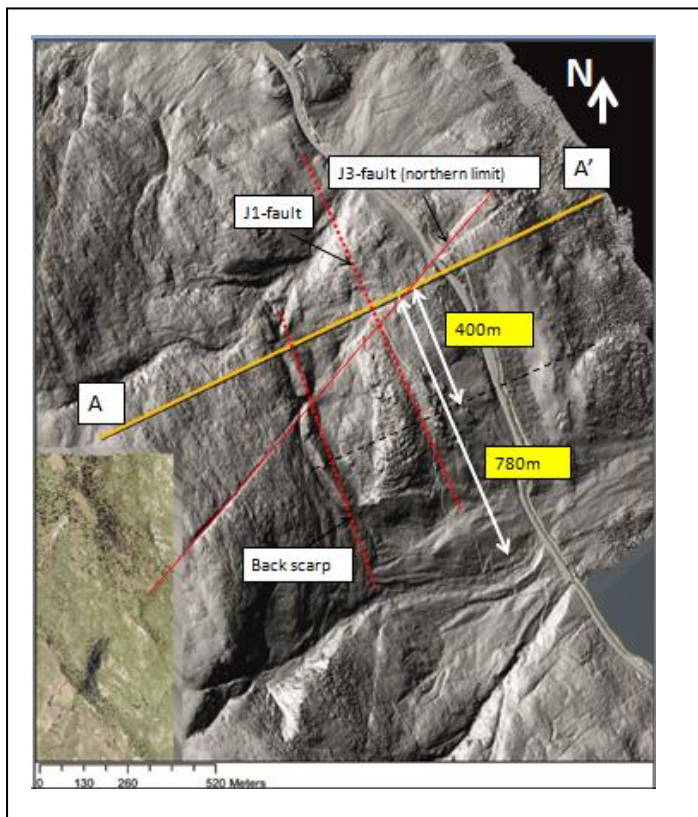
Håkåneset rockslide
 Analysis 4.4: Model 4 (all discontinuities), low GW
 Critical SRF = 1,1



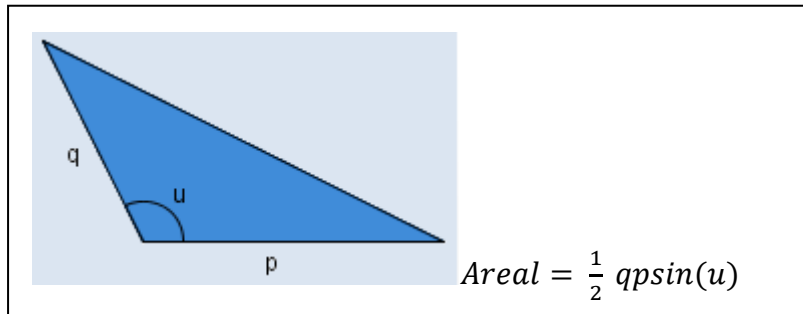
Appendix 9.2



Appendix 9.3



Appendix 9.4



Appendix 9.5

VOLUME ESTIMATION
(Analysis 4.4)

	Back scarp [m]	Basal plane [m]	Angle (deg)	Areal [m ²]	Length to buttress [m]	Volume [m ³]	Length to gulley [m]	Volume [m ³]
Basal surface at 100 m depth	594	699	117	184 976	780	144 280 989	400	73 990 251
	484	292	143	42 527	780	33 170 792	400	17 010 663

Basal surface at lake level	360	400	117	64 152	783	50 231 384	403	25 853 445
	180	100	143	5 416	784	4 246 407	404	2 188 199